(4

CONTRACTOR REPORT BRL-CR-627

BRL

AD-A220 153

THE XNOVAKTC CODE

PAUL S. GOUGH

DTIC
ELECTE
APR 06 1990
S
B
D

FEBRUARY 1990

U.S. ARMY LABORATORY COMMAND

BALLISTIC RESEARCH LABORATORY
ABERDEEN PROVING GROUND, MARYLAND

DESTRUCTION NOTICE

REPORT DOCUMENTATION PAGE

1. AGENCY USE ONLY (Leave blank)	2. REPORT DATE	3. REPORT TYPE AND DATES COVERED
	February 1990	Final, from Oct 85 to Mar 86

4. TITLE AND SUBTITLE
The XNOVAKTC Code

6. AUTHOR(S)
Paul S. Gough

5. FUNDING NUMBERS

C: DAAK11-85-D-0002

7. PERFORMING ORGANIZATION NAME(S) AND ADDRESS(ES)
Paul Gough Associates
1048 South Street
Portsmouth, NH 03801

8. PERFORMING ORGANIZATION REPORT NUMBER

9. SPONSORING / MONITORING AGENCY NAME(S) AND ADDRESS(ES)
US Army Ballistic Research Laboratory
ATTN: SLCBR-DD-T
Aberdeen Proving Ground, MD 21005-5066

10. SPONSORING / MONITORING AGENCY REPORT NUMBER

BRL-CR-627

11. SUPPLEMENTARY NOTES

12a. DISTRIBUTION / AVAILABILITY STATEMENT
Approved for Public Release; Distribution Unlimited.

12b. DISTRIBUTION CODE

13. ABSTRACT (Maximum 200 words)

A description of the one-dimensional two-phase with area change interior ballistic computer code XNOVAKTC (XKTC) is provided. XKTC has the tank gun and traveling charge features fully linked to the chemistry model. This version of the code has chemical kinetics, tank gun features (reactive sidewalls and boattail intrusion) and end burning traveling charge increments. Other extensions include the modeling of single perforated monolithic charges, charges bonded to the tube or the projectile, and a ballistic control tube.

The XKTC code was applied to the simulation of traveling charges with finite reaction zones. It was concluded that a reaction zone of several calibers can be tolerated without significant loss of performance. _Key words:_

14. SUBJECT TERMS
Interior Ballistics, Two-Phase Flow, XKTC Monolithic Charge, Traveling Charge, NOVA, Control Tube, Kinetics,

15. NUMBER OF PAGES
170

16. PRICE CODE

17. SECURITY CLASSIFICATION OF REPORT	18. SECURITY CLASSIFICATION OF THIS PAGE	19. SECURITY CLASSIFICATION OF ABSTRACT	20. LIMITATION OF ABSTRACT
UNCLASSIFIED	UNCLASSIFIED	UNCLASSIFIED	SAR

GENERAL INSTRUCTIONS FOR COMPLETING SF 298

The Report Documentation Page (RDP) is used in announcing and cataloging reports. It is important that this information be consistent with the rest of the report, particularly the cover and title page. Instructions for filling in each block of the form follow. It is important to *stay within the lines* to meet *optical scanning requirements*.

Block 1. Agency Use Only (Leave blank).

Block 2. Report Date. Full publication date including day, month, and year, if available (e.g. 1 Jan 88). Must cite at least the year.

Block 3. Type of Report and Dates Covered. State whether report is interim, final, etc. If applicable, enter inclusive report dates (e.g. 10 Jun 87 - 30 Jun 88).

Block 4. Title and Subtitle. A title is taken from the part of the report that provides the most meaningful and complete information. When a report is prepared in more than one volume, repeat the primary title, add volume number, and include subtitle for the specific volume. On classified documents enter the title classification in parentheses.

Block 5. Funding Numbers. To include contract and grant numbers; may include program element number(s), project number(s), task number(s), and work unit number(s). Use the following labels:

C	- Contract	**PR**	- Project
G	- Grant	**TA**	- Task
PE	- Program Element	**WU**	- Work Unit Accession No.

Block 6. Author(s). Name(s) of person(s) responsible for writing the report, performing the research, or credited with the content of the report. If editor or compiler, this should follow the name(s).

Block 7. Performing Organization Name(s) and Address(es). Self-explanatory.

Block 8. Performing Organization Report Number. Enter the unique alphanumeric report number(s) assigned by the organization performing the report.

Block 9. Sponsoring/Monitoring Agency Name(s) and Address(es). Self-explanatory.

Block 10. Sponsoring/Monitoring Agency Report Number. *(If known)*

Block 11. Supplementary Notes. Enter information not included elsewhere such as: Prepared in cooperation with...; Trans. of...; To be published in.... When a report is revised, include a statement whether the new report supersedes or supplements the older report.

Block 12a. Distribution/Availability Statement. Denotes public availability or limitations. Cite any availability to the public. Enter additional limitations or special markings in all capitals (e.g. NOFORN, REL, ITAR).

DOD - See DoDD 5230.24, "Distribution Statements on Technical Documents."
DOE - See authorities.
NASA - See Handbook NHB 2200.2.
NTIS - Leave blank.

Block 12b. Distribution Code.

DOD - Leave blank.
DOE - Enter DOE distribution categories from the Standard Distribution for Unclassified Scientific and Technical Reports.
NASA - Leave blank.
NTIS - Leave blank.

Block 13. Abstract. Include a brief *(Maximum 200 words)* factual summary of the most significant information contained in the report.

Block 14. Subject Terms. Keywords or phrases identifying major subjects in the report.

Block 15. Number of Pages. Enter the total number of pages.

Block 16. Price Code. Enter appropriate price code *(NTIS only)*.

Blocks 17. - 19. Security Classifications. Self-explanatory. Enter U.S. Security Classification in accordance with U.S. Security Regulations (i.e., UNCLASSIFIED). If form contains classified information, stamp classification on the top and bottom of the page.

Block 20. Limitation of Abstract. This block must be completed to assign a limitation to the abstract. Enter either UL (unlimited) or SAR (same as report). An entry in this block is necessary if the abstract is to be limited. If blank, the abstract is assumed to be unlimited.

SUMMARY

We describe the development of the INOVAKTC (XKTC) Code, a model of interior ballistic phenomena based on a numerical solution of the governing equations for one-dimensional, multi-phase flow. XKTC is an extension of the previously developed INOVAT Code. The extensions include revisions to the representation of reactive sidewalls such as combustible case elements, the modeling of monolithic charges, the analysis of charge increments bonded to the tube or the projectile, a representation of a ballistic control device intended to reduce the temperature coefficient of the charge, and the incorporation of logic to treat end-burning traveling charge increments. Moreover, the tank gun and traveling charge features have been fully linked to the chemistry models.

The XKTC Code is applied to the simulation of traveling charges with finite reaction zones to assess the extent to which the ballistic performance benefit of the traveling charge is degraded as the reaction zone thickness increases. It is concluded that reaction zone thicknesses of several calibers can be tolerated without a significant loss of performance.

INTENTIONALLY LEFT BLANK.

TABLE OF CONTENTS

INTENTIONALLY LEFT BLANK.

LIST OF ILLUSTRATIONS

Intentionally left blank.

viii

LIST OF TABLES

Intentionally left blank.

1.0 INTRODUCTION

The purpose of this report is to document the steps taken to create the XNOVAKTC (XKTC) Code from other recent versions of the NOVA Code. The XKTC Code is intended to provide digital simulations of the interior ballistics of a wide range of gun propelling charges. Like all versions of the NOVA Code,[1] XKTC is based on a numerical solution of the governing equations for the macroscopic, quasi-one-dimensional flow defined by the solid propellant and its products of combustion. The XKTC Code has been developed as an amalgam of the previously developed XNOVAT[2] and NOVATC[3] Codes which respectively address details of tank gun and traveling charges. Our intention in this report is to describe certain additional features which have been encoded into XKTC and to provide a completely updated description of the use of the code. However, we do not provide a complete description of the governing equations or the method of solution.

This introduction contains two sections. In Section 1.1 we provide some background information concerning the various versions of the NOVA Code which have led to the development of XKTC. In Section 1.2 we summarize the new features and cross-linkages which are particular to XKTC. Analysis pertinent to the new features is provided in Chapter 2.0. In Chapter 3.0 we describe the application of XKTC to the traveling charge; we investigate the extent to which the ballistic benefits of the end-burning traveling charge would be compromised by a reaction zone of finite thickness. In the Appendix we provide a complete description of the use of the XKTC Code.

1.1 Background Information

Our intention in this section is simply to clarify the nomenclature for the various versions of the NOVA Code without going into the detailed differences between them. The earlier reports cited here may be consulted for further discussion. The NOVA Code was originally developed to provide a means of analyzing the aspects of charge design which contribute to the formation of longitudinal pressure waves in the chamber of a gun. Although several earlier versions were developed, we understand the NOVA Code to be defined by the version described in Reference 1.

---

[1] G   P. S.   "The NOVA Code: A User's Manual"
Indian Head Contract Report   IHCR 80-8   1980

[2] Gough, P. S.   "XNOVAT – A Two-Phase Flow Model of Tank Gun Interior
Ballistics" Final Report, Task Order I, Contract DAAK11-85-D-0002   1985

[3] Gough, P. S.   "A Two-Phase Model of the Interior Ballistics of Hybrid
Solid-Propellant Traveling Charges"
Final Report, Task I, Contract DAAK11-82-C-0154   1983

Briefly, the NOVA Code was based on the balance equations for macroscopically one-dimensional two-phase flow. The state variables were to be thought of as averages of the local values or microproperties. Intractable microflow details such as drag, heat transfer and propellant combustion were assumed to be related to the macroscopic variables by means of empirical correlations. The NOVA Code allowed the simulation of a broad class of conventional charges consisting of granular or stick propellant arranged in several increments. The governing equations were solved by the method of finite differences with an explicit allowance for the discontinuities in the state variables at the internal boundaries defined by the ends of the increments.

The XNOVA Code[4] was developed to take advantage of more efficient computational procedures which had been established during work on a two-dimensional interior ballistics code.[5] From a modeling standpoint XNOVA retained most of the features of NOVA, only certain esoteric and seldom used options being deleted to produce a compact code. However, XNOVA also contained a modeling extension relative to NOVA in that a dual-voidage representation of perforated stick charges was admitted according to which interstitial properties were distinguished from those within the perforations.

The XNOVAK Code[6] was an extension of XNOVA in which the products of combustion of the propellant and igniter were permitted to react chemically. Whereas earlier code versions had always assumed combustion to proceed to completion locally and simultaneously with regression of the surface of the burning propellant, XNOVAK adopted the viewpoint that the products of combustion consisted of a homogeneous mixture of gases, droplets and particles in which a number of chemical reactions could occur.

XNOVAK was itself extended, as described in the previous task report, to become XNOVAT.[2] The XNOVAT Code incorporated numerous features pertinent to the modeling of tank gun propelling charges, including case combustion and projectile afterbody intrusion. While the chemistry options of XNOVAK were retained, they were not linked to the new tank gun options of XNOVAT.

---

[4] Gough, P. S. "XNOVA - An Express Version of the NOVA Code" Final Report   Contract N00174-82-M-8048   1983

[5] Gough, P. S. "Modeling of Rigidized Gun Propelling Charges" Contract Report   ARBRL-CR-00518   1983

[6] Gough, P. S. "Theoretical Modeling of Navy Propelling Charges" Final Report, Contract N00174-83-C-0241   PGA-TR-84-1   1984

Prior to the development of XNOVAK, the XNOVA Code was used to create the NOVATC Code which added to the features of XNOVA the possibility of modeling all or part of the charge as an end-burning traveling charge.[3] Combustion of the traveling charge was treated consistently with that of the conventional propellant. Regression of the rear face of the traveling charge was assumed to yield final products of combustion at an infinitesimal distance from the surface.

1.2 Objectives and Summary of Results

The objectives of the present effort have been two-fold. First, we have formed a new code by the replacement of XNOVA by XNOVAT in NOVATC. Second, we have added certain new features and encoded cross-linkages of the various options to produce the code which we refer to as the XNOVAKTC Code, or XKTC. Third, we have used XKTC to explore the extent to which the ballistic performance of a traveling charge would be compromised if the formation of final products of combustion were completed over a finite length, rather than at an infinitesimal distance from the base of the traveling charge, as assumed in NOVATC.

Figure 1.1 illustrates three types of propelling charge which can be modeled by XKTC. Figure 1.1 (a) represents a typical multi-increment charge of the type originally addressed by NOVA or XNOVA. Each increment may consist of granular or stick propellant. Unslotted perforated stick propellant is given a dual-voidage representation. Figure 1.1 (b) represents a multi-increment tank gun charge. The projectile afterbody is allowed to intrude into the region occupied by the charge and reactive sidewall components are admitted. It is also possible to model the presence of increment endwalls as reactive layers which resist penetration by the combustion products. The increments may also be described as parallel packaged with appropriate formulations of the flow resistance and heat transfer correlations. Figure 1.1 (c) represents a multi-increment charge in which some of the increments burn in a traveling charge mode, in successive planar layers from the rear. Reactive sidewalls are also admitted, in the region occupied by the conventional increments.

An effort has been made to link all the code options in a physically complete manner. However, it is assumed that there are no compactible filler materials present if the afterbody intrudes into the chamber or if the traveling charge option is exercised. It is also assumed that the projectile does not have an afterbody if the end-burning traveling charge option is used.

Apart from transfering the traveling charge model from NOVATC to XNOVAT, a number of revisions and extensions were added in the development of XKTC. These are described in full in Chapter 2.0. They may be summarized as follows.

3
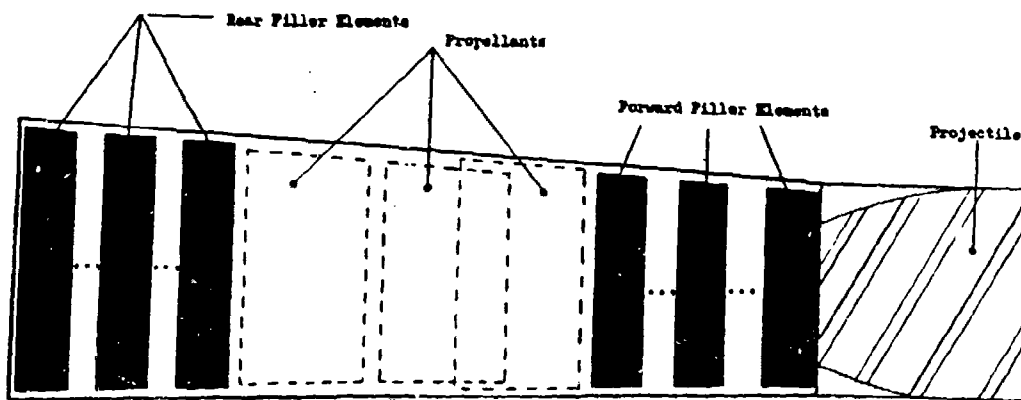
(a) Artillery or Navy Case Gun Charge
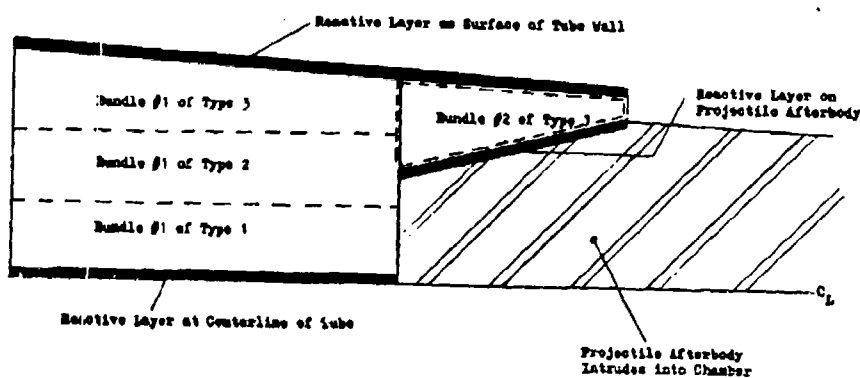
(b) Tank Gun Charge
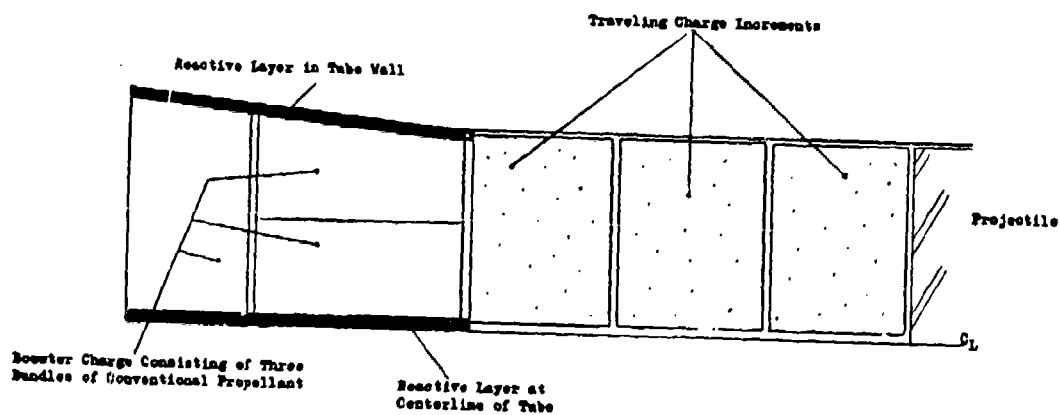
(c) Charge Comprising End Burning Traveling Charge Increments

Figure 1.1 Charge Configurations Represented by XKTC Code.

4

First, we have extended the representation of reactive sidewalls to admit a variation of thermochemical and mechanical properties with axial position. Second, we have encoded a form function for a monolithic charge which is bonded to the tube and burns only on the surface of a single internal perforation. The projectile afterbody is permitted to intrude into the perforation. Third, we have encoded logic to represent any charge increment as bonded either to the tube or to the projectile. This feature may be used to describe a traveling charge increment which burns in depth rather than at the rear surface, and also admits intrusion of the projectile afterbody. Fourth, we have encoded logic to describe a ballistic control device whose purpose is to reduce the temperature coefficient of the charge through the use of a separately burned sub-charge. Finally, we have linked the chemistry options to the sidewall and endwall reactivity models and to the combustion of the traveling charge.

2.0 REVISIONS AND EXTENSIONS TO EQUATIONS

As discussed in Chapter 1.0, most of the governing equations for the XKTC Code have been documented in previous reports and it is not an objective of the present report to provide a comprehensive statement of all the model details. However, we do discuss those equations and linkages which are new. This chapter contains four sections. In Section 2.1 we discuss the revised representation of the reactive sidewalls and endwalls. In Section 2.2 we discuss the representation of the monolithic charge. In Section 2.3 we discuss the treatment of a charge increment which is bonded either to the projectile or to the tube of the gun. Finally, in Section 2.4 we discuss the analysis of a ballistic control device which is intended to reduce the temperature coefficient of the charge.

2.1 Revised Representation of Reactive Sidewalls and Endwalls

In the previous report,[2] which described the development of INOVAT, we discussed the representation of reactive sidewalls and endwalls. The sidewalls were intended to represent combustible case components and/or ignition elements and were understood to be attributes of any or all of the following: the tube, the centerline, the projectile afterbody. The sidewalls were characterized by local values of thickness and surface regression rate. Both ignition and compressibility were taken into account and provision was made for a layer of deterrent. However, each sidewall was considered to have the same mechanical and thermochemical properties over its entire length. The sidewall on the tube was permitted to have different properties from that on the centerline or the projectile afterbody but it was not considered to consist of a number of segments of differing properties.

In XKTC the representation of the sidewalls has been revised so that each sidewall may be characterized as consisting of up to three segments as shown schematically in Figure 2.1. All the mechanical and thermochemical properties may vary from segment to segment. The initial thickness of the layer remains an arbitrary function of position. However, discontinuities in thickness are not recognized explicitly by the numerical method of solution. We also do not track the segment boundaries with precision. The properties of the sidewall at each mesh location are those of the segment in which the mesh point lies and no attempt is made to average sidewall properties when the mesh point is close to a segment boundary.

An additional modification in XKTC is concerned with the treatment of heat transfer to the tube. At a tube wall location which is covered by the sidewall, the heat transfer is assumed to be zero until the sidewall is completely burned through.
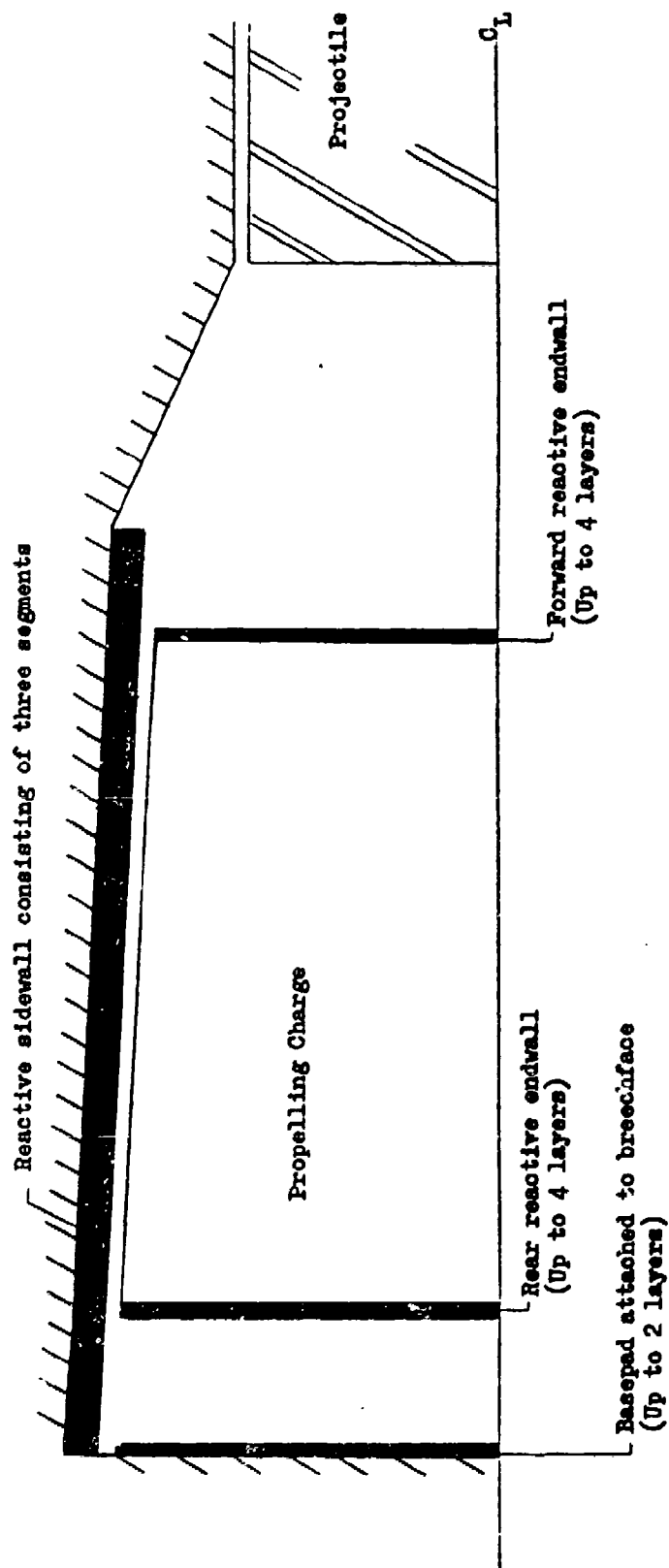
Figure 2.1 Representation of Reactive Sidewalls and Endwalls in XKTC

7

We have also completed the linkage of sidewall reactivity to the chemistry submodels of XNOVAK.[6] In the previous report[2] we had noted the governing equation for the rate of change of Y_i, the mass fraction of species i in the form

$$\varepsilon\rho\frac{DY_i}{Dt} = \varphi\left[Y_{IG_i} - Y_i\right] + \dot{m}_{s_e}\left[Y_{sei} - Y_i\right] + \dot{m}_{s_i}\left[Y_{sii} - Y_i\right]$$

$$+ \sum_{j=1}^{J}\left[Y_{ij,o} - Y_i\right]\dot{m}_j - \dot{w}_i + Y_i\sum_{n=1}^{N}\dot{w}_n + \sum_{k=1}^{K}\dot{r}_{ik} \qquad (2.1.1)$$

where Y_{IG_i}, Y_{sei} and Y_{sii} are the mass fractions of species i in the products of combustion of the igniter, the outer sidewall and the inner sidewall respectively; $Y_{ij,o}$ is the mass fraction of species i produced by the near field (fizz) reaction of propellant j, and $\dot{r}_{ik}$ is the rate of production of species i by reaction k. We also have ε, porosity; ρ, density; φ, $\dot{m}_{s_e}$, $\dot{m}_{s_i}$ and $\dot{m}_j$ as rates of production per unit volume of igniter products, outer sidewall products, inner sidewall products and near field products of propellant j respectively. Finally, $\dot{w}_i$ is the rate of loss of species i due to deposition on the surface of the solid propellant.

In the present code, the values of Y_{sei} and Y_{sii} are fully supported when the user elects to exercise both the tank gun and chemistry options at the same time.

A similar extension applies to the reactive endwalls. Whereas the analysis of the endwalls was previously unlinked to the chemistry option, XKTC requires that the composition of the products of combustion of each of the substrates be specified when the chemistry option is in effect. The internal boundary conditions are then solved subject to the additional balance laws

$$\dot{m}_1 Y_{i_1} + \sum_{j=1}^{4}\dot{m}_{s_j}Y_{s_ji} = \dot{m}_2 Y_{i_2} \qquad (2.1.2)$$

8

where $\dot{m}_1$ is the mass flux from the mixture region at the boundary point inside the endwall, $\dot{m}_2$ is the mass flux at the boundary point outside the endwall, $\dot{m}_{s_j}$ is the rate of reaction of the j-th sublayer, and Y_{i_1}, Y_{i_2}, Y_{sji} are mass fractions of species i corresponding to $\dot{m}_1$, $\dot{m}_2$ and $\dot{m}_{s_j}$ respectively.

2.2   Representation of Monolithic Charge

In Figure 2.2 we illustrate a propelling charge which comprises a monolithic increment. Such an increment is assumed to be bonded to the tube and inhibited on its end surfaces so that combustion is confined to the surface of the single central perforation. Moreover, we consider the possibility that the afterbody of the projectile may penetrate the perforation of the monolithic increment.

We represent the monolithic charge in XKTC as a single voidage stick bonded to the tube. Since end burning of stick propellant is neglected in the code, the inhibition of the ends is automatically captured. However, it is necessary to take care with the definition of the porosity and the form functions in order to model properly the rate of heat transfer during the ignition phase and the subsequent rate of pressurization due to combustion.

Let d_0 be the initial diameter of the perforation and let d be the local surface regression. We assume that d_0 is a function of position, as suggested by Figure 2.2. Let A_t and A_a respectively denote the cross-sectional areas of the tube and the afterbody, corrected for the presence of any reactive sidewalls. The cross-sectional area for the two-phase flow is considered to be

$$A = A_t - A_a \qquad . \qquad\qquad\qquad (2.2.1)$$

Let $A_p = \pi/4 \, (d_0 + 2d)^2$ be the area of the perforation. Then the porosity, or fraction of the flow cross-section occupied by the products of combustion, is

$$\varepsilon = \frac{A_p - A_a}{A} \qquad . \qquad\qquad\qquad (2.2.2)$$

It follows that if we define

$$S_{\bar{p}} = \pi \, (d_0 + 2d) \qquad , \qquad\qquad\qquad (2.2.3)$$

Outside conforms to tube geometry, is bonded and does not burn.

Projectile

C_L

Conventional Increment

Monolithic Charge Increment

Inside has arbitrary initial geometry and is the only burning surface.
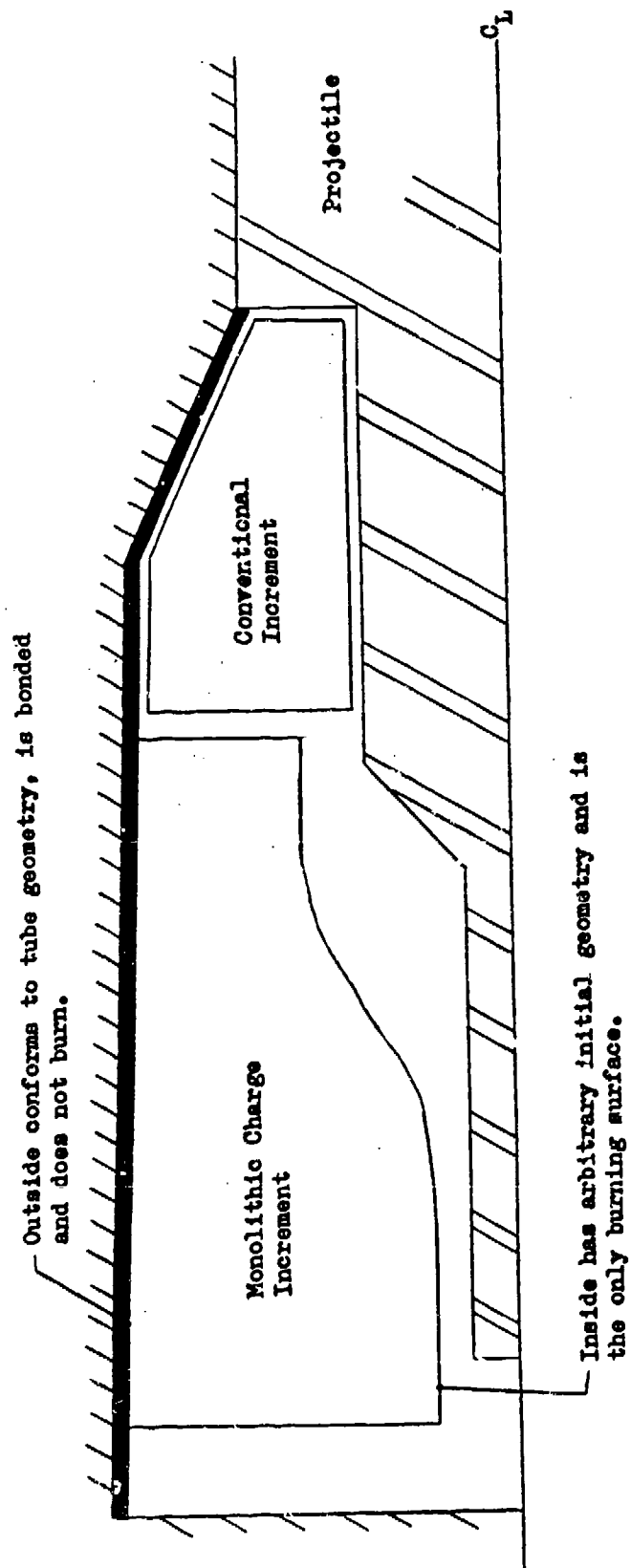
Figure 2.2 Representation of Single Perforation Monolithic Charge by XKTC

$$V_p = A - (A_p - A_a) \qquad , \qquad\qquad (2.2.4)$$

then the ratio S_p/V_p will yield the correct rate of pressurization of the perforation when combustion occurs. However, the heat transfer to the solid propellant during the ignition phase must be based on the hydraulic diameter

$$D_p = \frac{4(A_p - A_a)}{(S_p + S_a)} \qquad\qquad (2.2.5)$$

where S_p is given by (2.2.3) and S_a is the circumference of the afterbody.

We have already commented on the fact that we treat the monolithic grain as bonded to the tube. We discuss the analysis of bonded grains in the next section where we also consider the possibility of bond rupture. However, rupture of the bond which attaches the monolithic grain is presently assumed never to occur. If we do consider rupture we have also to consider the possibility that the outer surface of the grain will no longer conform with the inner surface of the tube. This will affect the c. culation of the form functions and, more importantly, will lead to a consideration of the formation of an outer annular ullage region and the possibility of ignition of the outside of the grain. Since combustion of the outer surface could well result in the consideration of mass addition in a region of arbitrarily small flow cross-section, we have regarded this topic as being beyond the scope of the present effort.

If a reactive layer is attached to the tube wall in the region occupied by the consolidated charge, it is assumed to be thermally insulated until the charge has completely burned through.

2.3 Analysis of Bonded Charge Increment

Figure 2.3 illustrates a charge increment which is bonded to the projectile. Rather than writing a momentum equation for the projectile and bonded charge as a system, we consider the equations of motion for each and introduce an explicit force of bonding which ensures that they remain in contact. This approach is computationally convenient as it allows us to make use of existing coding structures with only minor modifications. Also, the explicit computation of the bonding force allows us to consider a rupture criterion according to which the charge may separate from the projectile. We first consider a charge bonded to the projectile as in Figure 2.3. Subsequently, we comment on the case when the increment is bonded to the tube of the gun.
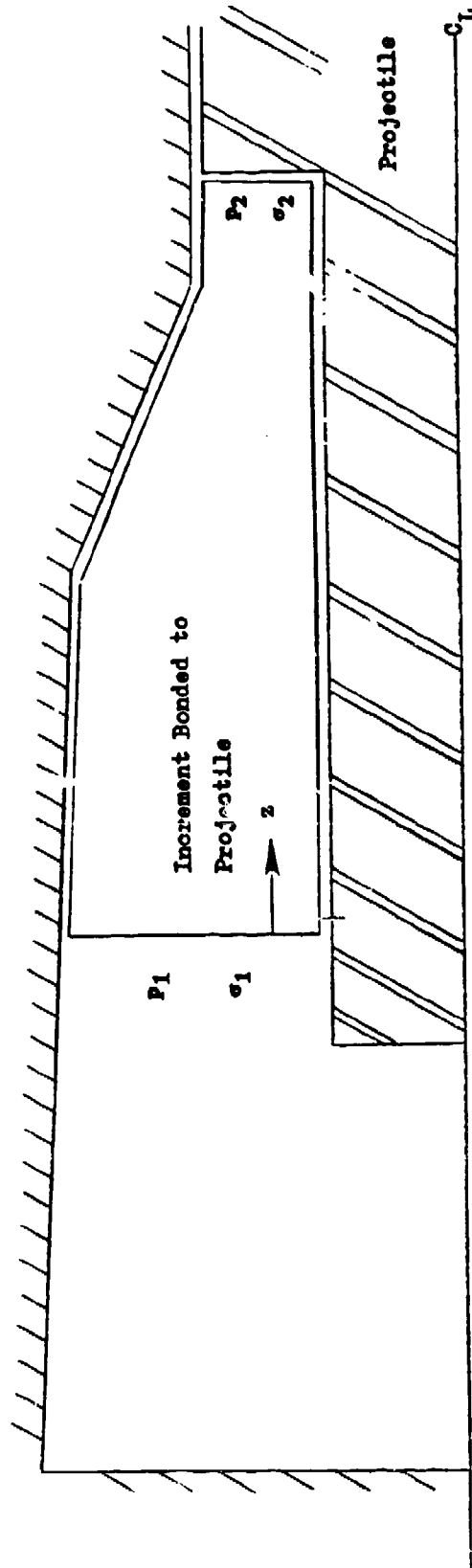
Figure 2.3 Charge Increment Bonded to Projectile

12

The equation of motion of the projectile is

$$M_p \frac{dv_p}{dt} = g_0(p_2 + \sigma_2)A_2 + g_0 \int_{z_3}^{z_2} (p + \sigma) \frac{dA_a}{dz} dz + g_0 \int_{z_1}^{z_2} \tau dz + \phi - F \tag{2.3.1}$$

where M_p is the mass of the projectile, v_p is the projectile velocity, p_2 and σ_2 are the pressure and intergranular stress at the base of the projectile and A_2 is the flow cross-sectional area at the same point and is defined by Equation (2.2.1). We assume that the charge is bonded to the afterbody over the interval $[z_1, z_2]$ and that τ is the bonding force. The symbol ϕ denotes the force due to gas pressure and intergranular stress over that part of the afterbody to the rear of the bonded increment. F is the bore resistance. We use the constant g_0 to reconcile units of measurement. As in the previous section, A_a is the cross-sectional area of the afterbody.

The equation of motion of the solid propellant is

$$(1 - \varepsilon)\rho_p \frac{Du_p}{Dt_p} + g_0(1 - \varepsilon) \frac{\partial p}{\partial z} + g_0 \frac{\partial \sigma}{\partial z} = f_s - \frac{\tau}{A} \tag{2.3.2}$$

where ρ_p is the density of the propellant, u_p is the velocity, f_s is the interphase drag and D/Dt_p is the convective derivative along the propellant streamline.

Now consider auxilliary variables v_p and u_p such that

$$M_p \frac{dv_p}{dt} = g_0(p_2 + \sigma_2)A_2 + g_0 \int_{z_1}^{z_2} (p + \sigma) \frac{dA_a}{dz} dz + \phi - F \quad , \tag{2.3.3}$$

$$(1 - \varepsilon)\rho_p \frac{Du_p}{Dt_p} + g_0(1 - \varepsilon) \frac{\partial p}{\partial z} + g_0 \frac{\partial \sigma}{\partial z} = f_s \quad . \tag{2.3.4}$$

13

We may multiply (2.3.4) by A, integrate over z and add to (2.3.3) and perform similar operations on (2.3.1) and (2.3.2) to obtain the physically expected result

$$M_p \frac{dv_p}{dt} + \int_{z_1}^{z_2} (1 - \varepsilon)\rho_p A \frac{Du_p}{Dt} dz = M_p \frac{dv_p}{dt} + \int_{z_1}^{z_2} (1 - \varepsilon)\rho_p A \frac{Du_p}{Dt} dz \qquad .$$

$$(2.3.5)$$

Since the condition of bonding requires $v_p = u_p$ it follows that the updated quantities obey

$$v_p^{n+1} \left\{ M_p + \int_{z_1}^{z_2} (1 - \varepsilon)\rho_p A dz \right\} = M_p v_p^{n+1} + \int_{z_1}^{z_2} (1 - \varepsilon)\rho_p A u_p^{n+1} dz \qquad . \quad (2.3.6)$$

The computational algorithm therefore requires that we first integrate (2.3.3) and (2.3.4) to get v_p^{n+1} and u_p^{n+1}. Then (2.3.6) yields v_p^{n+1} and hence u_p^{n+1}. We have assumed thus far that the bond between the propellant and the projectile does not rupture. The force of bonding may be determined as

$$F = \frac{v_p^{n+1} - v_p^{n+1}}{g\Delta t} M_p \qquad (2.3.7)$$

where $\Delta t = \Delta t$ on the predictor step and $\Delta t/2$ on the corrector step of the finite difference integration. Separation of the propellant from the projectile is assumed to occur if F exceeds a predetermined value.

The intergranular stress σ follows from the usual constitutive law according to which it is an irreversible function of porosity. Since axial strain cannot occur for the bonded charge, the stress will be controlled by combustion of the propellant and variations in tube area with travel. The boundary values of σ are likewise determined from the constitutive law and not from the characteristic forms.

14

The analysis of an increment bonded to the tube is analogous except that an obvious simplification arises since the tube is assumed to remain stationary. In place of (2.3.7) we evaluate the bonding force from

$$F = - \frac{\int_{z_1}^{z_2} u_p^{n+1} \rho_p A(1 - \varepsilon) dz}{g_o A t} \qquad (2.3.8)$$

We also note that the attribute of attachment to the projectile or to the tube applies to the increment as a whole. If the increment consists of a mixture of propellants or of several parallel packaged bundles, all the species or bundles are taken to be bonded until the rupture condition is achieved.

2.4 Representation of Ballistic Control Device

In Figure 2.4 we illustrate a ballistic control device whose intended purpose is the reduction of the temperature coefficient of the propelling charge. The small control charge is burned prior to or during the ignition of the main charge. Since thrust is supplied to the projectile via the base of the afterbody, the control charge has the effect of varying the position of the projectile during or prior to the ignition of the main charge. At higher temperatures the displacement of the projectile, at the time of ignition of the main charge, is expected to increase thereby offsetting the increased quickness of the main charge and reducing the temperature coefficient.

In our schematic illustration we show features of the XKTC representation which may or may not be present in actual designs. We show a combustion chamber within the device whose diameter differs from that of the propulsion tube into which the projectile afterbody intrudes. We also show sidevents along the device through which an ignition stimulus to the propelling charge may be induced prior to the uncorking of the afterbody. The XKTC Code also allows the exterior of the device to have an arbitrary shape.

The model of the ballistic control device includes the following details. Conditions within the device are presumed to be uniform since the device is not expected to be very long and the resolution of axial structure according to a continuum model does not seem worthwhile. The governing equations for the state of the gas within the device are therefore statements of the balance of mass and energy supported by a burn rate law for the control charge and a covolume equation of state. The control charge

15
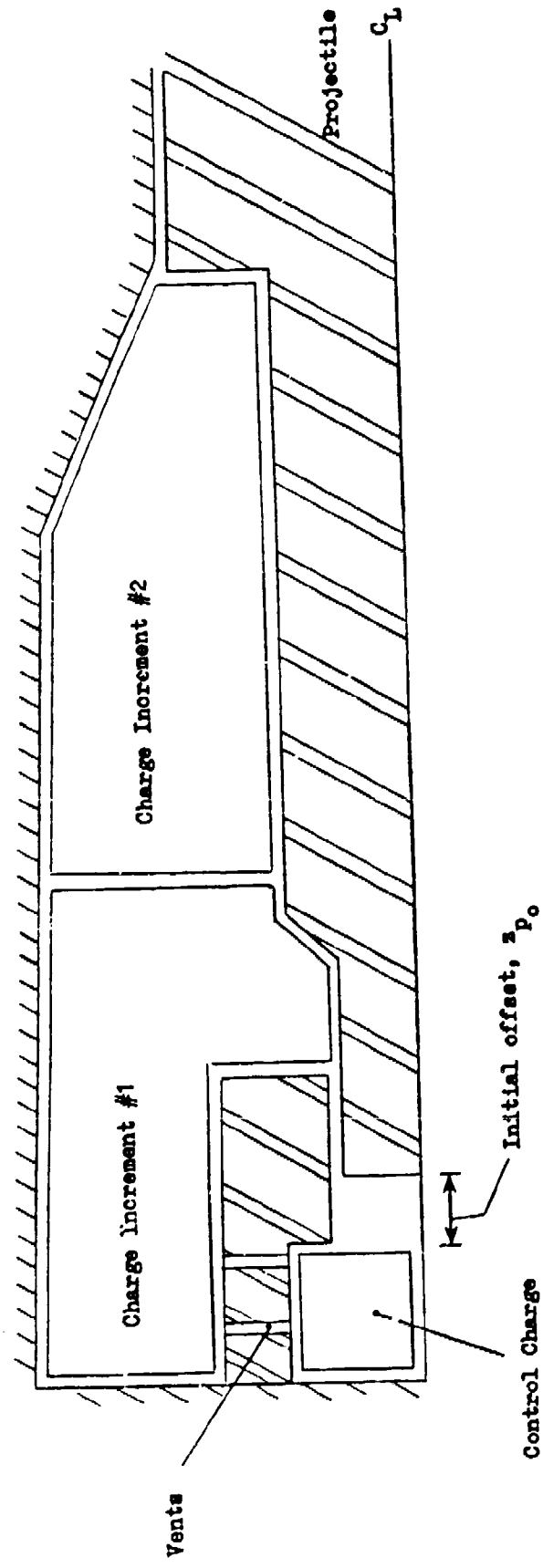
Figure 2.4 Schematic Illustration of Ballistic Control Device

is assumed to be granular and to consist of one of the following forms: sphere; cylinder; monoperforated with or without outside inhibition; seven-perforation. The control charge is assumed to be ignited after a predetermined delay.

The equation of motion of the projectile is modified to take into account the thrust due to the control charge until the instant when the projectile uncorks.

The external geometry of the device is used to correct the values of the cross-sectional area of the two-phase flow defined by the main charge. For the present we assume that the device is short enough that the vented gases can be coupled to the reponse of the main charge through representation as a basepad attached to the breechface. The rate of venting per unit vent area is deduced from the pressures within the control device and at the rear of the main charge according to an isentropic flow law with an allowance for choking. The total rate of flow follows from the total vent area which is exposed as the projectile moves. This total area consists of the sidewall contribution and, when the projectile uncorks, the area of the propulsion tube.

The total flux so computed is used to construct a surface source term which is expressed as an attribute of the breechface. Reversed flow into the control chamber is not presently considered. In subsequent work it is intended to provide the option of representing the flux from the control device as a sidewall source attributed to the internal boundary of the two-phase flow. This will permit the representation of longer devices than the present method.

The governing equations for the state of the gas within the device are easily derived and we simply summarize them here. The balances of mass and energy are

$$V_g \frac{d\rho}{dt} = \dot{m}_p \left[1 - \frac{\rho}{\rho_p} \right] - \dot{m}_e - \rho A_c v_p \qquad (2.4.1)$$

$$\rho V_g \frac{de}{dt} = \dot{m}_p (e_p - e) - \frac{p}{\rho} \dot{m}_e - p A_c v_p \qquad (2.4.2)$$

where ρ is density; p, pressure; e, internal energy; V_g, volume available to gas; A_c, cross-sectional area of propulsion tube; v_p, projectile velocity; $\dot{m}_p$, rate of combustion of control charge; ρ_p, density of control charge; e_p, chemical energy of control charge; $\dot{m}_e$, total mass flux to main charge, assumed to be always positive or zero.

17

The volume available to the gas is given by

$$V_g = V_0 + A_c z_p - \frac{M_p}{\rho_p} \qquad (2.4.3)$$

where V_0 is the volume of the combustion chamber; z_p is the displacement of the base of the afterbody relative to the entrance to the propulsion tube; m_p is the mass of the unburned propellant. We note that XKTC admits an initial gas volume V_{g_0} defined by

$$V_{g_0} = V_0 + A_c z_{p_0} \qquad (2.4.4)$$

where z_{p_0} is an initial standoff distance. The initial volume may be defined through either V_0, z_{p_0} or both.

The rate of combustion of the propellant is

$$\dot{m}_p = \frac{M_{p_0}}{V_{p_0}} S_p \dot{d} \qquad (2.4.5)$$

where S_p is the surface area of a grain; V_{p_0} is the initial volume of a grain; M_{p_0} is the initial mass of the charge and $\dot{d}$ is the surface regression rate and is assumed to obey the usual exponential dependence on pressure. We also have

$$M_p = \frac{M_{p_0}}{V_{p_0}} V_p \qquad (2.4.6)$$

where V_p is the current volume of a grain. The values of V_p and S_p are related to the total surface regression through the usual geometrical form functions.

18

The functional dependence of $\dot{m}_e$ on the pressures within the control device and at the breech of the main chamber is given by the isentropic flow law corrected for covolume as in Reference 1.

Provision is made for a deterrent layer in the control charge but there is no present linkage to the chemistry options.

3.0 EFFECT OF FINITE FLAME THICKNESS ON TRAVELING CHARGE PERFORMANCE

In conventional propelling charges the propellant tends to be distributed in a nearly uniform fashion over the length of the tube and the velocity distributions of both the propellant grains and the products of combustion tend to be nearly linear functions of axial position as suggested by Lagrange.[7] The kinetic energy of the propulsion gas is proportional to that of the projectile and represents a loss of ballistic efficiency. For artillery weapons operating with a muzzle velocity of approximately 1 km/sec the ratio of propellant mass to projectile mass (C/M) is about 0.2 and the loss is not very important. However, there is a current interest in weapons operating at a muzzle velocity of 3 km/sec. Estimates of the required value of C/M to achieve such velocities range from 3 to 8 and the kinetic energy of the propulsion gas therefore represents a significant loss.

The end-burning traveling charge has been proposed as a propulsion scheme whereby the loss due to the kinetic energy of the propulsion gas may be reduced.[8] A model of the traveling charge has been developed[9] and the theoretical advantages of this scheme have been demonstrated. However, theory has incorporated the assumption that the final products of combustion are formed an infinitesimal distance from the regressing rear surface of the traveling charge. This assumption has not been supported by experimental studies of those formulations which presently show the most promise.[10] Combustion has been observed to involve a complex series of steps which are strongly dependent on composition, confinement and density of the sample. Rather than consisting of a region of unburned propellant separated from a region of final combustion products by a thin reaction zone, the combustion process was seen to involve a preliminary penetration and partial consumption of the entire sample by a convective flamefront which was then followed by a relatively homogeneous consumption of the remainder of the propellant accompanied, in some cases, by deconsolidation.

---

[7] Corner, J. "Theory of the Interior Ballistics of Guns"
New York, John Wiley and Son, Inc   1950

[8] May, I. W., Baran, A. F., Baer, P. G. and Gough, P. S.
"The Traveling Charge Effect"
Proceedings of the 15th JANNAF Combustion Meeting   1978

[9] Gough, P. S. "A Model of the Traveling Charge"
Ballistic Research Laboratory Contract Report ARBRL-CR-00432   1980

[10] White, K. J., McCoy, D. G., Doali, J. O., Aungst, W. P.,
Bowman, R. E. and Juhasz, A. A.
"Closed Chamber Burning Characteristics of New VHBR Formulations"
Proceedings of the 21st JANNAF Combustion Meeting   1984

The objective of the present study is to investigate the ballistic consequences of a finite reaction zone at the base of the traveling charge. We do not attempt to model directly the complex phenomena reported by White et al.[10] The theoretical model is sufficiently broad that it does offer the prospect of future simulations of combustion mechanisms of the type described by these authors. In the present study, however, the model is simply exercised to describe a two-step combustion process in which regression of the base of the traveling charge yields a mixture of final (TC-F) and intermediate (TC-I) combustion products. The intermediate products react to completion at a finite rate over an extended region. The thickness of the combustion zone is varied by varying the ratio of final to intermediate products formed in the first step and the rate of reaction of the intermediate products.

We provide a summary of the physical content of the model in this introduction. The governing equations are summarized in Section 2.1. Before discussing the model we comment further on the differences between conventional and traveling charges.

We have already noted that the kinetic energy of the propellant and its products of combustion represent a ballistic loss whose importance increases with increasing muzzle velocity. The original concept of the traveling charge seems to be due to Langweiler[11] who proposed the development of an end-burning charge attached to the projectile base with a burn rate designed to yield products of combustion at rest relative to the tube. Apart from the purely technological problem of producing a propellant with the necessarily enormous burn rates and the required mechanical strength, it was observed by Vinti[12] that the proposed burn rates would, in general, require the development of a strong deflagration wave, one for which the products of combustion would be supersonic relative to the flame front. The strong deflagration wave is believed to be thermodynamically unstable[13,14] and

---

[11] Langweiler, H.
"A Proposal for Increasing the Performance of Weapons by the Correct Burning of Propellant"
British Intelligence Objective Sub-committee, Group 2,
Ft. Halstead Exploiting Center, Report 1247   undated

[12] Vinti, J. P. "Theory of the Rapid Burning of Propellants"
Ballistic Research Laboratory Report No. 841   1952

[13] Courant, R. and Friedrichs, K. O.
"Supersonic Flow and Shock Waves" Interscience, New York   1948

[14] Landau, L. D. and Lifschitz, E. M. "Fluid Dynamics"
Pergamon Press   1959

therefore to be incapable of existing in a steady flow. Although the traveling charge is burned in an inherently unsteady manner, the strong deflagration limit should nevertheless apply provided that the combustion zone is sufficiently thin that the rates of change of mass, momentum and energy within it remain negligible by comparison with the fluxes of these quantities through its bounding surfaces. We also note that even if the strong deflagration were achievable, it would not necessarily represent a useful state from an engineering standpoint due to the magnitude of the concomitant pressure drop across the reaction zone. At the theoretical limit of sonic or choked combustion the pressure on the unreacted side of the flame is approximately twice that on the reacted side. The ratio of pressures increases indefinitely with Mach number and, for the Langweiler proposal at least, it implies indefinitely increasing stress on the barrel throughout the combustion of the charge.

The foregoing objections are particular to the Langweiler concept. They do not rule out the possibility of improved ballistic performance through a more general traveling charge concept in which the rate of burning is simply required to be great enough to induce a substantial rearward blowing of the products of combustion.

An additional phenemenon to be considered is the rarefaction formed at the instant the traveling charge burns out. The local pressure drop may be so large that there is no further significant propulsion of the projectile following burnout. The projectile may even decelerate due to the resistive forces. The rarefaction also has the result that the velocity distribution of the combustion products is relaxed to the conventional linear Lagrange distribution with the result that the kinetic energy of the propellant gas is restored to the conventional value and the benefit of the traveling charge is apparently lost. It may be expected therefore that optimium traveling charge performance will involve burnout timed to occur just prior to muzzle exit.

Although the initial motivation for the traveling charge appears to have stemmed from a consideration of the velocity field of the propulsion gas, it is our view that attention is better directed towards the pressure distribution. Associated with the linear Lagrange velocity distribution is a parabolic pressure distribution whose gradient serves to accelerate the propulsion gas down the tube. The pressure at the projectile base is less than that at the breech. Accordingly, propulsion of the projectile is due to a lower pressure than that which the tube must withstand. We illustrate the conventional charge in Figure 3.1. We show the mixture region separated from the projectile base by a small region of ullage -- usually no more than one or two calibers -- which is due to the inability of the propellant grains to match exactly the projectile velocity. We also sketch the pressure distribution. According to the appoximate theory of Lagrange, the ratio of breech to base pressure is given by $1 + C/2M$, where C is the charge mass and M is the projectile mass. If $C/M = 0.2$ as is typically the case for artillery weapons firing at 1 km/sec then the ratio of pressures is 1.1 and the loss of efficiency is small. On the other hand, if a value of $C/M = 8$ is required to achieve velociti· of the order of 3 km/sec, then the
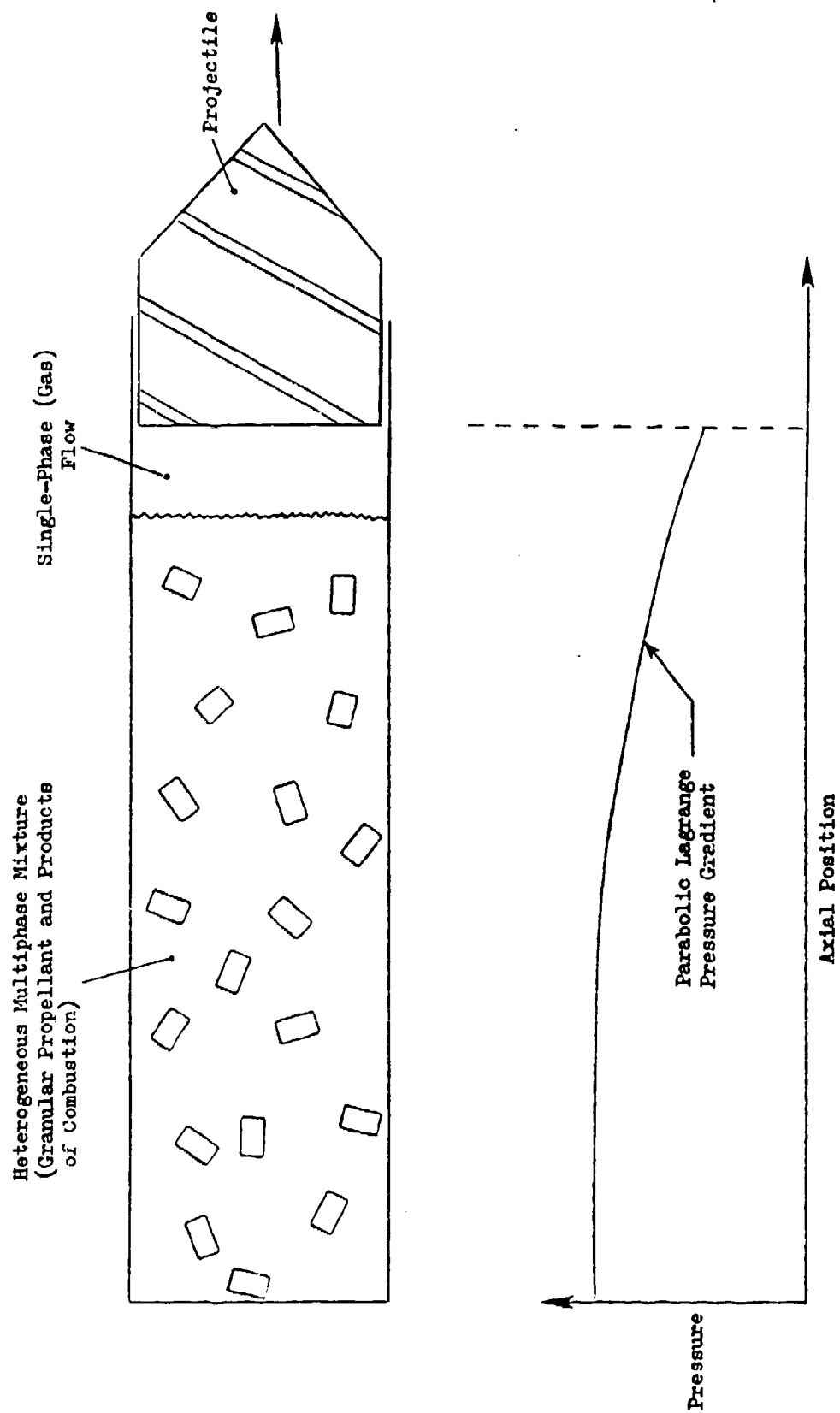
Figure 3.1 Structure of Flow for Conventional Propelling Charge

Projectile

Single-Phase (Gas) Flow

Heterogeneous Multiphase Mixture
(Granular Propellant and Products
of Combustion)

Parabolic Lagrange Pressure Gradient

Axial Position

Pressure

23

ratio becomes 5 and it is clear that the projectile is receiving little propulsive benefit from the pressure exerted on the tube. It should be said, however, that the Lagrange distribution may provide a very poor characterization of the pressure field in a conventional gun when C/M exceeds unity and the pressure drop may not in fact be as large as 1 + C/2M, particularly in the earlier stages of the propulsion cycle.

In Figure 3.2 we illustrate the situation for an ideal end-burning traveling charge. We assume that the traveling charge is ignited following the complete combustion of a booster charge. Therefore the unreacted propellant is separated from a region of single-phase flow by a thin reaction zone. We show a wave front moving to the rear. This compression front would not arise in the Langweiler cycle but would be expected for other types of burning schedules. The compression wave may also reflect from the breech and, at a later time, be observed traveling in the opposite direction. In the ideal representation of Figure 3.2, all the chemical energy of the traveling charge is released in a thin layer. We accordingly represent it as a discontinuity and we show a discontinuous drop in pressure as we pass from the unreacted to the reacted side of the combustion zone. We also show the pressure field dropping as we move through the unreacted traveling charge towards the base of the projectile. This pressure drop is expected to be linear, if the traveling charge is sufficiently rigid, and is analogous to the parabolic Lagrange pressure drop which occurs in the propulsion gas in a conventional charge. We therefore note that while the pressure distribution of Figure 3.2 is clearly different from that of Figure 3.1, both represent the propulsion of the projectile as due to a pressure which is less than the spacewise maximum.

When the traveling charge is compared with the conventional charge in terms of the relative ratios of the base pressure to the spacewise maximum it is not obvious that the one concept is necessarily superior to the other. Moreover, elementary interior ballistic theory is not much help since the Lagrange characterization of the pressure is not expected to be accurate even for conventional charges at the values of C/M of interest.

It is clear that theoretical comparison of conventional and ideal end-burning traveling charges can only be conducted by reference to a continuum model in which the pressure gradient is developed as a natural part of the solution. The BRLTC Code[9] was developed to permit such theoretical comparisons. The products of combustion were modeled as an inviscid, non-reacting one-dimensional gas flow subject to the covolume equation of state. The unreacted traveling charge was modeled as either rigid or as a one-dimensional elastic continuum. The reaction zone was represented as a discontinuity across which the solid propellant was transformed to final products of reaction. A number of combustion laws were encoded. The regression rate could be specified as a function of pressure or tailored to yield a predetermined value of pressure on the unreacted side or of projectile acceleration or of the Mach number of the combustion products relative to the regression front. Branching between the various laws was also admitted. The code was subsequently extended to incorporate multiple increment traveling charges and to provide a representation of booster
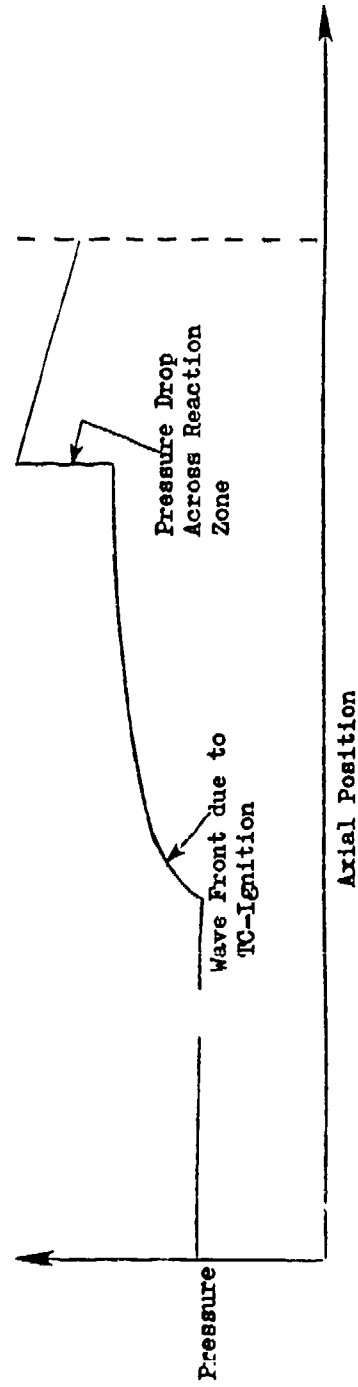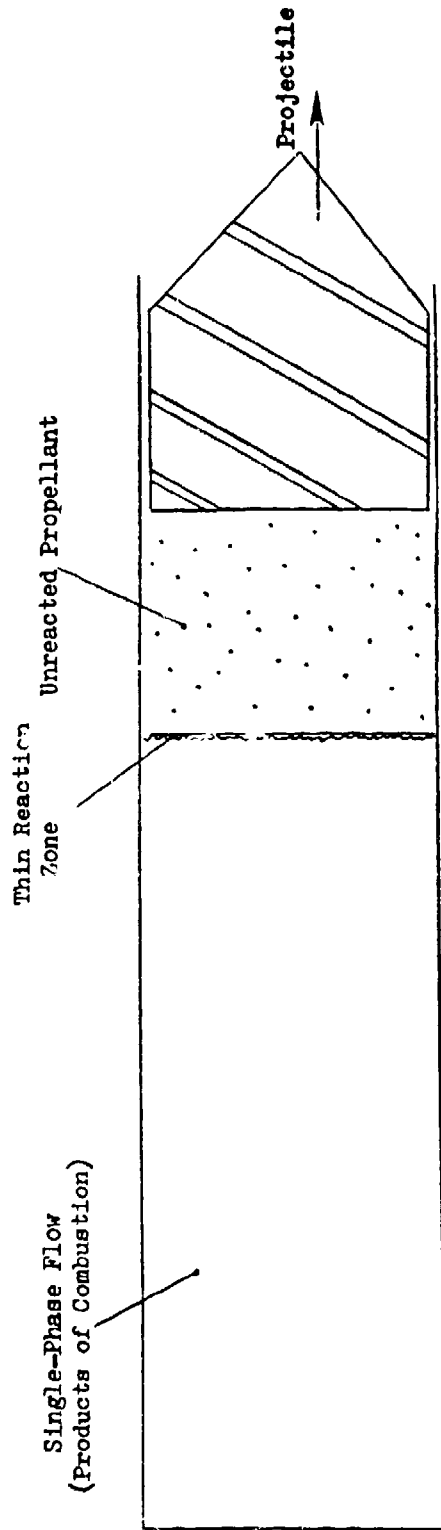
Figure 3.2 Structure of Flow for End-Burning Traveling Charge

Projectile

Thin Reaction Zone

Unreacted Propellant

Single-Phase Flow (Products of Combustion)

Pressure Drop Across Reaction Zone

Wave Front due to TC-Ignition

Axial Position

Pressure

25

combustion.[15] The booster was treated as a homogeneous mixture and computations of the pressure gradient were not expected to be reliable as the mass of the booster was increased to become comparable to that of the traveling charge. Accordingly, the NOVATC Code was developed[3] to provide a fully two-phase treatment of the booster propellant and its products of combustion. The ideal representation of the traveling charge combustion zone as a discontinuity was nevertheless retained in NOVATC.

Figure 3.3 illustrates the problem of interest here. We consider a hybrid charge consisting of a conventional booster increment and a traveling charge increment. Our approach is applicable to all values of the masses of each of the increments relative to the projectile mass. The combustion model for the traveling charge is extended relative to that of NOVATC. We still assume the existence of a thin reaction layer at the base of the traveling charge. However, this reaction zone yields a mixture of final products of combustion and intermediate products. The intermediate products react at a finite rate with the result that the traveling charge flame thickness also becomes finite. By varying the reaction rate we may vary the thickness of the the reaction zone. When short, the zone should approximate the behavior of the ideal traveling charger of Figure 3.2. When sufficiently extended, the zone should cause the release of energy by the intermediate products to yield a pressure distribution similar to that of a conventional charge. Assuming that we have identified an ideal traveling charge which is ballistically superior to a conventional equivalent subject to the assumption of a thin reaction zone, we may then allow the reaction zone to become finite and determine how the performance advantage of the traveling charge is eroded as the reaction zone increases in length.

Numerical simulations of the flow illustrated in Figure 3.3 are performed using the XNOVAKTC (XKTC) Code. The region between the breechface and the base of the traveling charge is modeled as a heterogeneous, multiphase flow which is macroscopically one-dimensional. The flow in this region is considered to consist of the solid booster propellant and a mixture of combustion products. The combustion products include those of the booster propellant and both intermediate (TC-I) and final (TC-F) products of combustion of the traveling charge. We distinguish between the velocities and temperatures of the solid propellant and those of the products of combustion. We also have as a field variable the porosity or fraction of a unit volume occupied by the mixture of combustion products. The mixture of combustion products is multiphase but homogeneous, all species having the same velocity and, except as specifically noted otherwise, the same temperature. An arbitrary scheme of chemical reactions is permitted to occur in the mixture of combustion products. The reactions may be either of the Arrhenius type or pressure dependent.

---

[15] Gough, P. S. "Extensions to BRLTC, A Code for the Digital Simulation of the Traveling Charge"
Ballistic Research Laboratory Contract Report ARBRL-CR-00511   1983

Heterogeneous Multiphase Mixture
(Granular Propellant, TC-Intermediate
and Products of Combustion)

This Reaction Zone Produces
some Final and some Intermediate
Products

Unreacted
Propellant

Projectile

Finite Reaction Zone:
Intermediates React to Final Products

Pressure Drop Across Thin
Reaction Zone

Pressure

Pressure Drop
Across Finite
Reaction Zone

Wave Front due to
TC-Ignition

Lagrange
Gradient

Pressure

Axial Position
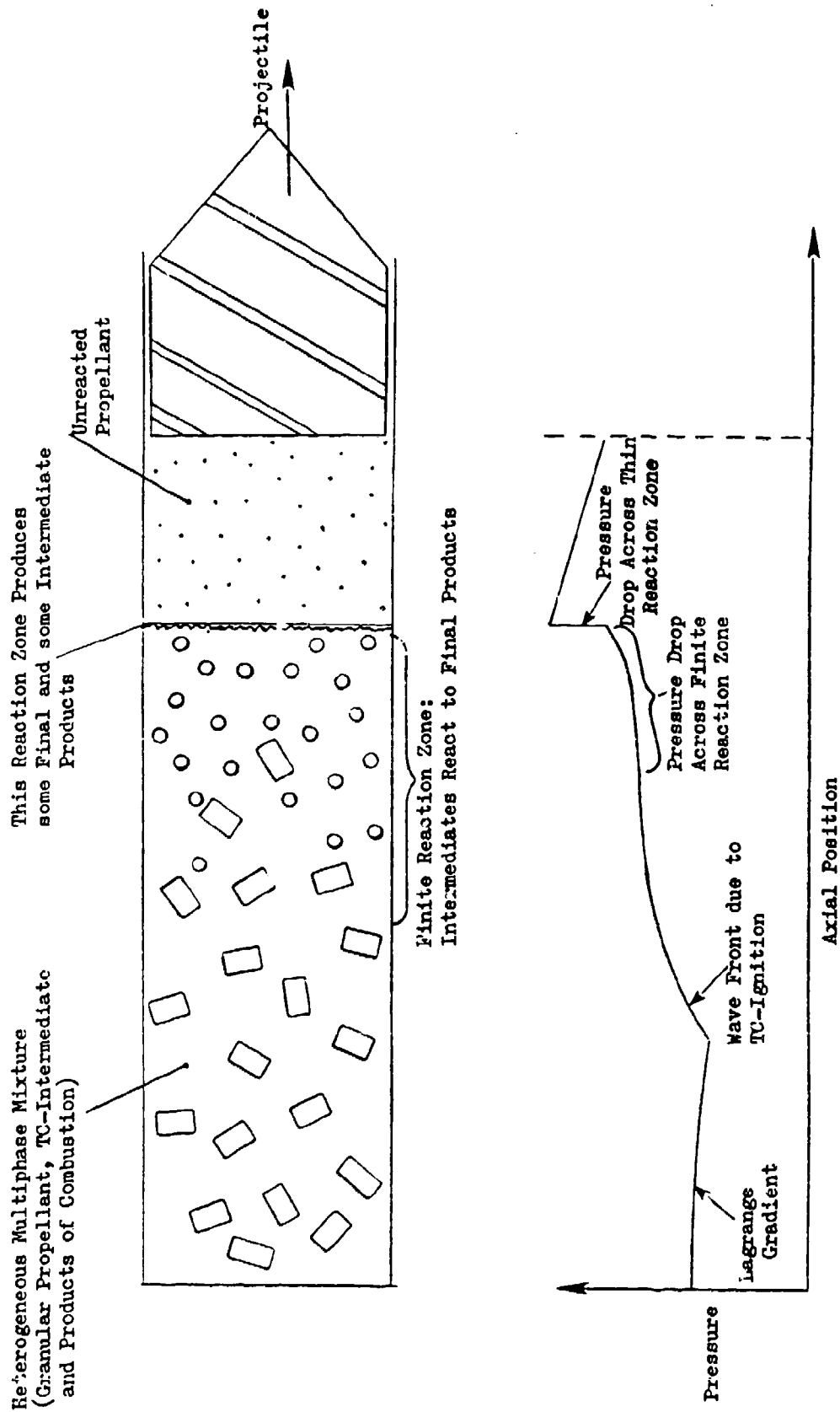
Figure 3.3   Structure of Flow for Hybrid Charge and Finite Reaction Zone
For Traveling Charge Products of Combustion

27

The balance equations are partial differential equations and have a partially hyperbolic structure. They are integrated using a two-step finite difference scheme of the MacCormack type[16] supplemented by characteristic forms at the boundaries. The chemical reaction rate equations are integrated using a simple predictor/corrector scheme which is adequate provided that the rates are comparable to the hydrodynamic time scales.

The traveling charge may be modeled either as rigid or as a one-dimensional elastic continuum. Integration in the latter case is also by the MacCormack scheme. The boundary conditions at the base of the ignited traveling charge consist of finite balances of mass, momentum and energy together with a burn rate law. Prior to ignition the boundary conditions are simple statements of contact. The projectile is taken to move as a rigid body opposed by friction due to the tube wall and the pressure in the compressed air in front of the projectile.

It may be seen that with suitable data to characterize the regression rate and the ratio TC-F:TC-I the model can be made to simulate the first step of the process described by White et al.[10] A suitable reaction rate model then permits the simulation of the second step, provided that deconsolidation is not a dominant mechanism. Such data are not presently available and it is not an objective of the present study to attempt such a direct simulation. When more precise simulation is required it will probably be appropriate to model the traveling charge increment according to the two-phase analysis presently used for the booster. This would allow a more natural treatment of the porous burning phase and the subsequent deconsolidation. However, the increased fidelity of representation would require considerably greater computer resources and the solution would involve a great deal of numerical stiffness which might well require algorithm revisions.

The major limiting assumption in the present study is that of the homogeneity of the mixture of combustion products. If the TC-I species consists of particles, they are required to be sufficiently small that their mechanical relaxation times are negligible by comparison with the hydrodynamic time scales. As is discussed by Wallis,[17] the characteristic time for the equilibration of the velocity of small spherical particles, in a gas stream is given by

$$\tau = \frac{d^2 \rho_s}{18\mu_g} \tag{3.1}$$

---

[16] MacCormack, R. W.
"The Effect of Viscosity in Hypervelocity Impact Cratering"
AIAA Paper 69-354   1969

[17] Wallis, G. B.
"One-Dimensional Two-Phase Flow" McGraw Hill New York   1969

where d is the particle diameter, ρ_s is the particle density and μ_g is the viscosity of the gas. We may estimate the gas viscosity at 1000C as 7.4×10^{-4} gm/cm-sec.[1] The value of ρ_s will be approximately 1.6 gm/cm^3. Thus we have $\tau \sim 1.2 \times 10^2 d^2$ sec and since a characteristic hydrodynamic time scale is 1 msec, it follows that d must be less than 30 microns for the assumption of mechanical equilibration to be satisfied. We note that the thermal relaxation time is expected to be of the same order as the mechanical relaxation time.

When we discuss the numerical solutions in Section 3.3 we will consider TC-I particle diameters considerably larger than 30μ. Failure to consider particle slip is not considered to be a serious omission in the context of the present study. The general relationship between reaction zone thickness and ballistic performance is not expected to be influenced strongly by the assumption of homogeneity. The assumption of homogeneity may be of greater concern if attempts are made to simulate more directly the behavior reported by White et al.[10] Apart from the previously mentioned possibility of representing the traveling charge as a two-phase region by means of XKTC, we note that research is in progress at BRL[18] and in France[19] to model the combustion of the traveling charge on a more fully non-equilibrium basis.

3.1 Governing Equations

We confine our discussion to a statement of the balance equations, the equation of state of the mixture of combustion products, the reaction rate law used in the present study, and the boundary conditions at the base of the traveling charge. Reference will be made to previous reports for further discussion, particularly in respect to the constitutive laws. Our main interest here is to show the difference between the non-equilibrium treatment of the heterogeneous mixture consisting of the solid propellant and its products of combustion and the equilibrium treatment of the combustion products which are viewed as a homogeneous multiphase mixture.

---

[18] Kooker, D. E. and Anderson, R. D.
"Modeling of Hivelite Solid Propellant Combustion"
Ballistic Research Laboratory Technical Report BRL-TC-2649   1985

[19] Briand, R., Deivaux, M. and Nicolas, M.
"Theoretical Study of Interior Ballistics of Guns with Traveling Charge"
Report communicated by W. Oberle   1986

3.1.1 Balance Equations for the Mixture of Combustion Products

These balance equations were developed in the previous report.[2] We reproduce them in full here even though they include certain terms which are not used in the present study. We emphasize, however, that the full equations stated here are completely linked to the traveling charge boundary conditions.

The mixture of combustion products is assumed to be homogeneous. All species are assumed to have the same velocity. In the previous report[2] we also assumed all species to have the same temperature. As we discuss in Section 3.1.3 we extend this in the present work to allow the species to be partitioned into two classes, one which is thermally equilibrated and the other which is thermally isolated. This extension was thought to be appropriate for the treatment of a mixture which contains burning particles.

As in Reference 2 we assume that the flow is quasi-one-dimensional and we recognize the possible presence of reactive sidewalls attached to the tube or to the centerline. Combustion of the sidewalls causes variations in flow area and results in mass addition to the mixture of combustion products. It is assumed, however, that there is no projectile afterbody intrusion to be considered simultaneously with the traveling charge boundary condition.

We assume that we have a total of N chemical species which may be either gas- or condensed- phases. A total of K chemical reactions takes place in the mixture of combustion products. A total of J types of propellant are present in a given cross-section of the flow.

We take A to be the area of the cross-section. We assume A is defined by the inner surface of the reactive layer on the tube wall and the outer surface of the reactive layer on the centerline and that A excludes the region occupied by the unburned igniter. The mass balance for the mixture may be written as

$$\frac{\partial}{\partial t}\, \varepsilon \rho A + \frac{\partial}{\partial z}\, \varepsilon \rho A u = \varphi + \dot{m}_{s_e} + \dot{m}_{s_i} + \sum_{j=1}^{J} \dot{m}_j - \sum_{i=1}^{N} \dot{w}_i \qquad (3.1.1)$$

30

where ε is the porosity; ρ, the density; u, the velocity; t, time; z, axial distance; φ, rate of addition of igniter products per unit volume; $\dot{m}_{s_e}$ and $\dot{m}_{s_i}$, rate of addition per unit volume of outer and inner sidewall products respectively; $\dot{m}_j$, rate of addition per unit volume of type j propellant products; and $\dot{w}_i$ is the rate of deposition of species i on the surface of the solid propellant. We note that when the time dependence of A is due solely to the combustion of the igniter we have $\partial A/\partial t = \varphi A/\rho_{IG}$, where ρ_{IG} is the density of the unburned igniter.

The momentum equation may be written as

$$\varepsilon\rho\,\frac{Du}{Dt} + \varepsilon g_0\,\frac{\partial p}{\partial z} = -f_s - \left[\varphi + \dot{m}_{s_e} + \dot{m}_{s_i}\right]u + \left[u_p - u\right]\sum_{j=1}^{J}\dot{m}_j \qquad (3.1.2)$$

where D/Dt is the convective derivative along the mixture streamline; g_0, a constant to reconcile units; f_s, the interphase drag; and u_p, the velocity of the solid propellant. The energy balance may be written in the following form:

$$\varepsilon\rho \frac{De}{Dt} - \frac{\varepsilon p}{\rho}\frac{D\rho}{Dt} = (u - u_p)\frac{\dot{f}_s}{g_0} - q_w - \sum_{j=1}^{J} q_{s_j}$$

$$+ \psi \left[e_{IG} - e + p\left[\frac{1}{\rho_{IG}} - \frac{1}{\rho}\right] + \frac{u^2}{2g_0} \right]$$

$$+ \dot{m}_{s_e} \left[e_{s_e} - e + p\left[\frac{1}{\rho_{s_e}} - \frac{1}{\rho}\right] + \frac{u^2}{2g_0} \right]$$

$$+ \dot{m}_{s_i} \left[e_{s_i} - e + p\left[\frac{1}{\rho_{s_i}} - \frac{1}{\rho}\right] + \frac{u^2}{2g_0} \right]$$

$$+ \sum_{j=1}^{J} \dot{m}_j \left[e_{p_j} - e + p\left[\frac{1}{\rho_{IG}} - \frac{1}{\rho}\right] + \frac{(u - u_p)^2}{2g_0} \right]$$

$$- \sum_{i=1}^{N} \dot{w}_i \left[c_{v_i}T - e + p\left[\frac{1}{\rho_{c_i}} - \frac{1}{\rho}\right] \right] + \sum_{k=1}^{K} Q_k \dot{r}_k \qquad .$$

$$(3.1.3)$$

Here we have e, the thermal part of the internal energy; q_w, heat loss to the tube wall; q_{s_j}, heat loss to propellant type j; e_{IG}, the chemical energy of the igniter; e_{s_e} and e_{s_i}, the chemical energies of the outer and inner

sidewall products; c_{v_i} and ρ_{c_i}, the constant volume heat capacity and density of condensed-phase species i; Q_k, the heat release per unit mass of reaction k; and $\dot{r}_k$ is the rate of reaction k. We note that the presence of the apparent heating term $Q_k \dot{r}_k$ is due to the convention adopted here of regarding e as excluding the chemical bonding energy.

Finally, we have the governing equation for each of the i species which constitute the mixture of combustion products

$$
\varepsilon \rho \frac{DY_i}{Dt} = \varphi \left[Y_{IG_i} - Y_i \right] + \dot{m}_{s_e} \left[Y_{s_{e_i}} - Y_i \right] + \dot{m}_{s_i} \left[Y_{s_{i_i}} - Y_i \right]
$$

$$
+ \sum_{j=1}^{J} \left[Y_{ij,o} - Y_1 \right] \dot{m}_j - \dot{r}_i + Y_i \sum_{n=1}^{N} \dot{w}_n + \sum_{k=1}^{K} \dot{r}_{ik}
$$

$$\tag{3.1.4}$$

where Y_i is the mass fraction of species i; Y_{IG_i}, $Y_{s_{e_i}}$, $Y_{s_{i_i}}$ are the mass fractions of species i in the products of combustion of the igniter, the outer sidewall and the inner sidewall respectively; $Y_{ij,o}$ is the mass fraction of species i produced by the near field (fizz) reaction of propellant j; and $\dot{r}_{ik}$ is the rate of production of species i by reaction k.

For computational purposes it is convenient to eliminate the derivative of e from Equation (3.1.3). Let ξ_j' represent the right hand side of Equation (3.1.3) and let ξ_{7_i} represent the right hand side of Equation (3.1.4) for the i-th species. Then if c is the the isentropic sound speed at constant composition it follows that the energy equation may be restated as

$$
\frac{Dp}{Dt} - \frac{c^2}{g_o} \frac{D\rho}{Dt} = \xi_{,}
$$

$$\tag{3.1.5}$$

where
$$\xi_s = \cfrac{1}{\varepsilon \rho \left[\dfrac{\partial e}{\partial p}\right]_{\rho, Y_i}} \left[\xi_s' - \sum_{i=1}^{N} \left[\dfrac{\partial e}{\partial Y_i}\right]_{p, \rho} \xi_{7_i}\right] \qquad (3.1.6)$$

We note that certain of the terms in Equations (3.1.1) – (3.1.4) will not be exercised in the present study. We will have $\varphi = \dot{m}_{s_e} = \dot{m}_{s_i} = \dot{w}_i = 0$.

3.1.2 Balance Equations for the Solid Propellant

The velocity and temperature of the solid booster propellant are distinguished from those of the mixture of combustion products. We have the balances of mass and momentum for the solid propellant in the following forms:

$$\frac{\partial}{\partial t}(1 - \varepsilon)\rho_p A + \frac{\partial}{\partial z}(1 - \varepsilon)\rho_p A u_p = -\sum_{j=1}^{J} \dot{m}_j \qquad , \qquad (3.1.7)$$

$$(1 - \varepsilon)\rho_p \frac{Du_p}{Dt_p} + (1 - \varepsilon)g_o \frac{\partial p}{\partial z} + g_o \frac{\partial \sigma}{\partial z} = f_s \qquad , \qquad (3.1.8)$$

where ρ_p is the density of the propellant, u_p is the velocity, σ is the intergranular stress and D/Dt_p is the convective derivative along the solid propellant streamline.

Since the solid propellant is assumed to be incompressible we do not state an energy balance. The thermal property of interest is the surface temperature which is initially deduced from the interphase heat transfer and a solution of the heat conduction equation applied to the interior of the solid propellant. When the surface temperature satisfies an ignition criterion, the heat transfer condition is replaced by a steady-state combustion law.

3.1.3 Constitutive Laws

The constitutive laws required for closure include the mixture equation of state, the intergranular stress law, the interphase drag and heat transfer correlations, the wall heat loss correlation, the ignition criterion, the booster burn rate law and the chemical reaction rate laws. Here we discuss only the mixture equation of state and the reaction rate laws as these incorporate some modifications. Reference may be made to earlier work for a discussion of the other constitutive laws.[1,2,6,20]

We have characterized the mixture in terms of density, ρ, pressure, p, internal energy, e and species mass fractions $Y_i, i = 1,\ldots\ldots,N$. We also introduce the temperature T and we assume that the mixture obeys an effective covolume equation of state

$$p(1 - b\rho) = \frac{\rho R_u T}{M_w} \tag{3.1.9}$$

where b is the effective covolume, R_u is the universal gas constant and M_w is the effective molecular weight of the mixture. Moreover, since e is understood to exclude the energy of chemical bonding we have the caloric equation of state

$$e = c_v T \tag{3.1.10}$$

where c_v is the effective specific heat at constant volume for the mixture.

We assume for the moment that thermal equilibrium prevails among the species so that all have the same temperature T. Then the values of b and M_w follow from a consideration of the covolume equation of state for the gas-phase components of the mixture. Consider a unit volume of the mixture.

---

[20] Gough, P. S. "Extensions to NOVA Flamespread Modeling Capacity" Final Report for Task I, Contract N00174-80-C-0316, PGA-TR-81-2 1981

The condensed phases occupy a fraction of the volume equal to

$$\sum_{i=n_g+1}^{N} \frac{\rho Y_i}{\rho_{c_i}}$$ where we assume species $i = n_g + 1, \ldots, N$ to be condensed

phases and ρ_{c_i} is the density of condensed-phase species i. Within the unit volume are $\rho Y_i / M_{w_i}$ moles of gas-phase species i, $i = 1, \ldots, n_g$ where M_{w_i} is the molecular weight of species i. The gas-phase molecules occupy a

volume $\sum_{i=1}^{n_g} \rho Y_i b_i$ where b_i is the covolume of species i. The mixture

consisting of the gas-phases alone evidently satisfies the covolume equation of state

$$p \left[1 - \sum_{i=n_g+1}^{N} \frac{\rho Y_i}{\rho_{c_i}} - \sum_{i=1}^{n_g} \rho Y_i b_i \right] = R_u T \sum_{i=1}^{n_g} \frac{\rho Y_i}{M_{w_i}} \qquad . \qquad (3.1.11)$$

Comparing (3.1.11) with (3.1.9) and (3.1.10) we see that

$$\frac{1}{M_w} = \sum_{i=1}^{n_g} \frac{Y_i}{M_{w_i}} \qquad , \qquad (3.1.12)$$

$$b = \sum_{i=1}^{n_g} Y_i b_i + \sum_{i=n_g+1}^{N} \frac{Y_i}{\rho_{c_i}} \qquad . \qquad (3.1.13)$$

36

With all species thermally equilibrated it is clear that the specific heats obey

$$c_v = \sum_{i=1}^{N} Y_i c_{v_i} \qquad , \tag{3.1.14}$$

$$c_p = \sum_{i=1}^{N} Y_i c_{p_i} \qquad , \tag{3.1.15}$$

where c_p is the specific heat at constant volume. We also have γ, the ratio of specific heats

$$\gamma = c_p / c_v \qquad . \tag{3.1.16}$$

We also recall that for the covolume equation of state

$$c_p - c_v = \frac{R_u}{M_w}$$

so that from (3.1.9), (3.1.10) and (3.1.16) we have

$$e = \frac{p}{(\gamma - 1)\rho} [1 - b\rho] \qquad . \tag{3.1.17}$$

We emphasize the importance of γ in respect to the thermal response of the mixture. Let heat ΔQ be added to the mixture at constant volume and negligible initial pressure. Then, neglecting the covolume, we have $p = (\gamma - 1)\rho\Delta Q$. The increase in pressure is proportional to $\gamma - 1$. For gas-phase species we will have typically $c_{p_i}/c_{v_i} \sim 1.25$. However, for condensed-phase species we will have $c_{p_i}/c_{v_i} \sim 1$. If the mixture consists of equal mass fractions of a gas and a solid then we will have $\gamma \sim 1.125$ and

the pressure increase due to ΔQ will be seen to be one half the increase that would occur if the mixture consisted only of a gas. This is the intuitively expected result, but it is important to see that it is conveyed through the dependence of γ on the composition of the mixture.

We have assumed thus far that all species have the same temperature. Now suppose that certain condensed species are thermally isolated as would be the case for large particles or for small particles surrounded by a flame zone. Let T be the temperature of the thermally equilibrated species. Then it is easy to see that (3.1.12) and (3.1.13) still apply since T is the temperature of the gases. Moreover, (3.1.16) and 3.1.17) also apply but it is necessary to replace (3.1.14) and (3.1.15) with

$$c_v = \sum_{i=1}^{N} E_i Y_i c_{v_i} \quad , \tag{3.1.18}$$

$$c_p = \sum_{i=1}^{N} E_i Y_i c_{p_i} \quad , \tag{3.1.19}$$

where $E_i = 1$ if species i is thermally equilibrated and $E_i = 0$ if species i is insulated. We emphasize that this simple modification is only appropriate when the insulated species are condensed-phases. A two-temperature gas mixture is not considered here.

The second constitutive law of interest here is that for the rate of chemical reaction $\dot{r}_{ik}$ which appears in Equation (3.1.4). We have previously assumed $\dot{r}_{ik}$ to be given by an Arrhenius law.[6] Here we wish to model the case in which reaction k represents the combustion of condensed species i by normal surface regression. Thus $\dot{r}_{ik}$ is the negative value of the rate of decomposition of species i per unit volume.

Let species i consist of an aggregate of droplets or particles which are locally identical. Let V_{p_i} and S_{p_i} be the volume and surface area of one particle. Then the number of particles per unit volume is given by

$$n_{p_i} = \frac{\varepsilon \rho Y_i}{\rho_{c_i} V_{p_i}} \quad . \tag{3.1.20}$$

38

If $\dot{d}_i$ is the rate of surface regression it follows that

$$\dot{r}_{ik} = -\rho_{c_i} S_{p_i} n_{p_i} \dot{d}_i$$

which, in view of (3.1.20) implies

$$\dot{r}_{ik} = -\frac{\varepsilon \rho Y_i \dot{d}_i}{D_{p_i}/6} \quad , \tag{3.1.21}$$

where we have introduced $D_{p_i} = 6V_{p_i}/S_{p_i}$ as the effective diameter of species i. We may assume that $\dot{d}_i$ is given in the usual form, having an exponential dependence on pressure.

In the present study we characterize the combustion of an aggregate of particles in terms of a characteristic diameter D_{p_i} and the burn rate $\dot{d} = Bp^n$. However, we do not follow the changes in particle diameter as combustion proceeds. This is not difficult to do but it was not thought to be worth the additional computational burden in the present context. However, we note that when D_{p_i} is allowed to vary, we expect that Y_i and D_{p_i} will tend to zero together, maintaining a finite value of $\dot{r}_{ik}$ and assuring a clean burn out of species i. If the value of Dp is kept constant, as is done here, $\dot{r}_{ik}$ tends asymptotically to zero with Y_i and the particles never quite burn out completely.

Accordingly, we use the following law to describe the pressure dependent rate of reaction of species i

$$\dot{r}_{ik} = -\frac{\varepsilon \rho B_i p^{n_i}}{D_{p_i}/6} \tag{3.1.22}$$

where B_i is the burn rate pre-exponent and n_i is the exponent. We note, in comparing (3.1.22) with (3.1.21) that we have simply dropped the factor of Y_i. When we characterize the rate of reaction by the input datum D_{p_i} we may interpret $\bar{D}_{p_i} = D_{p_i} Y_i$ as the initial particle diameter.

3.1.4 Traveling Charge Balance Equations

In order to distinguish them from the corresponding quantities for the booster charge, we denote the traveling charge solid-phase state variables by the subscript tc. Thus we have ρ_{tc}, u_{tc} and σ_{tc} which denote the density, velocity and pressure in the traveling charge. We have the bal•nces of mass and momentum

$$\frac{\partial \rho_{tc}}{\partial t} + \frac{\partial}{\partial z} \rho_{tc} u_{tc} = 0 \tag{3.1.23}$$

$$\rho_{tc} \frac{\partial u_{tc}}{\partial t} + \rho_{tc} u_{tc} \frac{\partial u_{tc}}{\partial z} + g_o \frac{\partial \sigma_{tc}}{\partial z} = f_w \tag{3.1.24}$$

where f_w is the frictional force exerted on the traveling charge by the wall of the tube. It is implicitly assumed that the traveling charge moves through a constant area section of the tube.

3.1.5 Boundary Conditions at the Base of the Traveling Charge

When the traveling charge has not ignited, the physical boundary condition at its base expresses the contact of the mixture of combustion products and the non-penetration of the solid propellant. Ignition of the traveling charge is taken to occur after a predetermined delay. Subsequently, the physical boundary conditions consist of the finite balances of mass, momentum and energy at the regression front and either one or two data to determine the regression rate. One datum is required to determine the regression rate if the products are subsonic relative to the front and two data are required if the products are sonic relative to the front. The condition of supersonic products — the strong deflagration wave — is not admitted.

The finite balances of mass, momentum and energy may be stated as

$$\rho A (u - u_s) = \rho_{tc} A_{tc} (u_{tc} - u_s) \qquad , \qquad (3.1.25)$$

$$A p + \frac{A \rho}{g_0} (u - u_s)^2 = A \sigma_{tc} + \frac{\rho_{tc} A_{tc}}{g_0} (u_{tc} - u_s)^2 \qquad , \qquad (3.1.26)$$

$$e + \frac{p}{\rho} + \frac{1}{2 g_0} (u - u_s)^2 = e_{tc} + \frac{\sigma_{tc}}{\rho_{tc}} + \frac{1}{2 g_0} (u_{tc} - u_s)^2 \qquad . \qquad (3.1.27)$$

Here we have u_s as the velocity of the regression front relative to the gun tube so that

$$u_s = u_{tc} + r_{tc} \qquad\qquad (3.1.28)$$

where r_{tc} is the regression rate relative to the unburned traveling charge. We have used the subscript tc to denote properties of the traveling charge and to distinguish them from the booster solid propellant. We note that we have introduced A_{tc}, the cross-sectional area of the traveling charge increment, which is not necessarily assumed equal to that of the tube, in order to account for the possible presence of an external liner used to support the traveling charge.

It remains to discuss the conditions which specify r_{tc}. We assume that r_{tc} obeys any of the following laws:

(a) Measured burn rate—r_{tc} is given as a function of the pressure on either side of the flame in either exponential or tabular form.

(b) Ideal burn rate—r_{tc} is chosen so as to yield a predetermined value of pressure on either side of the flame, or to yield a predetermined acceleration of the projectile, or to yield a predetermined value of the Mach number of the combustion products relative to the flame.

(c) Composite burn rate—r_{tc} may be required to satisfy a measured or ideal burn rate law subject to the constraint that the Mach number of the products be equal to one.

It is always assumed that the Mach number of the products of combustion of the traveling charge relative to the flame is less than or equal to one. If the Mach number is less than one it is assumed that the burning process is acoustically coupled to the state of mixture of combustion products and use is made of the appropriate characteristic constraint. If the Mach number is one, acoustic coupling is not assumed and the characteristic constraint is replaced by the condition of choking. In the latter case the traveling charge burns as a nozzleless rocket.

Ignition of the first increment is assumed to occur at a prespecified point in time. Following ignition, the full burn rate as described by the appropriate law is assumed to be reduced by a coefficient which increases from zero to one over a second user-selectable interval. When the flame passes from one increment to the next, a delay can be specified for the ignition of the new increment. The burn rate achieves the value given by the appropriate law for the new increment after an additional delay during which the actual value varies linearly in time from the final value for the previous increment to the full value for the new increment.

A strong rarefaction can be formed when the traveling charge burns out. As in BRLTC,[9] we use a simple wave solution for five steps after burnout to allow the state variables in the mixture of combustion products to become reasonably smooth.

3.2 Numerical Results

The numerical results presented here satisfy two different objectives. First, we seek to determine the effect of a finite length reaction zone on the interior ballistics of a traveling charge. A second objective, which had to be satisfied prior to the first, was to complete the development of XKTC, including in particular, the traveling charge option and its linkage to the chemistry option. To satisfy these objectives we started with a BRLTC data base which was considered to exhibit a reasonable level of ballistic benefit from a traveling charge increment. This data base was then made compatible with NOVATC and necessary algorithm revisions were identified and incorporated to achieve a satisfactory numerical solution. This solution then served as a benchmark against which the operability of XKTC could be verifed, at least for the ideal case of an infinitesimal traveling charge combustion zone. Finally, the chemistry option was invoked to generate a finite flame zone in the XKTC solutions and the effect of the flame thickness on ballistic performance was appraised.

42

Table 3.1 XKTC Input Data for Nominal Simulation of Traveling Charge with Finite Flame Thickness

CONTROL DATA

LOGICAL VARIABLES:

PRINT	T	DISK WRITE	F	DISK READ	F
I.B. TABLE	T	FLAME TABLE	F	PRESSURE TABLE(S)	F

EROSIVE EFFECT 0 WALL TEMPERATURE CALCULATION	0
BED PRECOMPRESSED	0
HEAT LOSS CALCULATION	1
BORE RESISTANCE FUNCTION	2
TRAVELING CHARGE OPTION (0=NO, 1=YES)	1
CONSERVATIVE SCHEME TO INTEGRATE SOLID-PHASE CONTINUITY EQUATION (0=NO,OLD; 1=YES,NEW)	0
KINETICS MODE (0=NONE; 1=GAS-PHASE ONLY; 2=BOTH PHASES)	1
TANK GUN OPTION (0=NO, 1=YES)	0
INPUT ECHO OPTION	0

INTEGRATION PARAMETERS

NUMBER OF STATIONS AT WHICH DATA ARE STORED	30
NUMBER OF STEPS BEFORE LOGOUT	5000
TIME STEP FOR DISK START	0
NUMBER OF STEPS FOR TERMINATION	5000
TIME INTERVAL BEFORE LOGOUT(SEC)	$.100 \times 10^{-3}$
TIME FOR TERMINATION (SEC)	10.00
PROJECTILE TRAVEL FOR TERMINATION (IN)	157.48 (400 cm)
MAXIMUM TIME STEP (SEC)	$.100 \times 10^{-2}$
STABILITY SAFETY FACTOR	2.00
SOURCE STABILITY FACTOR	.200
SPATIAL RESOLUTION FACTOR	.010
TIME INTERVAL FOR I.B. TABLE STORAGE(SEC)	$.100 \times 10^{-3}$
TIME INTERVAL FOR PRESSURE TABLE STORAGE (SEC)	$.100 \times 10^{-3}$

43

FILE COUNTERS

NUMBER OF STATIONS TO SPECIFY TUBE RADIUS	2
NUMBER OF TIMES TO SPECIFY PRIMER DISCHARGE	0
NUMBER OF POSITIONS TO SPECIFY PRIMER DISCHARGE	0
NUMBER OF ENTRIES IN BORE RESISTANCE TABLE	0
NUMBER OF ENTRIES IN WALL TEMPERATURE TABLE	0
NUMBER OF ENTRIES IN FORWARD FILLER ELEMENT TABLE	0
NUMBER OF TYPES OF PROPELLANTS	1
NUMBER OF BURN RATE DATA SETS	1
NUMBER OF ENTRIES IN VOID FRACTION TABLE(S)	0 0 0
NUMBER OF ENTRIES IN PRESSURE HISTORY TABLES	0
NUMBER OF ENTRIES IN REAR FILLER ELEMENT TABLE	0

GENERAL PROPERTIES OF INITIAL AMBIENT GAS

INITIAL TEMPERATURE (R)	540.0	(300K)
INITIAL PRESSURE (PSI)	14.7	(0.101 MPa)
MOLECULAR WEIGHT (LBM/LBMOL)	28.960	
RATIO OF SPECIFIC HEATS	1.400	

GENERAL PROPERTIES OF PROPELLANT BED

INITIAL TEMPERATURE (R)	540.0	(300K)

PROPERTIES OF PROPELLANT 1

PROPELLANT TYPE	BOOSTER
MASS OF PROPELLANT (LBM)	.5327 (242 gm)
DENSITY OF PROPELLANT (LBM/IN^3)	.0600 (1.66 gm/cm^3)
FORM FUNCTION INDICATOR	7
OUTSIDE DIAMETER (IN)	.2415 (0.613 cm)
INSIDE DIAMETER (IN)	.0281 (0.071 cm)
LENGTH (IN)	.5795 (1.472 cm)
NUMBER OF PERFORATIONS	7.
SLOT WIDTH (NFORM=11) OR SCROLL DIA. (NFORM=13) (IN)	0.0000
PROPELLANT STACKED (0=NO, 1=YES)	0
ATTACHMENT CONDITION (0=FREE, 1=ATTACHED TO TUBE, 2=ATTACHED TO PROJECTILE)	0
BOND STRENGTH (LBF) (N.B. ZERO DEFAULTS TO INFINITY)	0.

RHEOLOGICAL PROPERTIES

SPEED OF COMPRESSION WAVE IN SETTLED BED (IN/SEC)	17400 (44196 cm/sec)
SETTLING POROSITY	1.0
SPEED OF EXPANSION WAVE (IN/SEC)	50000. (127000 cm/sec)
POISSON RATIO (-)	0.0

SOLID PHASE THERMOCHEMISTRY

MAXIMUM PRESSURE FOR BURN RATE DATA (LBF/IN^2)	100000. (689.5 MPa)
BURNING RATE PRE-EXPONENTIAL FACTOR(IN/SEC-PSI^{BN})	.1790 X 10^{-3} (0.3368 cm/sec-MPa^{BN})
BURNING RATE EXPONENT	.8650
BURNING RATE CONSTANT (IN/SEC)	0.0000
IGNITION TEMPERATURE (R)	539.0 (299.4K)
THERMAL CONDUCTIVITY (LBF/SEC-R)	.2770 X 10^{-2} (2.22 X 10^{-3} J/cm-sec-K)
THERMAL DIFFUSIVITY (IN^2/SEC)	.1345 X 10^{-3} (8.677 X 10^{-4} cm^2/sec)
EMISSIVITY FACTOR	.600

GAS PHASE THERMOCHEMISTRY

CHEMICAL ENERGY RELEASED IN BURNING(LBF-IN/LBM)   .17280 X 10^8 (4304 J/gm)

MOLECULAR WEIGHT (LBM/LBMOL)   19.4000

RATIO OF SPECIFIC HEATS   1.2500

COVOLUME   32.9000 (1.189 cm^3/gm)

LOCATION OF PACKAGE(S)

PACKAGE	LEFT BDDY (IN)	RIGHT BDDY (IN)	MASS (LBM)	INNER RADIUS (IN)	OUTER RADIUS (IN)
1	0.000	7.963 (20.22 cm)	0.533 (241.8 gm)	0.000	0.000

PARAMETERS TO SPECIFY TUBE GEOMETRY

DISTANCE(IN)	RADIUS(IN)
0.000	.787
200.000 (508 cm)	.787 (2.0 cm)

THERMAL PROPERTIES OF TUBE

THERMAL CONDUCTIVITY (LBF/SEC-R)   7.770 (0.662 J/cm-sec-K)

THERMAL DIFFUSIVITY (IN^2/SEC)   .2280 X 10^{-1} (0.147 cm^2/sec)

EMISSIVITY FACTOR   .700

INITIAL TEMPERATURE (R)   540.00 (300K)

PROJECTILE AND RIFLING DATA

INITIAL POSITION OF BASE OF PROJECTILE(IN)   0.000

MASS OF PROJECTILE (LBM)   0.000

POLAR MOMENT OF INERTIA ($LBM-IN^2$)   0.000

ANGLE OF RIFLING (DEG)   0.000

CHEMISTRY OPTION DATA

NUMBER OF SPECIES	4
NUMBER OF GAS-PHASE REACTIONS	1
NUMBER OF SOLID-PHASE REACTIONS	0

PROPERTIES OF SPECIES

NAME	PHASE	CV	CP	COVOLUME	MOL.WGT	DENSITY	TRANSFER	KTEQL
		LBF-IN/LBM-R	LBF-IN/LBM-R	IN^3/LBM	LB/LBMOL	LBM/IN^3	COEF.	
AIR	G	3824.7	4780.9	32.900	19.400	0.00000	0.	0
BOOSTER	G	3824.7	4780.9	32.900	19.400	0.00000	0.	0
TCI	S	3824.7	3824.7	0.000	0.000	.06000 (1.66 gm/cm^3)	0.	1
TCF	G	3824.7 (1.715 J/gm-K)	4780.9 (2.144 J/gm-K)	32.900 (1.189 cm^3/gm)	19.400	0.00000	0.	0

COMPOSITION OF LOCAL COMBUSTION PRODUCTS OF PROPELLANT   1

ENERGY	MASS FRACTIONS (-)			
LBF-IN/LBM	YO(1)	YO(2)	YO(3)	YO(4)
17280000. (4304 J/gm)	0.00000	1.00000	0.00000	0.00000

COMPOSITION OF LOCAL COMBUSTION PRODUCTS OF TRAVELING CHARGE

ENERGY	MASS FRACTIONS (-)			
LBF-IN/LBM	YTCO(1)	YTCO(2)	YTCO(3)	YTCO(4)
8640000. (2152 J/gm)	0.00000	0.00000	0.50000	0.50000

COMPOSITION OF COMBUSTION PRODUCTS OF IGNITER

ENERGY	MASS FRACTIONS (-)			
LBF-IN/LBM	YO(1)	YO(2)	YO(3)	YO(4)
0.	0.00000	0.00000	0.00000	0.00000

COMPOSITION OF AMBIENT GAS

```
ENERGY          MASS FRACTIONS (-)
LBF-IN/LBM      YO( 1)    ' YO( 2)     YO( 3)     YO( 4)

864727.         1.00000    0.00000    0.00000    0.00000
( 215 J/gm)
```

GAS-PHASE REACTION DATA

REACTION   1

```
REACTANT SPECIES                 3   0   0   0   PRODUCT SPECIES   4   0   0   0
STOICHIOMETRIC COEFFICIENTS (LBM) 1.  0.  0.  0.                    1.  0.  0.  0.
```

HEAT OF REACTION (LBF-IN/LBM)   17280000.   (4305 J/gm)

PARTICLE DIAMETER (IN)   0.1 (0.254 cm)

BURN RATE ADDITIVE CONSTANT (IN/SEC)   0.

BURN RATE COEFFICIENT (IN/SEC-PSI^{BN})   .17900 X 10^{-2}

BURN RATE EXPONENT (-)   .8650

T.C. CONTROL DATA

IDEAL BURN RATE LAW	2
CONTINUUM MODEL OF UNREACTED PROPELLANT	1
NUMBER OF PROPELLANTS	1
PROPELLANT WALL FRICTION PARAMETER	0
NUMBER OF ENTRIES IN PROJECTILE BORE RESISTANCE TABLE	2
INDICATOR FOR AIR RESISTANCE	1
NUMBER OF ENTRIES IN OBTURATOR FRICTION TABLE	0

INTEGRATION PARAMETERS

MAXIMUM NUMBER OF MESH POINTS   11

MINIMUM MESH SIZE (IN)   .200 (0.508 cm)

PROJ. AND TRAV. CHARGE PROPERTIES

T.C. DIAMETER (IN)	1.575	(4.0 cm)
INITIAL POSITION OF REAR FACE OF PROPELLANT (IN)	7.963	(20.22 cm)
PROJECTILE MASS (LBM)	.35270	(160 gm)
CHARGE MASS (LBM)	.542	(245.8 gm)
MAXIMUM PRESSURE IN UNREACTED PROPELLANT (PSI), IF IDEAL=2	100000.	(689.5 MPa)
MAXIMUM MACH NUMBER OF REACTION PRODUCTS	.999	
MAXIMUM ACCELERATION OF PROJECTILE (G)	0.	
RATIO OF SPECIFIC HEATS OF AIR (-)	1.4000	
PRESSURE OF AIR IN BARREL (PSI)	14.700	(0.101 MPa)
TEMPERATURE OF AIR IN BARREL (R)	540.0	(300K)
MOLECULAR WEIGHT OF AIR IN BARREL (LBM/LBMOL)	28.9600	

RESISTIVE PRESSURE DUE TO OBTURATOR

TRAVEL (IN)	RESISTIVE PRESSURE (PSI)	
0.000	800.	(5.52 MPa)
.500 (0.27 cm)	500.	(3.45 MPa)

PROPERTIES OF PROPELLANT NUMBER 1

RATIO OF SPECIFIC HEATS (-)	1.250	
COVOLUME (IN^3/LBM)	32.900	(1.189 cm^3/gm)
MOLECULAR WEIGHT (LBM/LBMOL)	19.400	
CHEMICAL ENERGY OF PROPELLANT (LBF-IN/LBM)	17280000.	(4304 J/gm)
DENSITY OF PROPELLANT (LBM/IN^3)	.0466	(1.290 gm/cm^3)
INITIAL MASS (LBM)	.5415	(160 gm)
IGNITION DELAY (MSEC)	1.800	
DELAY FOR TRANS. TO FULL BURN RATE (MSEC)	.100	
BURNING RATE ADDITIVE CONSTANT (IN/SEC)	-I	
BURNING RATE PRE-EXPONENTIAL FACTOR (IN/SEC-PSI^{BN})	-I	
BURNING RATE EXPONENT (-)	-I	
TC GRAIN LENGTH (IN)	5.966	(15.15 cm)
LENGTH BREECH TO PROJECTILE BASE (IN)	13.929	(35.38 cm)
COMPRESSION WAVE SPEED IN PROPELLANT (IN/SEC)	118110.	(300000. cm/sec)
EXPANSION WAVE SPEED IN PROPELLANT (IN/SEC)	0.	
BURN RATE FORMAT (0=EXP, 1=TABULAR)	0	
BURN RATE DEPENDENCE (0=PRES; 1=STRESS)	1	

A representative XKTC data base, including the chemistry data, is presented in Table 3.1. The problem of interest involves a total propellant mass of 488 gm and a projectile mass of 160 gm so that C/M is approximately equal to 3. The gun bore diameter is 4.0 cm and the projectile travel is 400 cm. The charge is divided into a booster component, consisting of seven-perforation granular propellant and having a mass of 242 gm, and a traveling charge component whose mass is 246 gm. The booster granulation is selected to achieve a maximum breech pressure of approximately 690 MPa which occurs at about 1.2 msec after the booster is ignited. Ignition of the traveling charge occurs at 1.8 msec when the breech pressure has fallen to approximately 250 MPa. The rate of surface regression of the traveling charge is required to yield a stress, on the unreacted side of the flame, equal to 690 MPa, provided that the Mach number of the products does not exceed 0.999. If the stress cannot be achieved without violating the Mach number constraint, the regression rate is chosen to yield a Mach number of 0.999. The solution within the traveling charge is assumed always to be acoustically coupled to that in the mixture of combustion products.

The data of Table 3.1 were developed from a BRLTC data base which we refer to as 40MTC3. Certain modifications were incorporated in order to arrive at the data of Table 3.1, apart from considerations of a chemical reaction in the mixture of combustion products. BRLTC models the booster increment as a single-phase substance and the pressure gradient responds only to the momentum of the combustion products. Accordingly, BRLTC tends to underestimate the pressure gradient when compared with the more complete two-phase analysis of NOVATC or XKTC. The NOVA data bases therefore incorporated a somewhat lower burn rate coefficient to produce the same maximum chamber pressure as BRLTC. It also became necessary in the NOVA runs to advance slightly the time of ignition of the traveling charge increment in order to assure burnout prior to muzzle exit. In Table 3.2 we compare the predictions of BRLTC, NOVATC and XKTC for the 40MTC3 data base.

Table 3.2   Code Dependence of Nominal Thin Flame TC Data Base (40MTC3)

Code	Max Press. (MPa)	Muzzle Velocity (m/sec)	$\Delta m\%$	$\Delta e\%$
BRLTC*	699	2879	0.67	0.36
NOVATC**	691	2860	-1.9	0.04
XKTC**	687	2854	-2.1	-0.95

*   Booster burn rate = $0.00185p^{0.865}$, TC ignition at 2.0 msec, maximum of 31 points for booster and TC combined.

**   Booster burn rate = $0.000179p^{0.865}$, TC ignition at 1.8 msec, 16 points for booster, maximum of 11 for TC.

Good agreement is seen between the three sets of calculations. These results serve to demonstrate the operability of XKTC for the thin flame traveling charge calculations and to confirm the data of Table 3.1 as reproducing the performance of 40MTC3 in BRLTC. We note that we have also tabulated values of the final percent mass and energy defects, $\Delta m\%$ and $\Delta e\%$, as indicators of numerical accuracy. Values of these quantities less than 1% would be desirable, but we have accepted results in this study for which the final defects were as large as 2 or 3%.

To verify that these mass and energy defects did not imply excessive mesh dependence we present solutions for three different problems obtained with 30 and 60 mesh points for the region occupied by the mixture of combustion products. The first problem, identified as the thin flame TC,

Table 3.3 Mesh Dependence of XKTC Solutions

Problem	Number of Booster Mesh Points	Max Press. (MPa)	Muzzle Vel. (m/sec)	$\Delta m\%$	$\Delta e\%$
Thin Flame TC	30	692	2875	-2.4	-1.4
	60	598	2875	-1.9	-1.3
Conventional Equivalent	30	689	2476	-1.16	-0.54
	60	696	2483	-0.38	-0.11
Finite Flame TC*	30	684	2603	-1.58	-2.22
	60	689	2589	-1.23	-1.82

* Burn rate = $0.000179p^{0.865}$, TC-I/TC-F = 50/50, Dp = 0.254 cm

is the 40MTC3 data base adapted to XKTC. The second problem, identified as the conventional equivalent, is a charge consisting entirely of granular propellant and having the same total mass as 40MTC3. The third problem, identified as the finite flame TC, corresponds precisely to the data of Table 3.1. Good mesh indifference is exhibited for all three problems and it is assumed, unless otherwise explicitly noted, that the solutions presented here have an accuracy of 1 or 2%.

The conventional equivalent data base was formed by taking the traveling charge increment to be a conventional granular increment of the same mass and chemical energy. In order to obtain a conventional loading density of approximately 60% it was necessary to move the projectile forward a distance of 5 cm. The travel was still assumed to be 400 cm so that the conventional equivalent result corresponds to a slightly longer gun than the traveling charge results. This difference is not believed to be

significant. The granulation of the conventional equivalent was varied to achieve a maximum breech pressure of approximately 690 MPa. Table 3.3 therefore shows a ballistic benefit of the traveling charge in the sense that the muzzle velocity exceeds that of the conventional equivalent by 400 m/sec at the same maximum pressure.

It should be noted that the maximum pressure for the traveling charge is achieved not only at the breech but also further downbore in the regions occupied by the traveling charge following ignition. We do not consider the extent to which the ballistic benefit is offset by the potentially increased structural burden on the tube.

The finite flame TC calculation shown in Table 3.3 assumes that the regression of the base of the traveling charge yields a mixture of final combustion products (TC-F) and intermediate products (TC-I) in the ratio TC-F/TC-I = 50/50. The intermediates are assumed to react according to Equation (3.1.22) with $D_{p_i} = 0.254$ cm. We understand this value to correspond to an initial particle diameter equal to 0.127 cm.

We note that the maximum pressure in the finite flame TC calculation is essentially identical to that in the two preceding cases. This will be true of all the calculations considered here. Accordingly, the evaluation of ballistic performance is reduced to an examination of the muzzle velocities. It is evident, in Table 3.3, that this particular finite flame TC data base exhibits considerable degradation of performance, the muzzle velocity exceeding that of the conventional equivalent by only 125 m/sec.

In order to relate the degradation of the traveling charge performance benefit to the thickness of the flame zone we introduce the characteristic reaction zone length L^* defined as

$$L^* = \frac{\int_0^L \varepsilon \rho A x Y_i^2 \, dx}{\int_0^L \varepsilon \rho A Y_i \, dx} \quad . \tag{3.2.1}$$

Here x is a coordinate originating at the base of the traveling charge and L is the distance to the breechface. We have ε, porosity; ρ, mixture density; A, cross-sectional area of the tube; and Y_i is the mass fraction of the intermediate product species TC-I.

It should be noted that we have Y_i^2 in the numerator and Y_i in the denominator. Hence L^* is a measure not only of the length of the reaction zone but also the concentration of TC-I.

It is easy to verify that if

$$Y_i = \begin{cases} Y_o & 0 \leq x \leq L_f \quad , \\ 0 & x > L_f \quad , \end{cases} \tag{3.2.2}$$

where Y_o is constant and L_f is the flame thickness, then

$$L^* = \frac{Y_o L_f}{2} \quad . \tag{3.2.3}$$

In such a case $L_f = 2L^*/Y_o$ and will be equal to $4L^*$ if $Y_o = 0.5$. The distribution (3.2.2) corresponds to a flamesheet model with TC-I being consumed very rapidly at a standoff distance L_f. If we have a distribution more appropriate to our particle burning model in the form

$$Y_i = \begin{cases} Y_o \left[1 - \frac{x}{L_f}\right] & 0 \leq x \leq L_f \quad , \\ 0 & x > L_f \quad , \end{cases} \tag{3.2.4}$$

then we see that

$$L^* = \frac{Y_o L_f}{6} \quad . \tag{3.2.5}$$

We may therefore interpret values of L^* as corresponding to an ideal flame length $L_f = 6L^*/Y_o$ if the distribution (3.2.4) applies.

Our subsequent results will introduce a non-dimensional flame length L_{ND}^* which is simply related to L^* by

$$L_{ND}^* = \frac{L^*}{D_T} \tag{3.2.6}$$

where D_T is the diameter of the bore.

Table 3.4 presents the relationship between muzzle velocity and flame thickness for a series of data bases corresponding to Table 3.1 Only the composition of the products of surface decomposition TC-F/TC-I and the particle diameter D_p are varied.

Table 3.4 Relation Between Muzzle Velocity and Flame Thickness
(TC-I Burn Rate = $0.337p^{0.865}$ cm/sec)

TC-F/TC-I	D_p cm	$L_{ND,MAX}^{*}$	Muzzle Vel. m/sec	f-TCI	Δm%	Δe%
50/50	0.127	0.40	2889	0.000	3.37	2.89
50/50	0.254	1.52	2603	0.050	-1.58	-2.22
50/50	0.381	3.36	2502	0.123	-2.17	-2.77
50/50	0.508	5.56	2461	0.188	-2.25	-2.86
75/25	0.127	0.14	2906	0.000	0.46	1.61
75/25	0.254	0.45	2793	0.007	-2.21	-1.39
75/25	0.381	0.89	2732	0.021	-2.45	-1.69
75/25	0.508	1.45	2703	0.037	-2.58	-1.86
25/75	0.127	0.79	2830	0.000	2.58	1.23
25/75	0.254	2.54	2434	0.131	1.60	-1.51
25/75	0.381	6.07	2249	0.301	-0.18	-3.38
25/75	0.508	8.42	2175	0.389	-0.91	-4.17

For each run we tabulate TC-F/TC-I, the ratio of the mass fractions of the final and intermediate TC products at the base of the traveling charge; D_p, the particle diameter; $L_{ND,MAX}^{*}$, the maximum value of L_{ND}^{*} which occurs in the solution; the muzzle velocity; f-TCI, the value of the mass of the unburned intermediates at muzzle exit divided by the initial mass of the traveling charge; and Δm%, Δe%, the final mass and energy defects.

It is evident in Table 3.4 that many of these runs involved an appreciable quantity of unburned traveling charge intermediates at muzzle exit. In order to remove the complicating influence of unburned propellant from the relation between muzzle velocity and flame length, we repeated the matrix of runs with a particle burn rate calculated to ensure complete burnout of the intermediates. These results are shown in Table 3.5.

Table 3.5 Relation Between Muzzle Velocity and Flame Thickness
(TC-I Burn Rate = 50.8 cm/sec)

TC-F/TC-I	D_p cm	$L^*_{ND,MAX}$	Muzzle Vel. m/sec	f-TCI	$\Delta m\%$	$\Delta e\%$
50/50	0.127	0.54	2832	0.000	1.10	0.12
50/50	0.254	1.27	2726	0.000	-1.68	-2.38
50/50	0.381	1.90	2659	0.000	-2.10	-2.77
50/50	0.508	2.50	2604	0.000	-2.17	-2.82
75/25	0.127	0.14	2883	0.000	-0.37	0.54
75/25	0.254	0.33	2824	0.000	-2.23	-1.41
75/25	0.381	0.48	2792	0.000	-2.47	-1.68
75/25	0.508	0.64	2766	0.000	-2.51	-1.77
25/75	0.127	1.12	2774	0.000	1.25	-0.51
25/75	0.254	2.04	2665	0.000	0.95	-2.56
25/75	0.381	2.92	2556	0.000	-0.27	-3.71
25/75	0.508	3.70	2459	0.000	-0.77	-4.23

The results of Tables 3.4 and 3.5 are presented graphically in Figure
3.4. It is evident that, for those data corresponding to complete
combustion, there is quite a good correlation between muzzle velocity and
$L^*_{ND,MAX}$. We also indicate the muzzle velocities obtained with the ideal
thin flame traveling charge and its conventional equivalent. It is further
evident from Tables 3.4 and 3.5 and from Figure 3.4 that there are solutions
with values of $L^*_{ND,MAX}$ of the order of 0.5 to 1.0 for which the degradation
of traveling charge performance benefit is quite small. Thus we conclude
that a characteristic flame length of one caliber is quite compatible with
the theoretical benefit of the traveling charge. Since Equation (3.2.4) is
a reasonable representation of the distribution of the intermediate species
and since Y_o corresponds to a value between 0.25 and 0.75 in these
calculations, we may say that a physical combustion zone thickness of five
to ten calibers appears tolerable without substantial degradation of
performance.
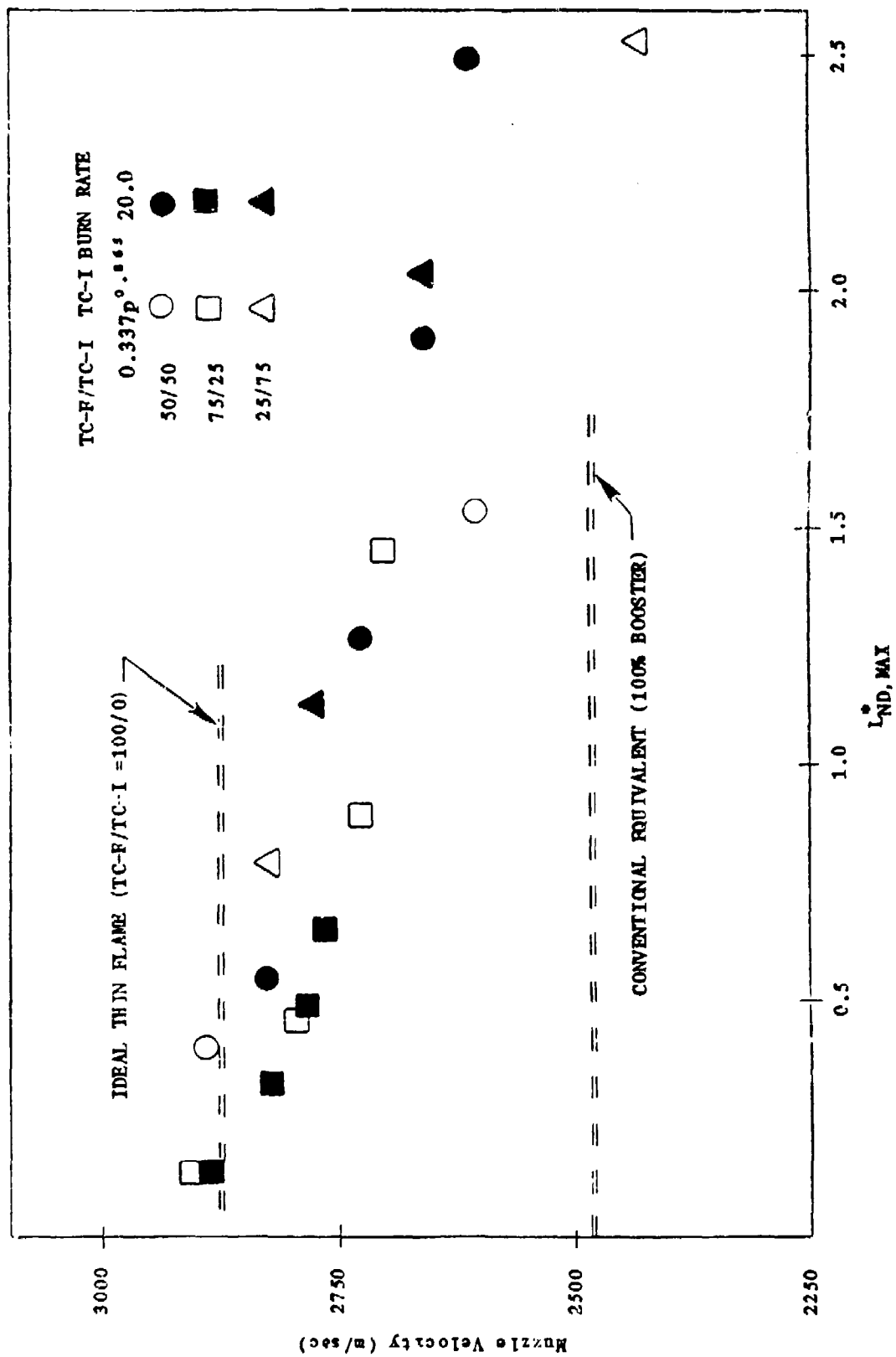
Figure 3.4   Relation Between Muzzle Velocity and Non-Dimensional TC Flame Thickness

We conclude our discussion with one other comment. In Table 3.6 we examine the effect on performance of the time of ignition of the traveling charge for the case TC-F/TC-I = 50/50, D_p = 0.508 cm in Table 3.5. The nominal delay is 1.8 msec and we consider a range from 1.4 to 2.4 msec. It is evident that for this problem there is virtually no dependence of muzzle velocity on ignition delay. Accordingly, the loss of performance due to flame thickness cannot be compensated by a change in ignition delay, at least in this case.

Table 3.6 Effect of TC-Ignition Delay on Finite Flame TC Performance
(TC-F/TC-I = 50/50, D_p = 0.508, B.R. = 50.8 cm/sec)

TC-Ignition Delay msec	Muzzle Velocity m/sec	$L^*_{ND, MAX}$	f-TCI	$\Delta m\%$	$\Delta e\%$
1.4	2575	2.28	0.000	-2.21	-3.08
1.6	2590	2.43	0.000	-2.14	-2.85
1.8	2604	2.50	0.000	-2.17	-2.82
2.0	2605	2.46	0.000	-2.23	
2.2	2607	2.39	0.009	-1.79	·.
2.4	2592	2.30	0.044	-0.87	-2.._

REFERENCES

1. Gough, P. S.
    "The NOVA Code: A User's Manual"
    Indian Head Contract Report   IHCR 80-8   1980

2. Gough, P. S.
    "XNOVAT - A Two-Phase Flow Model of Tank Gun Interior Ballistics"
    Final Report, Task Order I, Contract DAAK11-85-D-0002   1985

3. Gough, P. S.
    "A Two-Phase Model of the Interior Ballistics of Hybrid
    Solid-Propellant Traveling Charges"
    Final Report, Task I, Contract DAAK11-82-C-0154   1983

4. Gough, P. S.
    "XNOVA - An Express Version of the NOVA Code"
    Final Report   Contract N00174-82-M-8048   1983

5. Gough, P. S.
    "Modeling of Rigidized Gun Propelling Charges"
    Contract Report   ARBRL-CR-00518   1983

6. Gough, P. S.
    "Theoretical Modeling of Navy Propelling Charges"
    Final Report, Contract N00174-83-C-0241,   PGA-TR-84-1   1984

7. Corner, J.
    "Theory of the Interior Ballistics of Guns"
    New York, John Wiley and Son, Inc   1950

8. May, I. W., Raran, A. F., Baer, P. G. and Gough, P. S.
    "The Traveling Charge Effect"
    Proceedings of the 15th JANNAF Combustion Meeting   1978

9. Gough, P. S.
    "A Model of the Traveling Charge"
    Ballistic Reearch Laboratory Contract Report ARBRL-CR-00432   1980

10. White, K. J., McCoy, D. G., Doali, J. O., Aungst, W. P.,
    Bowman, R. E. and Juhasz, A. A.
    "Closed Chamber Burning Characteristics of New VHBR Formulations"
    Proceedings of the 21st JANNAF Combustion Meeting   1984

11. Langweiler, H.
    "A Proposal for Increasing the Performance of Weapons by the
    Correct Burning of Propellant"
    British Intelligence Objective Sub-committee, Group 2,
    Ft. Halstead Exploiting Center, Report 1247   undated

12. Vinti, J. P.
     "Theory of the Rapid Burning of Propellants"
     Ballistic Research Laboratory Report No. 841   1952

13. Courant, R. and Friedrichs, K. O.
     "Supersonic Flow and Shock Waves"
     Interscience, New York   1948

14. Landau, L. D. and Lifschitz, E. M.
     "Fluid Mechanics"
     Pergamon Press   1959

15. Gough, P. S.
     "Extensions to BRLTC, A Code for the Digital Simulation of the
     Traveling Charge"
     Ballistic Research Laboratory Contract Report ARBRL-CR-00511   1983

16. MacCormack, R. W.
     "The Effect of Viscosity in Hypervelocity Impact Cratering"
     AIAA Paper 69-354   1969

17. Wallis, G. B.
     "One-Dimensional Two-Phase Flow"
     McGraw-Hill New York   1969

18. Kooker, D. E. and Anderson, R. D.
     "Modeling of Hivelite Solid Propellant Combustion"
     Ballistic Research Laboratory Technical Report BRL-TR-2649   1985

19. Briand, R., Dervaux, M. and Nicolas, M.
     "Theoretical Study of Interior Ballistics of Guns with
     Traveling Charge"
     Report communicated by W. Oberle   1986

20. Gough, P. S.
     "Extensions to NOVA Flamespread Modeling Capacity"
     Final Report for Task I, Contract N00174-80-C-0316,
     PGA-TR-81-2   1981

NOMENCLATURE

A	Cross-sectional area of flow. Equals area of tube minus intrusions of reactive sidewalls, unburned igniter and projectile afterbody.
B_i	Burn rate coefficient.
b	Covolume.
c	Isentropic sound speed in mixture of combustion products at constant composition.
c_p	Specific heat at constant pressure.
c_v	Specific heat at constant volume.
D_p	Effective diameter of particle.
d	Surface regression.
d_0	Initial diameter of perforation.
e	Internal energy. Thermal component only.
e_{IG}	Heat released per unit mass of igniter.
e_{Pj}	Heat released per unit mass of propellant type j.
e_s	Heat released per unit mass of sidewall.
f_s	Steady-state interphase drag.
f_w	Friction force between traveling charge and tube wall.
g_0	Constant used to reconcile units of measurement.
J	Total number of types of solid propellant.
K	Total number of reactions in mixture of combustion products.
M_p	Mass of projectile.
M_w	Molecular weight.
$\dot{m}_j$	Rate of decomposition per unit volume of propellant type j.
$\dot{m}_s$	Rate of decomposition per unit volume of reactive sidewall.
N	Total number of species in mixture of combustion products.

n_i Burn rate exponent.

p Pressure.

Q_k Heat released per unit mass by reaction k.

q_w Heat loss per unit volume to tube wall.

q_{s_j} Heat loss per unit volume to propellant type j.

R_u Universal gas constant.

$\dot{r}_k$ Rate of reaction k per unit volume.

$\dot{r}_{ik}$ Rate of production of species i by reaction k.

r_{tc} Rate of regression of rear surface of traveling charge.

S_p Surface area of a grain.

T Temperature.

t Time.

u Velocity of mixture of combustion products.

u_p Velocity of solid propellant.

u_{tc} Velocity of traveling charge.

V_p Volume of a grain.

v_p Projectile velocity.

$\dot{w}_i$ Rate of deposition of condensed-phase species i onto surface of solid propellant.

Y_i Mass fraction of species i in mixture of combustion products.

$Y_{ij,o}$ Mass fraction of species i in near field products of combustion of propellant type j.

Y_{IG_i} Mass fraction of species i in products of combustion of igniter.

Y_{s_i} Mass fraction of reactive sidewall.

z Axial coordinate.

Greek Symbols

γ Ratio of specific heats.

ε Porosity or fraction of unit volume occupied by mixture of combustion products.

ζ Non-homogeneous term in balance equations.

ρ Density of mixture of combustion products.

ρ_{c_i} Density of condensed species in mixture of combustion products.

ρ_{IG} Density of unburned igniter

ρ_s Density of sidewall.

ρ_{tc} Density of traveling charge.

σ Intergranular stress.

σ_{tc} Stress in traveling charge

φ Rate of decomposition of igniter.

Special Symbols

$\dfrac{D}{Dt}$ Convective derivative along streamline of mixture of combustion products.

$\dfrac{D}{Dt_p}$ Convective derivative along solid-propellant.

Intentionally left blank.

64

APPENDIX:

XNOVAKTC (XKTC)--STRUCTURE AND USE

INTENTIONALLY LEFT BLANK.

Our intention in this Appendix is to provide the user of the code with some understanding of its macrostructure and full details of the specification of input data. We do not attempt to document the code in such detail as to permit revisions by the user. XKTC is an extension of NOVATC, XNOVAT and XNOVAK which are, in turn, extensions of the express version of the NOVA Code known as XNOVA. XNOVA is a subset of the NOVA Code and certain of the details of the original versions of the NOVA Code which were deleted in the preparation of XNOVA are also absent from its successors XNOVAK and XNOVAT. Discussions of the structure of NOVA, NOVATC, XNOVA, XNOVAK and XNOVAT may be found in earlier reports.[1,3,4,6,2] Although we provide a complete tabulation of the present set of code subroutines and functions, our general discussion is confined to the differences between XKTC and its predecessors.

The discussion of structure and of input is contained in the two following Sections. Before proceeding, however, we wish to draw the user's attention to certain general restrictions on the use of the code.

First, it should be noted that existing NOVA, XNOVA and NOVATC data bases cannot be read by XNOVAK, XNOVAT or XKTC. Although we always attempt to maintain data base compatibility between the various code versions, XNOVAK, XNOVAT and XKTC do require a minor change to pre-existing data bases. File [M4], described in Table A.5, always consists of two cards in XNOVAK/XNOVAT/XKTC data sets. Pre-existing NOVA, XNOVA and NOVATC data sets in which File [M4] consisted of just one card may be made compatible with XNOVAK/XNOVAT/XKTC by the incorporation of a single blank card following the pre-existing File [M4]. No change is required to pre-existing data bases for which [M4] already consisted of two cards. A corresponding revision to XNOVAK/XNOVAT/XKTC data bases is required if they are to be run on NOVATC, XNOVA or NOVA. However, all XNOVAK data bases can be read by XNOVAT and XKTC.

Second, in regard to the summarized solution histories given at the conclusion of each run, it should be noted that the energy defect calculation does not presently support the full chemistry option. If intermediate combustion products are present, the tabulated energy defect may become quite large. Only the mass defect can be depended upon to gage the accuracy of the numerical solution in such cases. The single exception to this statement is that of the traveling charge with a finite flame thickness. In this special case, where there is just one intermediate species, the energy defect calculation reflects the chemical energy stored in the intermediates. Moreover, in this special case, the mass fraction calculation for propellant type three in the summary table is used to tabulate the ratio of the mass of the unburned intermediates to that of the original traveling charge increment.

STRUCTURE AND LINKAGES

A complete summary of the routines and their linkages is given in Table A.1. The overall macrostructure is unchanged from that of XNOVA as documented in Reference 4. The following brief comments provide a summary of the routines which were added to XNOVA to produce XNOVAK, the revisions which subsequently transformed XNOVAK into XNOVAT, and the final amalgam of XNOVAT and BRLTC[9] to produce XKTC. It should be noted that we have previously commented on the fact that XNOVAK was written on a 32-bit word machine in double precision,[6] and that users who implement the Code on a 60-bit machine such as the CYBER 7600 might wish to convert the Code to single precision. The version of XNOVAK used to develop XKTC was implemented on the CYBER at BRL as a single precision code. Accordingly, XKTC is a single precision code and it follows that implementation of XKTC on a 32-bit word machine should incorporate a conversion to double precision.

Routines Added in Preparation of XNOVAK

XNOVAK was developed as an extension of XNOVA. Accordingly, XNOVA is a subset of both XNOVAK and NOVA. Moreover, in developing XNOVAK it was found necessary to restore certain capabilities which had been removed from NOVA during the preparation of XNOVA. Specifically, we restored the invariant embedding solution for the thermal response of the solid propellant. Thus, in addition to the capabilities of XNOVA, XNOVAK and NOVA also share a transient combustion modeling capability.

The NOVA routines restored to XNOVAK were CMBUST, FBAK, IMBED and ROOT together with necessary I/O linkages. The routines were then modified to support the XNOVAK features of subsurface reactivity and the evaporative boundary condition. New routines added to support the kinetics option included CHEMR, CHEMRS, CONLOS, COVC and GAMMOL. The new routine FILLBR implements the analysis of the rear filler elements and was created by making appropriate editing changes to the pre-existing routine FILLER. One additional routine, AVN, was included for the purpose of documenting Code revisions and printing the version number on each run.

Routines Added in Preparation of XNOVAT

Several routines were required to produce XNOVAT. Subroutine INTRPC determines the rate of combustion of the reactive layers ascribed to the tube wall, the centerline, and the projectile afterbody. To support the new form functions we have added the routines BLSL, HEX19, and SLIVER. To treat the reactivity and flow resistance of the endwalls of the bundles of propellant we added the routines CALFLO, CALPRM, FLUX, FLUXDR AND TDBCAL, all

of which were adapted from the TDNOVA Code.[5] The routine TDBUF acts as a link between the existing boundary value solver BCAL and the routine TDBCAL. In addition we added the routines JCON, SETSUB and RCASE which perform various utility functions.

Structure of NOVATC

XKTC was essentially formed by substituting XNOVAT in place of XNOVA in the previously developed NOVATC Code.[3] As we have previously discussed,[3] NOVATC is an amalgam of XNOVA and BRLTC.[4,9]

In forming the amalgam care was taken to minimize cross-contamination of the coding. The approach was to take BRLTC and delete all references to the flow behind the base of the traveling charge while retaining the storage, data reads and processing pertinent to the regression of the surface, the traveling charge and the projectile. This stripped down code was linked to a complete version of XNOVA[4] in which a minimal number of linking subroutine calls were placed. Although a more tightly written code could have been developed it would have been more difficult to maintain such a code in a form compatible with future versions of XNOVA and BRLTC. Also, it is the case that XNOVA and BRLTC have many variables whose Fortran names are identical, but whose meanings differ and, conversely, some variables with different names but identical meanings.

It will be noted in Table A.1 that all routines pertinent to the traveling charge have the prefix TC. A single routine, TCLINK, has the function of reconciling the storage conventions of the two codes and of passing data between them. Processing follows the usual NOVA conventions with the traveling charge logic activated at a number of places. NOVSUB calls TCDATA and TCLINK to read and initialize data. INTEG calls TCLINK, TCOUT to print the solutions and TCBR4 to determine the traveling charge time step constraint. INTAL calls TCLINK and TCXC, the main integration executive for the traveling charge. TABLES calls TCLINK. It was also necessary to restructure slightly the routines BCAL and BDMOV.

Routines Added in Preparation of XKTC

The approach followed in the development of NOVATC made the replacement of XNOVA by XNOVAT fairly straightforward. It should be noted, however, that the present effort involved substantial exercising of the algorithm and several revisions were made to the analysis of the boundary values at the base of the burning traveling charge. Accordingly, the versions of TCLINK and TCBASE used here differ from those in earlier versions of NOVATC.

69

Apart from linking the kinetics, tank gun and traveling charge options in a physically complete fashion, it was necessary to add several new routines in the development of XKTC. Subroutine GETLS computes the values of L^* for the intermediate products of combustion of the traveling charge. ATACH enforces the attachment of a propellant type to the tube or to the projectile. Subroutine LPBV provides an update of the combustion chamber of a control charge. It is supported by FORMCR which computes the form functions, and by the previously developed NOVA routine FRATE which computes mass transfer rates.

DESCRIPTION OF INPUT FILES

We preface the detailed description of the input file structure with some general observations. We note, in particular, the nomenclature for the definition of the geometry of the propelling charge.

Figure A.1 illustrates a charge configuration which does not make use of the tank gun option (MODET = 0). We illustrate the base of the projectile, an arbitrary number of filler elements -- some at the rear and some at the front of the charge -- and two types of propellant, the first of which is in two increments, the latter increment overlapping that of the second propellant. The figure also illustrates the significance of the input data ZGR, XEL, XBL and ZBPR.

Figure A.2 illustrates a charge configuration which does make use of the tank gun option (MODET = 1). We illustrate the intrusion of the projectile afterbody into the combustion chamber, the reactive layers on the tube wall, the centerline and the projectile afterbody, and three types of propellant, the first of which is present as two increments. To the rear of the afterbody we represent the three types of propellant as being parallel packaged and we illustrate the significance of the input data RGRI and RGRO.

Figures A.1 and A.2 both assume that the propellant is of the conventional type Figure A.3 illustrates a charge configuration in which a traveling charge is present. We note that the traveling charge may consist of several increments, each having distinct mechanical and thermochemical properties. The simulation of the traveling charge may be performed in conjunction with an arbitrarily configured conventional charge. It is assumed, however, that when the traveling charge is present there are no compactible filler materials at the front of the chamber, as in Figure A.1, and that the projectile does not have an afterbody as in Figure A.2. Reactive sidewalls may nevertheless be present, as shown in Figure A.3.

70
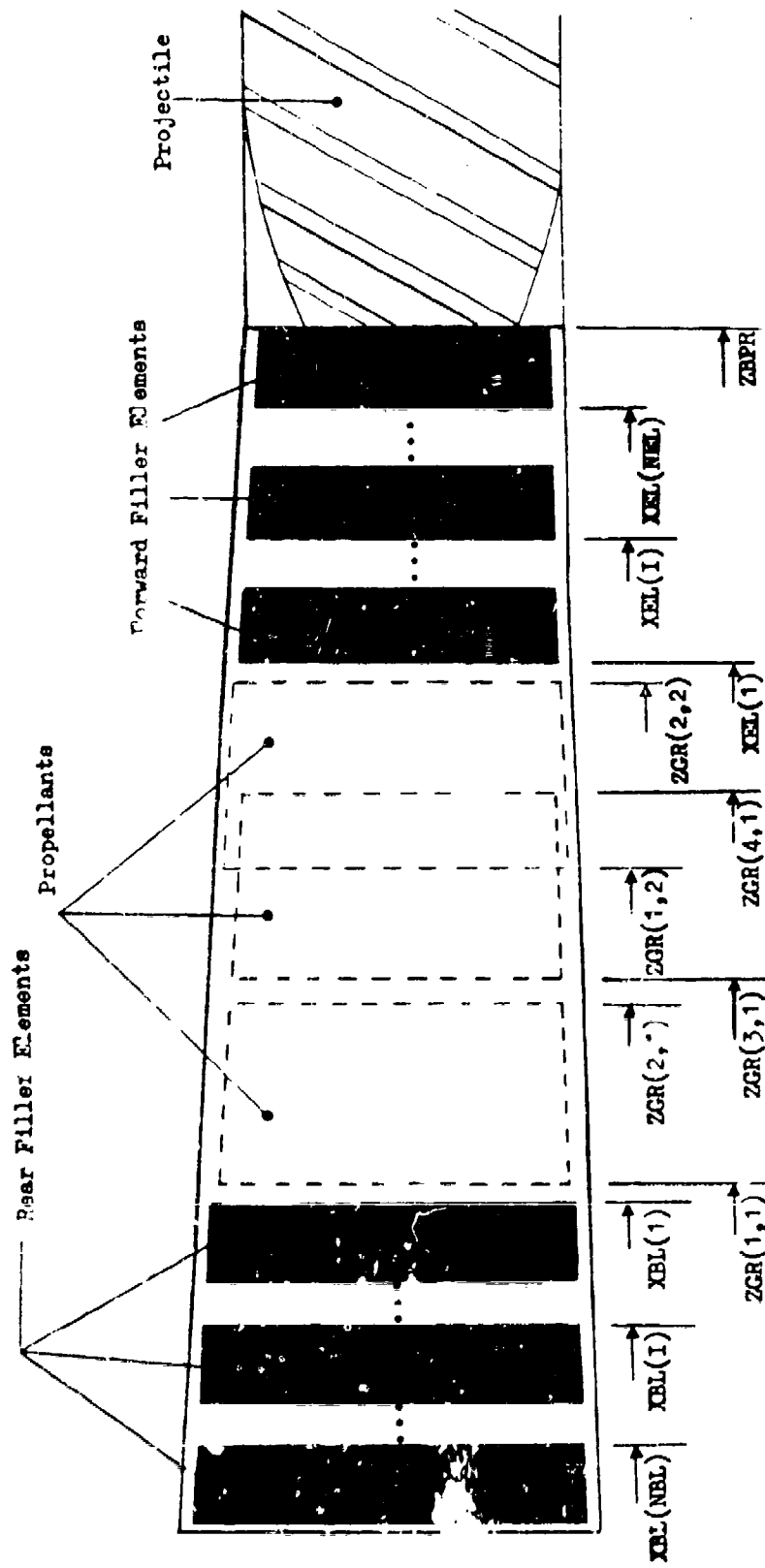
Figure A.1 Nomenclature for Definition of Charge Configuration in XNOVAT with MODET = 0
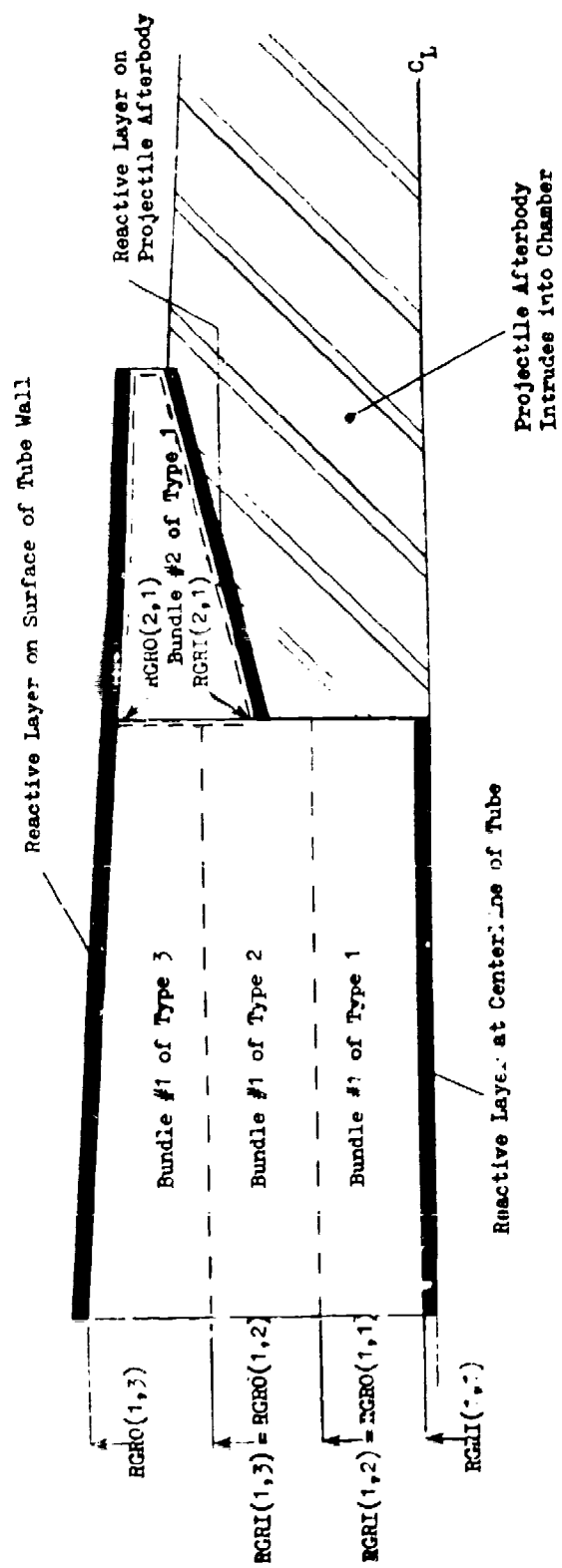
Figure A.2 Nomenclature for Definition of Charge Configuration in XNOVAT with MODET = 1.

Labels within figure:
- Reactive Layer on Surface of Tube Wall
- Reactive Layer on Projectile Afterbody
- RGRO(2,1)
- Bundle #2 of Type 1
- RGRI(2,1)
- Projectile Afterbody Intrudes into Chamber
- C_L
- Bundle #1 of Type 3
- Bundle #1 of Type 2
- Bundle #1 of Type 1
- Reactive Layer at Centerline of Tube
- RGRO(1,3)
- RGRI(1,3) = RGRO(1,2)
- RGRI(1,2) = RGRO(1,1)
- RGRI(1,1)

72

Projectile

C_L

Traveling Charge Increments

Reactive Layer in Tube Wall

Reactive Layer at
Centerline of Tube

Booster Charge Consisting of Three
Increments of Conventional Propellant

Figure A.3   Example of a Hybrid Charge Consisting of Conventional and Traveling Charge Increments.

73

Input to XKTC consists of XNOVAT data followed by a subset of the BRLTC data base when the traveling charge option is selected in the control data field of XKTC. Tables A.2, A.3 and A.4 enumerate the "Mandatory", Cont'agent and Traveling Charge data files. The files prefixed with an M are always mandatory in XNOVAT. Here, File [M13] is optional. We have retained the file labels of XNOVAT, in spite of this minor inconsistency, to promote commonality among the various codes.

The enumeration of the M and C files follows that for the NOVA Code. We have attempted to maximize the compatibility of XKTC, XNOVAT, XNOVAK, XNOVATC, XNOVA and NOVA data bases. As noted in the introduction to this appendix, compatibility is complete with the possible exception of File [M4]. In XKTC, XNOVAT and XNOVAK, File [M4] always consists of two cards. In XNOVATC, XNOVA and NOVA it may consist of either one or two cards. Existing NOVATC, XNOVA and NOVA data sets for which File [M4] consists of only one card may be made compatible with XKTC, XNOVAT and XNOVAK by the insertion of a single blank card after the existing [M4] data card. NOVA files not supported by XKTC, XNOVAT and XNOVAK are read and subsequently ignored. The tabulation of data by XKTC only includes those elements which are supported.

All mandatory files, Table A.2, are common to all codes. However, not all the members of every file are supported by XKTC, XNOVAT and XNOVAK. The detailed definition of the input files given in Table A.5 describes all the elements which are supported and simply denotes the others as "Inactive." Those contingent files, Table A.3, which are supported are defined while the others are denoted as "not supported." Only those contingent files which are supported by XKTC appear in the detailed discussion of Table A.5.

The program input files are structured to permit the running of only one problem at a time. A problem may be restarted from disc, provided suitable options have been selected in a prior run. Each problem may be terminated according to a criterion of number of integration steps, projectile displacement or problem time. Termination occurs at whichever of the three criteria is first satisfied.

It should be noted that file counters are edited by subroutine NOVSUB to establish their conformality with internal storage dimensions. However, other data are not edited, and it is recommended that the program user perform a first run on a new problem with termination set to follow initial set-up, so that all data may be validated.

The following notes (1) - (10) apply whether or not the traveling charge option is exercised. Subsequent notes (11) - (16) pertain to the traveling charge option.

(1) For problems involving only granular propellant, the representations of the grain distributions are arbitrary. The granular propellants may doubly or triply overlap. However, a region occupied by stick propellant may not be shared by any other type unless MODET = 1. IF MODET = 1, it is permissible to have an increment of stick propellant parallel packaged with another increment of stick or granular propellant. The monolithic charge is not permitted to share a cross-section of the tube with any other type. If a given type is specified as bonded to the tube or projectile, the bonding will be presumed to apply to any other propellant which shares a region with the given type.

(2) The mode of representation of one type of propellant is independent of the mode of representation of any other. If tables of volume fractions are used, it should be recalled that the volume fraction is the complement of the porosity, being zero when no propellant is present and increasing to unity as the pore volume vanishes. The volume fraction defaults to zero outside the range of positions defined by the tables.

(3) An internal boundary is identified at any location in which any volume fraction is discontinuous. Thus an internal boundary may be established at a point at which the porosity is continuous.

(4) Absolutely no restrictions, other than that on note (1), are placed on the relative positions of the bags of propellant. After the data are read, they are all converted internally to volume fraction tables. These are all then scanned to create a list of internal boundary positions. This list is then sorted to put them into order and to define the computational regions.

(5) The right-hand boundary is always set equal to XEL(1). If NEL = 0, XEL(1) defaults to ZBPR. Similarly, the left-hand boundary is always set equal to XBL(1). If NBL = 0, XBL(1) defaults to zero. It should be noted that the configuration of the forward elements is specified by reference to the position of the left-hand or rear boundary of each element. Conversely, the configuration of the rear elements is specified by reference to the position of the right-hand or forward boundary of each element. In both cases the elements are ordered so that the first is closest to the propelling charge.

(6) Although filler elements may be included if MODET = 1, the coding does not consider the influence of the afterbody on the behavior of the filler elements.

75

(7) It is emphasized that every case closure element must be accounted for, including spaces. Any element, other than the first, may be entered as a space by setting its mass equal to zero.

(8) It is noted that one may use a single element to represent more than one physical component and that conversely, one may use several elements to characterize a single component.

(9) The present storage allocation in the code imposes certain restrictions on the modeling of subsurface reactions in the propellant. It is assumed that only one type of propellant is present if an invariant embedding solution of the thermal response is desired (KMODE = 2 in File [M2]). At most 21 stations are permitted for the analysis of the thermal response. At most two chemical species can be associated with the subsurface chemistry. While these limits are thought to be adequate for present needs, they may readily be relaxed by means of changes in certain dimension statements.

(10) It will be noted that the data required when KMODE $\neq$ 0 Files ([C23.1] – [C23.6]) are to some extent already provided by the data of Files [M7] – [C7]. The latter data are superseded in such a case and consistency between the two sets of data is not essential. However, inconsistencies may yield an apparent energy defect in the summarized interior ballistics table.

(11) Unit 9 is reserved for storage of the traveling charge data if disk logout is specified.

(12) The code does not support the traveling charge option simultaneously with the compactible case closure option. It is also assumed that the projectile has no afterbody if the traveling charge option is exercised.

(13) The code termination data are always specified according to the NOVA format. The projectile data follow the NOVA format only if the traveling charge option is not in effect.

(14) Due to the cross-linking of the codes, no more than 98 mesh points and no more than 9 increments can be specified for the booster region when the traveling charge option is in effect.

(15) A composition dependent covolume is not considered. The covolume for the calculation is presently based on the booster charge data according to the NOVA convention.

(16) The gun tube is assumed to have a constant area in the region occupied by the unreacted traveling charge.

TABLE A.1 SUMMARY OF ROUTINES AND LINKAGES

XKTC   Purpose: XKTC is a dummy main routine which immediately
                          transfers control to NOVSUB.

            Calls: NOVSUB.

            Called by: None.

ATACH   Purpose: Subroutine ATACH enforces the attachment of a charge
                          increment to either the tube or the projectile.

            Calls: None.

            Called by: INTAL.

AVN   Purpose: Subroutine AVN is used to document code revisions
                          and print the version number.

            Calls: None.

            Called by: NOVSUB.

BCAL   Purpose: Subroutine BCAL accepts trial boundary values for
                          the gas- and solid-phases and adjusts them so as to
                          satisfy simultaneously the physical and character-
                          istic boundary conditions.

            Calls: COVC, EPTOR, GAMMOL, LUMPS, OUTPUT, PRTOC,
                          PRTOE, TABLES, TDBUF.

            Called by: INTAL.

BDMOV   Purpose: Subroutine BDMOV updates the position of the region
                          boundaries. It also updates the projectile
                          displacement and velocity, making use of FILLEX
                          and/or FILLBR when case closure elements are present.

            Calls: FILLBR, FILLER, RCASE, RESFUN, RHEC.

            Called by: INTAL.

BLKDAT   Purpose: BLKDAT performs block data initialization.

            Calls: None.

            Called by: None.

77

BLSL   Purpose: Subroutine BLSL computes the volume and surface area for the blind slit form function during the slivering phase

Calls: None.

Called by: FORM.

BRNOUT   Purpose: Subroutine BRNOUT detects the instant when all the propellant has been consumed and then consolidates all the computational regions into a single region with uniform mesh spacing.

Calls: FITSP, REG21.

Called by: None.

CALFLO   Purpose: Subroutine CALFLO computes the rate of reaction of the surface fluxes associated with the endwalls of the charge increments.

Calls: None.

Called by: TDBUF.

CALPRM   Purpose: Subroutine CALPRM computes the flow resistance co-efficient for the endwalls of the charge increments.

Calls: None.

Called by: TDBUF.

CHEMR   Purpose: Subroutine CHEMR computes the effects of chemical reactions on the species mass fractions in the combustion product mixture and returns the value of the heat liberated by chemical reaction.

Calls: None.

Called by: INTAL, LUMPS.

CHEMRS   Purpose: Subroutine CHEMRS performs a function similar to that of CHEMR; however it addresses the reactions within the solid propellant.

Calls: None.

Called by: IMBED.

CMBUST   Purpose: Subroutine CMBUST interfaces the invariant embedding solution of the solid propellant thermal response with the macroscopic two-phase flow.

Calls: FBAK, IMBED.

Called by: INTEG, NOVSUB.

CONLOS   Purpose: Subroutine CONLOS computes the rate of transfer of condensed species from the combustion product mixture to tne surface of the solid propellant.

Calls: None.

Called by: HEATP.

COVC   Purpose: Function COVC computes the covolume of the combustion product mixture.

Calls: None.

Called by: BCAL, FRICT, HEATP, HEATW, INTAL, INTEG, INTRPC, LUMPS, REG12, REG32, STATES, TCLINK, TDBCAL, TDBUF.

DINT   Purpose: Function DINT performs a truncation of a floating point variable to its integer part.

Calls: None.

Called by: TABLES.

DPDER   Purpose: Function DPDER computes the partial derivative $(\partial p/\partial e)_\rho$ for the covolume equation of state.

Calls: None.

Called by: LUMPS.

DFDRE Purpose: Function DPDRE computes the partial derivative $(\partial p / \partial \rho)_e$ for the covolume equation of state.

Calls: None.

Called by: LUMPS.

EPTOR Purpose: Function EPTOR evaluates the density as a function of internal energy and pressure for the covolume equation of state.

Calls: None.

Called by: BCAL, FRICT, HEATP, HEATW, INTRPC, NOVSUB, TDBCAL.

ERTOP Purpose: Function ERTOP evaluates the pressure as a function of internal energy and density for the covolume equation of state.

Calls: None.

Called by: INTAL, LPVB, LUMPS, NOVSUB, REG12, REG32.

FBAK Purpose: Function FBAK computes the temperature gradient at the surface of the solid propellant taking into account heat transfer from the igniter and heat feedback from the flame.

Calls: None.

Called by: CMBUST, NOVSUB.

FILLBR Purpose: Subroutine FILLBR updates the motion of the rear case closure elements.

Calls: OUTPUT, TABLES.

Called by: BDMOV, NOVSUB.

FILLER Purpose: Subroutine FILLER updates the motion of the forward case closure elements and the projectile.

Calls: OUTPUT, TABLES.

Called by: BDMOV, NOVSUB.

FITSP	Purpose:	Subroutine FITSP sets values of the state variables, following re-allocation of the mesh, by means of a cubic spline interpolation scheme.
	Calls:	SETSUB.
	Called by:	BRNOUT, MESH, NOVSUB.

FLUX	Purpose:	Subroutine FLUX computes the state of gas at the boundaries of the reactive endwalls.
	Calls:	None.
	Called by:	FLUXDR, TDBCAL.

FLUXDR	Purpose:	Subroutine FLUXDR computes the derivatives of the state variables in a lumped parameter region with respect to the fluxes to that region from the contiguous continuum regions.
	Calls:	FLUX.
	Called by:	TDBUF.

FORM	Purpose:	Subroutine FORM computes the surface area and volume of the propellant grains. It is supported by PERF19 which treats the slivering phase of nineteen perforation propellant.
	Calls:	BLSL, HEX19, PERF19.
	Called by:	INTEG, NOVSUB.

FORMCR	Purpose:	Subroutine FORMCR computes the form functions for grains used to define a control charge.
	Calls:	None.
	Called by:	LPVB.

FRATE	Purpose:	Function Frate computes the rate of mass transfer through a nozzle subject to the assumption of isentropic flow.
	Calls:	None.
	Called by:	LPVB.

FRICT   Purpose: Subroutine FRICT computes the interphase drag for granular propellant.

         Calls: COVC, EPTOR, VIS.

         Called by: INTEG.

GAMMOL   Purpose: Subroutine GAMMOL computes the ratio of specific heats and the molecular weight of the combustion product mixture.

         Calls: None.

         Called by: BCAL, LUMPS, STATES, TCLINK, TDBCAL, TDBUF.

GEILS   Purpose: Subroutine GEILS computes L^* values for the intermediate combustion products of the traveling charge.

         Calls: None.

         Called by: INTAL, INTEG.

HEATP   Purpose: Subroutine HEATP determines the interphase heat transfer, updates the surface temperature of the solid-phase prior to ignition, and also determines the interphase drag in stick propellant.

         Calls: CONLOS, COVC, EPTOR, VIS.

         Called by: INTEG.

HEATW   Purpose: Subroutine HEATW determines the rate of heat transfer to the tube wall and updates the tube surface temperature.

         Calls: COVC, EPTOR, VIS.

         Called by: INTEG, NOVSUB.

HEX19   Purpose: Subroutine HEX19 computes the volume and surface area of nineteen-perforation hexagonal grains.

         Calls: SLIVER.

         Called by: FORM.

IGNITE	Purpose:	Subroutine IGNITE determines the time of ignition of the propellant.
	Calls:	None.
	Called by:	INTEG.

IMBED	Purpose:	Subroutine IMBED integrates the thermal profile in the solid propellant by means of the method of invariant embedding.
	Calls:	CHEMRS, ROOT, ROOTR.
	Called by:	CMBUST, NOVSUB.

INTAL	Purpose:	Subroutine INTAL updates the principal state variables, p, ρ, u, s, u_p, σ at all interior mesh points. It also determines trial update boundary values together with characteristic coefficients which are transmitted to BCAL for imposition of the physical boundary conditions.
	Calls:	ATACH, BCAL, BDMOV, CHEMR, COVC, ERTOP, GETLS, INTRP1, LPVB, PRTOC, PRTOE, RCASE, RDEDPR, RHEO, TCLINK, TCXC.
	Called by:	INTEG.

INTEG	Purpose:	Subroutine INTEG is the principal integration executive. It is cycled twice per time step, once for the predictor level and once for the corrector level. It establishes the constitutive data by calls to individual subroutines and effects the update of the principal state variables by a call to INTAL. INTEG itself updates the surface regression and thermal parameter H for the solid-phase and, if KMODE =0 (File [M2] of Table A.4), it also updates the molecular weight and ratio of specific heats for the gas phase.
	Calls:	CMBUST, COVC, FORM, FRICT, GETLS, HEATP, HEATW, IGNITE, INTAL, INTRPC, INTRP1, INTRP2, JCON, MESH, OUTPUT, PRTOC, REGRES, STATES, TABLES, TCBR4, TCLINK, TCOUT, TERMIN, VOIDS, WALTEM.
	Called by:	NOVSUB.

INTRPC   Purpose: Subroutine INTRPC computes the local mass addition due to combustion of the reactive sidewalls.

           Calls: COVC, ERTOR, JCON, RCASE, VIS.

           Called by: INTEG, NOVSUB.

INTRP1   Purpose: Subroutine INTRP1 determines the cross-sectional area of the tube at each mesh point, including an allowance for the unburned portion of the primer.

           Calls: JCON.

           Called by: INTAL, INTEG, NOVSUB, REG12, REG21, REG32, TABLES.

INTRP2   Purpose: Subroutine INTRP2 computes the rate of discharge of the igniter at each mesh point.

           Calls: None.

           Called by: INTEG, NOVSUB, REG12, REG32.

JCON   Purpose: Function JCON locates the nearest continuum mesh point.

           Calls: None.

           Called by: INTEG, INTRPC, INTRP1, LUMPS.

LPDATA   Purpose: Subroutine LPDATA converts the XNOVA data base into an equivalent data base for a lumped parameter interior ballistic model.

           Calls: None.

           Called by: NOVSUB.

LPVB   Purpose: Subroutine LPVB updates the state of the control charge combustion chamber and prepares data to permit the mass transfer to the chamber of the gun to be represented as a source term.

           Calls: ERTOP, FORMCR, FRATE.

           Called by: INTAL, NOVSUB.

LUMPS   Purpose: Subroutine LUMPS provides a trial update of the state of all lumped parameter regions. It also computes derivatives of the state variables with respect to the mass fluxes to the lumped parameter region. These are used by BCAL to enforce the physical boundary conditions.

           Calls: CHEMR, COVC, DPDER, DPDRE, ERTOP, GAMMOL, JCON, RCASE.

           Called by: BCAL, TDBUF.

MESH   Purpose: Subroutine MESH determines the level of modeling of each region and assigns mesh points to the continuum regions on the basis of their relative sizes.

           Calls: FITSP, OUTPUT, REG12, REG21, REG32, STATES.

           Called by: INTEG, NOVSUB.

NOVSUB   Purpose: Subroutine NOVSUB reads and prints the input data used to define the problem. NOVSUB also performs all the initialization of variables which is not accomplished through BLKDAT. Some of the initialization is performed by executing a call to certain subroutines with an appropriately set switch. Following initialization, NOVSUB transfers program control to INTEG.

           Calls: AVN, CMBUST, EPTOR, ERTOP, FBAK, FILLBR, FILLER, FITSP, FORM, HEATW, IMBED, INTEG, INTRPC, INTRP1, INTRP2, LPDATA, LPVB, MESH, SETSUB, TABLES, TCDATA, TCINIT, TCLINK.

           Called by: XKTC.

OUTPUT   Purpose: Subroutine OUTPUT is responsible for logout of the solution to the printer and/or direct access device unit 8.

           Calls: TABLES.

           Called by: BCAL, FILLBR, FILLER, INTEG, MESH.

PERF19	Purpose:	Subroutine PERF19 computes the surface area and covolume of nineteen-perforation propellant during the slivering phase.
	Calls:	None.
	Called by:	FORM.
PRTOC	Purpose:	Function PRTOC computes the square of the speed of sound according to the covolume equation of state.
	Calls:	None.
	Called by:	BCAL, INTAL, INTEG, TDBUF.
PRTOE	Purpose:	Function PRTOE computes the internal energy from the pressure and density according to the covolume equation of state.
	Calls:	None.
	Called by:	BCAL, INTAL, STATES, TCLINK, TDBCAL, TDBUF.
RCASE	Purpose:	Subroutine RCASE determines the density of the case as a function of pressure.
	Calls:	None.
	Called by:	BDMOV, INTAL, INTRPC, LUMPS.
RDEDPR	Purpose:	Function RDEDPR computes the quantity $\rho(\partial e/\partial p)_\rho$ according to the covolume equation of state.
	Calls:	None.
	Called by:	INTAL.
REGRES	Purpose:	Subroutine REGRES computes the rate of regression of the surface of the propellant.
	Calls:	None.
	Called by:	INTEG.

86

REG12 Purpose: Subroutine REG12 transforms data for a region of continuum ullage into data for a region of lumped parameter ullage.

Calls: COVC, ERTOP, INTRP1, INTRP2.

Called by: MESH.

REG21 Purpose: Subroutine REG21 transforms data for a region of lumped parameter ullage into data for a region of continuum ullage.

Calls: INTRP1.

Called by: BRNOUT, MESH.

REG32 Purpose: Subroutine REG32 sets initial data for a lumped parameter region of ullage which is newly opened.

Calls: COVC, ERTOP, INTRP1, INTRP2.

Called by: MESH.

RESFUN Purpose: Function RESFUN computes the resistance to projectile motion due to interference of the rotating band with the gun tube.

Calls: None.

Called by: BDMOV.

RHEO Purpose: Subroutine RHEO computes the rate of propagation of intergranular disturbances.

Calls: None.

Called by: BDMOV, INTAL.

ROOT Purpose: Subroutine ROOT selects a new value for the solution of an arbitrary equation by the method of regula falsi.

Calls: None.

Called by: IMBED.

ROOTR   Purpose: Subroutine ROOTR is similar to ROOT, but contains additional logic for the situation in which the slope of the test function vanishes.

Calls: None.

Called by: IMBED.

SETSUB   Purpose: Subroutine SETSUB sets the reactivity and permeability pointers.

Calls: None.

Called by: FITSP, NOVSUB.

SLIVER   Purpose: Subroutine SLIVER computes the volume and surface area of nineteen-perforation hexagonal grains during the slivering phase.

Calls: None.

Called by: HEX19.

STATES   Purpose: Subroutine STATES computes certain of the dependent state variables from the principal storage arrays for the gas-phase.

Calls: COVC, GAMMOL, PRTOE.

Called by: INTEG, MESH, TERMIN.

TABLES   Purpose: Subroutine TABLES compiles the summary data which describe the conventional interior ballistic quantities such as histories of breech and base pressure and of the projectile trajectory.

Calls: DINT, INTRP1, TCLINK.

Called by: BCAL, FILLBR, FILLER, INTEG, NOVSUB, OUTPUT.

TCARAC	Purpose:	Subroutine TCARAC defines characteristic data in conjunction with the determination of boundary values for the traveling charge when modeled as a continuum.
	Calls:	TCBR2, TCDSDR.
	Called by:	TCBASE, TCBPR, TCONTC.

TCBASE	Purpose:	Subroutine TCBASE determines the regression rate of the traveling charge and provides trial boundary values for the unreacted side.
	Calls:	TCARAC, TCBURN, TCDSDR, TCIG, TCLINK, TCPROP, TCRESP, TCRNOM.
	Called by:	TCXC.

TCBMDC	Purpose:	Subroutine TCBMDC computes mechanical properties of the traveling charge when its rheology is specified in tabular format.
	Calls:	ISCICU (An IMSL routine).
	Called by:	TCDATA, TCDSDR, TCRNOM, TCSNOW.

TCBPR	Purpose:	Subroutine TCBPR updates the boundary values of the traveling charge at the base of the projectile.
	Calls:	TCARAC, TCDSDR, TCRNOM.
	Called by:	TCXC.

TCBR1	Purpose:	Subroutine TCBR1 initializes the computational arrays associated with the traveling charge.
	Calls:	TCRFIT, TCRNOM.
	Called by:	TCINIT.

TCBR2	Purpose:	Subroutine TCBR2 moves the traveling charge computational arrays into working arrays. This routine performs a trivial function in the present code but it is retained in order to maintain structural commonality with BRLTC where its function is non-trivial.
	Calls:	None.
	Called by:	TCARAC, TCBR3, TCBR4, TCOUT.

TCBR3	Purpose:	Subroutine TCBR3 updates the state variables for the traveling charge at all internal mesh points.
	Calls:	TCBR2, TCDSDR, TCWFR.
	Called by:	TCXC.

TCBR4	Purpose:	Subroutine TCBR4 determines the CFL time step restriction for the traveling charge.
	Calls:	TCBR2, TCDSDR, TCLINK.
	Called by:	INTEG.

TCBURN	Purpose:	Subroutine TCBURN calculates the regression rate of the traveling charge when specified as an empirical function of pressure (on the reacted side) or stress (on the unreacted side).
	Calls:	TCDVDI.
	Called by:	TCBASE.

TCDATA	Purpose:	Subroutine TCDATA reads and prints the input data associated with the traveling charge.
	Calls:	TCBMDC, TCINIT.
	Called by:	NOVSUB.

TCDSDR	Purpose:	Function TCDSDR calculates the speed of sound in the traveling charge.
	Calls:	TCBMDC, TCSNOM.
	Called by:	TCARAC, TCBASE, TCBPR, TCBR3, TCBR4, TCONTC.

TCDVDI   Purpose: Subroutine TCDVDI performs interpolation by the method of divided differences.

Calls: None.

Called by: TCBURN.

TCGETK   Purpose: Subroutine TCGETK updates the ordinary differential equations associated with the traveling charge.

Calls: TCRESP.

Called by: TCXC.

TCIG   Purpose: Subroutine TCIG determines the time at which ignition occurs for the traveling charge.

Calls: None.

Called by: TCBASE.

TCINIT   Purpose: Subroutine TCINIT performs the initialization of constants and pointers for the traveling charge.

Calls: TCBR1, TCRFIT, TCVUPD.

Called by: NOVSUB, TCDATA.

TCLINK   Purpose: Subroutine TCLINK transfers data between the NOVA routines and the BELTC routines.

Calls: COVC, GAMMOL, PRTOE, TCPROP.

Called by: INTAL, INTEG, NOVSUB, TABLES, TCBASE, TCBR4, TCOUT, TCXC.

TCONTC   Purpose: Subroutine TCONTC updates the boundary values for the traveling charge at the interfaces between increments.

Calls: TCARAC, TCDSDR, TCRNOM.

Called by: TCXC.

TCOUT   Purpose: Subroutine TCOUT performs the logout of the traveling charge state variables.

            Calls: TCBR2, TCLINK.

            Called by: INTEG.

TCPROP   Purpose: Subroutine TCPROP moves the traveling charge property data from vector into scalar storage.

            Calls: None.

            Called by: TCBASE, TCLINK.

TCRESP   Purpose: Subroutine TCRESP computes the resistance on the projectile when the traveling charge option is in effect.

            Calls: None.

            Called by: TCBASE, TCGETK.

TCRFIT   Purpose: Subroutine TCRFIT performs the mesh allocation for the traveling charge and the interpolation of data associated with revisions to the number of points.

            Calls: None.

            Called by: TCBR1, TCINIT, TCXC.

TCRNOM   Purpose: Function TCRNOM computes the density of the traveling charge as a function of pressure on the nominal loading curve.

            Calls: TCBMDC.

            Called by: TCBASE, TCBPR, TCBR1, TCONTC.

TCSCHK   Purpose: Subroutine TCSCHK enforces the requirement that the pressure in the traveling charge not exceed the nominal loading value for the current value of density.

            Calls: TCSNOM.

            Called by: TCXC.

TCSNOM	Purpose:	Function TCSNOM computes the pressure in the traveling charge as a function of density on the nominal loading curve.
	Calls:	TCBMDC.
	Called by:	TCDSDR, TCSCHK.
TCVCHK	Purpose:	Subroutine TCVCHK checks that the velocity in the traveling charge has not been reversed as a consequence of the friction term.
	Calls:	None.
	Called by:	TCXC.
TCVUPD	Purpose:	Subroutine TCVUPD updates the continuum boundary velocities for the traveling charge.
	Calls:	None.
	Called by:	TCINIT, TCXC.
TCWFR	Purpose:	Subroutine TCWFR computes the friction between the traveling charge and the tube wall.
	Calls:	None.
	Called by:	TCBR3.
TCXC	Purpose:	Subroutine TCXC is the integration executive for the traveling charge state variables.
	Calls:	TCBASE, TCBPR, TCBR3, TCGETK, TCLINK, TCONTC, TCRFIT, TCSCHK, TCVCHK, TCVUPD, TCZUPD.
	Called by:	INTAL.
TCZUPD	Purpose:	Subroutine TCZUPD updates the positions of the continuum boundaries associated with the traveling charge.
	Calls:	None.
	Called by:	TCXC.

TDBCAL   Purpose: Subroutine TDBCAL uses the physical boundary conditions and the characteristic forms to determine the boundary values at each time step.

           Calls: COVC, EPTOR, FLUX, GAMMOL, PRTCE.

           Called by: TDBUF.

TDBUF   Purpose: Subroutine TDBUF acts as an interface from the NOVA storage conventions to those of the solver TDBCAL.

           Calls: CALFLO, CALPRM, COVC, FLUXDR, GAMMOL, LUMPS, PRTOC, PRTOE, TDBCAL.

           Called by: BCAL.

TERMIN   Purpose: Subroutine TERMIN tests for the termination of the calculation.

           Calls: STATES.

           Called by: INTEG.

VIS   Purpose: Function VIS computes the viscosity of the gas-phase as a function of temperature.

           Calls: None.

           Called by: FRICT, HEATP, HEATW, INTRPC.

VOIDS   Purpose: Subroutine VOIDS updates the volume fractions of each of the constituent solid-phase species from the history of the porosity.

           Calls: None.

           Called by: INTEG.

WALTEM   Purpose: Subroutine WALTEM updates the thermal equation for the tube wall temperature determined according to a cubic profile approximation.

           Calls: None.

           Called by: INTEG.

TABLE A.2   SUMMARY OF XKTC "MANDATORY" INPUT FILES

FILE NUMBER   FILE NAME

M1   Problem Name

M2   Control Data

M3   Integration Parameters

M4   File Counters

M5   Properties of Ambient Gas

M6   General Properties of Propellant Bed

M7   Ith Propellant Type, Location and Mass

M8   Ith Propellant Form Function Data

M9   Ith Propellant Rheology

M10   Ith Propellant Solid-Phase Thermochemistry

M11   Ith Propellant Gas-Phase Thermochemistry

M12   Tube Geometry

*M13   Projectile and Rifling Characteristics

----

* File M13 is not mandatory in XKTC. It is required only if the
traveling charge option is not exercised.

TABLE A.3   SUMMARY OF XKTC CONTINGENT INPUT FILES

FILE NUMBER	FILE NAME
C1	Logout Counters
C2	Erosive Burn Rate Parameters
C3	Not Supported.
C4	Position and Mass of Additional Bags of Ith Propellant
C5	Distribution of Volume Fraction of Ith Propellant
C5.1	Ith Propellant Port Diameter File Counter
C5.2	Ith Propellant Port Diameter
C6	Not Supported.
C7	Ith Propellant Deterred Layer Properties
C8	Igniter Thermochemistry
C9	Igniter Discharge Times
C10	Igniter Discharge Positions
C11	Igniter Rate of Discharge
C12	Bore Resistance
C13	Tube Thermal Properties
C14	Tube Initial Temperature Profile
C15	Not Supported.
C16	Not Supported.
C17	Not Supported.
C18	Ith Forward Compactible Filler Element Properties
C19	Constitutive Data for Ith Forward Element
C19.1	Ith Rear Compactible Filler Element Properties
C19.2	Constitutive Data for Ith Rear Element
C20	Not Supported.
C21	Not Supported.
C22	Not Supported.

FILE NUMBER	FILE NAME
C23	Positions for Pressure Table Storage
C23.01	Projectile Afterbody Pressure History Option
C23.1	Kinetics Option Counters
C23.2	Properties of Species
C23.3	Composition of Propellant Near Field Combustion Products
C23.4	Composition of Igniter Discharge Combustion Products
C23.5	Composition of Initial Ambient Gas
C23.6	Initial Composition of Solid Propellant
C23.61	Composition of Traveling Charge Near Field Combustion Products
C23.62	Types of Reactions in Mixture of Combustion Products
C23.63	Species Thermal Equilibration Switches
C23.7	Description of Arrhenius Reactions in Mixture of Combustion Products
C23.71	Description of Pressure-Dependent Reactions in Mixture of Combustion Products
C23.8	Description of Reactions in Solid Propellant
C23.9	Solid Propellant Thermal Response Parameters
C24	Parameters to Define Mesh in Invariant Embedding Analysis
C25	Tank Gun Option Control Data
C25.1	Geometry of Projectile Afterbody
C25.2	Thickness and Density Counters for Reactive Layer I
C25.3	Thickness of Reactive Layer I
C25.31	Segment Pointers for Reactive Layer I
C25.4	Density of Reactive Layer I
C25.5	Counter to Describe Discharge of Reactive Layer I
C25.6	Positions to Describe Discharge of Reactive Layer I

TABLE A.3 continued

FILE NUMBER	FILE NAME
C25.7	Times to Describe Discharge of Reactive Layer I
C25.8	Rate of Discharge of Reactive Layer I
C25.9	Burn Rate Counters for Reactive Layer I
C26	Burn Rate Data for Reactive Layer I
C26.1	Ignition Data for Reactive Layer I
C26.2	Thermochemical Data for Reactive Layer I
C26.21	Composition of Reactive Layer Near Field Combustion Products
C26.3	Properties of Deterred Layer of Reactive Layer 1
C26.4	Endwall Property Pointers
C26.5	Permeability Model Data
C26.6	File Counters for I-th Reactivity Model
C26.7	Thermochemical Data for I-th Reactivity Model
C26.71	Composition of Near Field Combustion Products of I-th Reactivity Model
C26.8	Ignition Value for I-th Reactivity Model
C26.9	Burn Rate Data for I-th Reactivity Model
C27	Tabular Description of I-th Reactivity Model
C28	Internal Properties of Control Charge Combustion Chamber
C28.1	External Properties of Control Charge Combustion Chamber
C28.2	Control Charge Type
C28.3	Control Charge Form Function
C28.4	Control Charge Burn Rate Counter
C28.5	Control Charge Burn Rate Description
C28.6	Control Charge Thermochemistry
C28.7	Properties of Deterred Layer

TABLE A.4 SUMMARY OF XKTC TRAVELING CHARGE INPUT FILES

File Number	File Name
TC1	Traveling Charge Control Data
TC2	Mesh Parameters
TC3	General Properties
TC4	Propellant Thermochemical Properties
TC5	Burn Rate Switches
TC6	Tabular Burn Rate Data
TC7	Tabular Burn Rate Data (cont'd)
TC8	Exponential Burn Rate Data
TC9	Propellant Analytical Rheology Data
TC10	Propellant Tabular Rheology Data
TC11	Propellant Tabular Rheology Data (cont'd)
TC12	Ablative Film Data
TC13	Propellant Friction Data
TC14	Tabular Bore Resistance Data
TC15	Barrel Shock Resistance Data
TC16	Obturator Setback Resistance Data
TC17	Obturator Friction Data

TABLE A.5   DESCRIPTION OF INPUT FILES

File [M1]	"Problem Name" (15A4) One Card

TITLE	Problem name. May be up to 60 alphanumeric characters.

File [M2]	"Control Data" (7L1,33I1) One Card

NPRINT	1 if print on logout, 0 otherwise.
NGRAPH	Inactive.
NDISK	1 if disc write on logout, 0 otherwise.
DSKRD	1 if disc start, 0 otherwise.
IBTABL	1 if summarized interior ballistic data are required, 0 otherwise.
NFLAM	1 if summary of ignition delay data required, 0 otherwise.
NPTABL	1 if summarized pressure, pressure difference data are required, 0 otherwise.
NEROS	1 if erosive effect to be included in propellant combustion, 0 otherwise. If NEROS = 1, File [C2] is required.
NDYN	Inactive.
NHTW	0 if wall temperature is not updated. 1 if cubic profile update is used.
NBC(1)	Inactive.
NBC(2)	Inactive.
NRES(1)	Inactive.
NRES(2)	Inactive.
LDBED	0 if propellant beds initially uncompacted, 1 otherwise. See comment in File [M9].

JHTW	0 if heat loss to tube is neglected.
	1 if heat loss is calculated by empirical correlation for fully developed turbulent flow. File [C13] is required.
LYER	Inactive.
IBRES	1 if linear interpolation of tabular data from File [C12] is used to define bore resistance. No velocity dependence is considered.
	2 if the interpolated value is multiplied by $7.2V^{-0.6}$, where V is the projectile velocity (ft/sec), provided $V \geq 27$ fps.
	3 if the interpolated value is multiplied by $(1 + 0.0004414V)/(1 + 0.005046V)$ where V is the projectile velocity (in/sec).
	If any other value is used, IBRES will default to the value 2.
NTC	0 if traveling charge option not required.
	1 if traveling charge option is in effect.
	When NTC = 1, NUNIN and NUNOUT (File [M3]) must not be entered as nine (default values are eight); NEL (File [M4]) must be entered as zero; NDIM (File [M3]) must not exceed ninety-eight for a granular booster or forty-nine for a stick booster. Files [TC1] through [TC17] are required.
INHIB(1)	0 if propellant type 1 does not have a deterred layer.
	1 if propellant type 1 does have a deterred layer. File [C7] is required in this case.
INHIB(2)	As per INHIB(1), but for second propellant type.
INHIB(3)	As per INHIB(1), but for third propellant type.
NXCW	Inactive.
NBLDWN	Inactive.
NSWSOL	0 if non-conservative form of solid-phase continuity equation is to be used.
	1 if conservative form is to be used. It is recommended that this option be selected only if excessive mass defects result from the use of the non-conservative form.
KMODE	0 if kinetics option not desired.
	1 if gas-phase is to be treated as a reacting, homogeneous mixture. See Files [C23.1] through [C23.9].
	2 if, in addition to treatment of gas-phase as a mixture, subsurface reactivity and/or finite difference solution of solid-phase thermal response is desired. See Files [C23.1] through [C23.9].

MODET   0 if tank gun option not desired.
1 if tank gun option is desired. See Files [C25.1] through [C27].

NECHO   0 if interpretation of input and normal run desired.
1 if input data not interpreted but normal run desired.
2 if interpretation of input data with no subsequent run desired.

Note: Independently of the value of NECHO, the Code prints an image of the card input file.

File [M3]   "Integration Parameters"   (6I5,F10.0/8F10.0)   Two Cards

---

NDIM   Number of grid points to be used in calculation. In general, NDIM must not exceed 99. If perforated stick propellant is present, NDIM must not exceed 49.

NSTEP   Number of integration steps before logout. (Each step consists of a predictor followed by a corrector.) If NSTEP = 0, logout follows every predictor as well as every corrector. If NSTEP < 0, File [C1] is required with |NSTEP| pairs of data. NSTEP $\geq$ -10.

NDTST   Step number for disc start.

NSTOP*   Number of steps for termination.

NUNIN   Unit number for disc read. If NUNIN = 0, it is defaulted to 8.

NUNOUT   Unit number for disc logout. If NUNOUT = 0, it is defaulted to 8.

DTPRT   Time interval before logout (sec). If entered as zero, it is defaulted to 10^{10}.

TSTOP*   Time for termination (sec).

ZSTOP*   Projectile travel for termination (in).

TINT   Maximum time step (sec).

SAFE   Stability safety factor. Recommended value is 1.1 although larger values may sometimes be required.

CRIT   Stability safety factor for source terms. Recommended value is 0.05.

RZOLV	Spatial resolution factor. Recommended range of values is $0.01 \leq RZOLV \leq 0.05$. If RZOLV is entered as zero, it will default internally to $1/(NDIM - 1)$.
TABLIB**	Time interval for storage of summarized interior ballistic data.
TABLP**	Time interval for pressure table storage.

---

* Termination occurs at whichever of NSTOP, TSTOP or ZSTOP is first satisfied.

** Table sizes are dimensioned to 100. When overflow is imminent, tables are condensed by deleting every second datum. Subsequently, storage time is doubled.

File [C1]	"Logout Counters" (16I5) One or Two Cards

N.B. File required if and only if NSTEP < 0. (See File [M3].)

NDTEP(1)	Maximum value of integration step number for which MSTEP(1) is to be used.
MSTEP(1)	Number of integration steps (predictor plus corrector count as one unit) between logout cycles.
.	
.	
.	
NDTEP($\|$NSTEP$\|$)*	Maximum value of integration step number for which MSTEP($\|$NSTEP$\|$) is to be used.
MSTEP($\|$NSTEP$\|$)	Corresponding value of number of steps between logout cycles.

---

* If NDTEP($\|$NSTEP$\|$) is exceeded during the calculation, the value MSTEP($\|$NSTEP$\|$) will be used as a default quantity.

File [M4]	"File Counters" (16I5) Two Cards

NSTA	Number of entries in tube geometry table. $2 \leq$ NSTA $\leq$ 10.
JJ	Number of times at which primer discharge is specified. $0 \leq$ JJ $\leq$ 40. If II and JJ $\geq$ 2, Files [C8] – [C11] are required.
II	Number of positions at which primer discharge is specified. $0 \leq$ II $\leq$ 40.
NBRES	Number of entries in bore resistance table. $0 \leq$ NBRES $\leq$ 20. If NBRES $\geq$ 2, File [C12] is required.
NTEM	Number of entries in tube initial temperature profile. If NTEM = 0, tube temperature defaults to TEMST (see File [M5]). If NTEM $\neq$ 0, File [C14] is required. $0 \leq$ NTEM $\leq$ 10.
NEL	Number of elements to characterize compactible filler between bed and projectile. If NEL = 0, projectile base is taken as right-hand boundary for computational domain. If NEL $\neq$ 0, File [C18] is required. $0 \leq$ NEL $\leq$ 10.
NPROP	Number of types of propellant grains. $1 \leq$ NPROP $\leq$ 3.
NBRDS	Number of burn rate data sets to describe pressure dependence of exponent and pre-exponential factors. See File [M10]. Note that the same value is assumed for all propellant species, if more than one are defined.
NEPS(1)	Number of entries in initial distribution of volume fraction of propellant type 1. If NEPS = 0, porosity is calculated from mass and position data given in File [M7]. If NEPS $\neq$ 0, File [C5] is required. Propellant types may be entered in either mode, independently of the representation of other types. $0 \leq$ NEPS(1) $\leq$ 10.
NEPS(2)	Number of entries for type 2.
NEPS(3)	Number of entries for type 3.
NZPT	Number of entries in table of positions for summarized pressure data. If NZPT $\neq$ 0, File [C23] is required. $0 \leq$ NZPT $\leq$ 8.
NMS(1)	Inactive.

NMS(2)	Inactive.
NWIB	Inactive.
MORE(1)	Number of additional bags of propellant of type 1. If MORE(1) > 0, File [C4] is required. $0 \le$ MORE(1) $\le$ 9.
MORE(2)	Number of additional bags of propellant of type 2. Only required if NPROP $\ge$ 2. Starts a new card.
MORE(3)	Number of additional bags of propellant of type 3. Only required if NPROP = 3.
NBL	Number of elements to characterize compactible filler between bed and breech. If NBL $\neq$ 0, File [C19.1] is required. $0 \le$ NBL $\le$ 10.

File [M5]	"Properties of Ambient Gas" (8F10.0) One Card

TEMST	Initial temperature (R).
PST	Initial pressure (psi).
GMST	Molecular weight (lbm/lbmol).
GAMST	Ratio of specific heats (-).

File [M6]	"General Properties of Propellant Bed" (8F10.0) One Card

TP0	Initial temperature (R).

File [C2]	"Erosive Burn Rate Parameters" (8F10.0) One Card

N.B.   File required if and only if NEROS = 1. (See File [M2].)

CEROS	Erosive burning pre-exponential factor (in^2 $^\circ$R/lbf).
BEROS	Erosive burning exponential factor (-).

Note: The subsequent files [M7], [C4], [C5], [M8], [M9], [M10], [C6], [M11] and [C7] are repeated, as a group for each of the NPROP (see (File [M4]) types of propellant which constitute the solid-phase.

File [M7]	"Ith Propellant Type, Location and Mass" (5A4,6F10.0) One Card

---

GRNAM(I)   Name of propellant. Up to 20 alphanumeric characters.

ZGR(1,I)   Left-hand boundary of first bag of propellant of type I (in).

ZGR(2,I)   Right-hand boundary of first bag of propellant of type I (in).

WTGRA(1,I)   Mass of first bag of propellant of type I (1bm). A negative value of WTGRA may be entered. In such a case, the absolute value is used to define the mass. The negative sign is used to set an internal switch which causes the computation of initial porosity to reflect the assumption that the propellant is packaged as a cylinder rather than filling uniformly each cross-section of the tube.

RHOP(I)   Density of propellant type I (1bm/in^3).

RGRI(1,I)   Inner radius of rear of bag (in). Only required if MODET = 1. (See File [M4].) If RGRI(1,I) is input as zero it is assumed to coincide with the inner radius of the available flow cross-section.

RGRO(1,I)   Outer radius of rear of bag (in). Only required if MODET = 1. (See File [M4].) If RGRO(1,I) is input as zero it is assumed to coincide with the outer radius of the available flow cross-section.

File [C4]	"Position and Mass of Additional Bags of Ith Propellant" (8F10.0) MORE(I) Cards

N.B.   File required if and only if MORE(I) = 0.   (See File [M4].)

ZGR(3,I)	Left-hand boundary of second bag of propellant of type I (in).
ZGR(4,I)	Right-hand boundary of second bag of propellant of type I (in).
WTGRA(2,I)	Mass of second bag of type I (1bm).
RGRI(2,I)	Inner radius of second bag (in).
RGRO(2,I)	Outer radius of second bag (in).
ZGR(5,I)*	Left-hand boundary of third bag.
.	
.	
.	
.	
ZGR(2*MORE(I)+2,I)	Right-hand boundary of bag MORE(I)+1 (last bag).
WTGRA(MORE(I)+1)	Mass of last bag.
RGRI(MORE(I)+1)	Inner radius of last bag (in).
RGRO(MORE(I)+ 1)	Outer radius of last bag (in).

*   Begin new card for each bag.

File [C5]	"Distribution of Volume Fraction of Ith Propellant" (8F10.0) One to Three Cards

N.B.   File required if and only if NEPS(I) = 0.   (See File [M4].)

ZEPS(1,I)	First position relative to breech (in).
EPSO(1.I)	Corresponding volume fraction of propellant type I.
.	
.	
.	
.	
ZEPS(NEPS(I),I)	Last position.
EPSO(NEPS(I),I)	Corresponding volume fraction.

File [M8]	"Ith Propellant Form Function Data" (I5,5F10.0,I5,F10.0)
	One Card

NFORM(I)   Form function indicator. $1 \le |NFORM(I)| \le 16$. NFORM may be entered as a negative number. In such a case, the absolute value is used to determine the form function, but the grains are taken to be stacked. This option allows granular propellant to respond as though it had the flow resistance of stick propellant.

OD(I)   Grain dimension (in). (See table below.)

DPERF(I)   Grain dimension (in). (See table below.)

GLEN(I)   Grain length (in).

NPERF(I)   Number of perforations (-) except for NFORM = 14 in which case NPERF is the number of slots.

SLW(I)   Grain dimension (in). (See table below.)

NFIX(I)   If 0, grains are assumed to be free to move.
If 1, grains are assumed to be attached to the tube.
If 2, grains are assumed to be attached to the projectile.

BONDX(I)   Strength of bond to tube or projectile (1bf). If BONDX(I) is entered as zero, it is taken to be infinite. Separation from tube or projectile occurs when absolute value of force required to maintain attachment exceeds BONDX(I).

FORM FUNCTION PARAMETERS

NFORM	GRAIN TYPE	OD	DPERF	SLW
1	Sphere	Diameter (in)	-	-
2	Cylinder	Diameter (in)	-	-
3	Stick*	Diameter (in)	Perforation Diameter (in)	-
4	Strip*	Width (in)	Thickness (in)	-
5	Monoperforated	Diameter (in)	Perforation Diameter (in)	-
6	Monoperforated with outside inhibition	Diameter (in)	Perforation Diameter (in)	-
7	Seven Perforations	Diameter (in)	Perforation Diameter (in)	-
9	Nineteen Perforations	Diameter (in)	Perforation Diameter (in)	-
10	Hexagonal Seven-Perforation Stick*	Distance between flats (in)	Perforation Diameter (in)	-
11	Slotted stick* (single-voidage)	Diameter (in)	Perforation Diameter (in)	Slot Width(in)
12	Scroll* (single-voidage)	Width (in)	Thickness (in)	-
13	Scroll* (dual-voidage)	Width (in)	Thickness (in)	External Diameter of Scroll (in)
14	Blind slit	Diameter (in)	Diameter of slotted core (in)	-
15	Hexagonal Nineteen-Perforation	Diameter (in)**	Perforation Diameter (in)	-
16	Monolithic Grain with central port***	Port diameter at rear (in)	Port diameter at front (in)	-

* End burning is neglected for these forms. Hence GLEN (File [M8]) may be entered arbitrarily.

** Grain assumed to have rounded corners. Diameter is between opposite corners.

*** Burning is assumed to take place only on the surfaces of the internal port. Projectile afterbody may intrude into port. NFIX(I) and BONDX(I) default to 1 and 0 respectively. If OD(I) = 0, or DPERF(I) = 0, then Files [C5.1], [C5.2] are required to define the diameter of the port as a function of position.

File [C5.1]   "Ith Propellant Port Diameter File Counter" (I5) One Card

---

N.B. File required if and only if NFORM (I) = 16 and either OD(I) = 0 or
      DPERF(I) = 0. (See File [M8].)

MNOP(I)   Number of entries in file to define diameter of port of
                monolithic grain. $2 \leq MNOP(I) \leq 8$.

File [C5.2]   "Ith Propellant Port Diameter" (8F10.0) One to Two Cards

---

N.B. File required if and only if NFORM(I) = 16 and either OD(I) = 0 or
      DPERF(I) = 0. (See File [M8].)

ZMNO(1,I)   First axial position relative to rear surface of
               grain (in).

DMNO(1,I)   Corresponding diameter of port (in).
  .
  .
  .
  .

ZMNO(MNOP(I),I) Last axial position.

DMNO(MNOP(I),I) Corresponding diameter.

File [M9]   "Ith Propellant Rheology" (8F10.0) One Card

GAP(I)   Rate of propagation of intergranular stress in
               settled, loading granular bed of type I (in/sec). If
               propellant I consists of stick then GAP(I) is independent
               of the settling porosity.

GEPO(I)   Porosity of settled bed for type I propellant. If
               LDBED = 0 (see File [M2]) and the porosity of the bed is
               less than GEPO(I) at any point where type I is present,
               GEPO(I) is automatically defaulted to the smallest value of
               porosity which occurs in the initial distribution. This
               property may be used to avoid calculating GEPO(I).

GCAP(I)	Rate of propagation of intergranular stress during unloading and reloading of propellant type I (in/sec). Not required for stick propellant.
PRPYLD	Inactive.
ANU(I)	Poisson ratio of propellant (-). Must be specified for stick propellant. ANU(I) defaults to 0.5 internally if propellant I is granular or if ANU(I) is entered as zero.

File [M10]	"Ith Propellant Solid-Phase Thermochemistry" (8F10.0) One to Three Cards

---

UPPR(1,I)	Maximum value of pressure for corresponding values of burn rate pre-exponential and exponential factors (psi).
B22(1,I)	Burning rate pre-exponential factor (in/sec-ps^n).
BNN(1,I)	Burning rate exponent (-).
.	
.	
.	
UPPR(NBRDS,I)*	Maximum value for last set of burn rate data.
B22(NBRDS,I)	Corresponding pre-exponential factor.
BNN(NBRDS,I)	Corresponding exponent.
B1(I)	Burning rate additive constant (in/sec .
TEMPIG(I)	Ignition temperature (R).
KP(I)	Thermal conductivity (lbf/sec/R).
ALPHAP(I)	Thermal diffusivity (in^2/sec).
ALPHA(I)	Emissivity factor (-).

---

* If pressure exceeds UPPR(NBRDS,I), the corresponding values of pre-exponential and exponential factors are used as default values.

File [M11]	"Ith Propellant Gas-Phase Thermochemistry" (8F10.0) One Card

ECHEM(I)	Internal energy released in combustion (lbf-in/lbm).
GMW(I)	Molecular weight (lbm/lbmol).
GAMMA(I)	Ratio of specific heat (-).
BV(I)	Covolume (in³/lbm).

File [C7]	"Ith Propellant Deterred Layer Properties" (8F10.0) One Card

N.B. File required if and only if INEIB(I) ≠ 0. (See File [M2].)

ECHIB(I)[*]	Internal energy released in combustion at start of deterred layer (lbf-in/lbm).
ECHIB2(I)	Internal energy released in combustion at end of deterred layer (lbf-in/lbm).
RGFAC(I)[*]	Factor by which burn rate is multiplied at start of deterred layer (-).
RGFAC2(I)	Factor by which burn rate is multiplied at end of deterred layer (-).
HIBX(I)	Depth of inhibited layer (in).

[*]   Values within deterred layer deduced by linear spacewise
interpolation. Final values need not be the same as those of the
undeterred propellant.

File [C8]	"Igniter Thermochemistry" (8F10.0) One Card

N.B. File required if and only if II, JJ ≥ 2. (See File [M4].)

EIG	Internal energy released in combustion (lbf-in/lbm).
GMIG	Molecular weight (lbm/lbmol).
GAMIG	Ratio of specific heats(-).
VIG	Specific volume of igniter solid-phase (in³/lbm).

| File [C9] | "Igniter Discharge Times" | (8F10.0) One to Five Cards |

N.B. File required if and only if II, JJ $\geq$ 2. (See File [M4].)

TPHI(1)　　　　First time in tabular representation of igniter discharge
.　　　　　　　　　(sec).
.
.
.
TPHI(JJ)　　　　Last time.

| File [C10] | "Igniter Discharge Positions" | (8F10.0) One to Five Cards |

N.B. File required if and only if II, JJ $\geq$ 2. (See File [M4].)

ZPHI(1)　　　　First position in tabular representation of igniter
.　　　　　　　　discharge (in).
.
.
.
ZPHI(II)　　　　Last position.

| File [C11] | "Igniter Rate of Discharge" | (8F10.0) Two to Two Hundred Cards |

N.B. File required if and only if II, JJ $\geq$ 2. (See File [M4].)

PHI(1,1)　　　　Igniter discharge per unit length per unit time at first
　　　　　　　　position and first time (lbm/in/sec).

PHI(2,1)　　　　Discharge at second position and first time.
.
.
.
PHI(II,1)　　　　Discharge at last position and first time.

PHI(1,2)*　　　　Discharge at first position and second time.
.
.
.
PHI(II,JJ)　　　　Discharge at last position and last time.

---

*　　PHI(1,J) begins a new card, J = 1, ... , JJ.

113

File [M12]	"Tube Geometry" (8F10.0) One to Three Cards

ZA(1)	First axial location relative to breech (ins).
RA(1)	Corresponding radius of bore (ins).
.	
.	
.	
.	
ZA(NSTA)	Last axial location.
RA(NSTA)	Corresponding radius.

File [C12]	"Bore Resistance" (8F10.0) One to Five Cards

N.B File required if and only if NBRES ⩾ 2. (See File [M4].)

BRZ(1)	First axial location. If BRZ(1) > 0 it is understood to be relative to breech (in). If BRZ(1) is entered as zero, however, all values of BRZ are understood to be relative to the initial position of the projectile.
BR(1)	Corresponding resistance exerted on projectile when base is at BRZ(1) (psi).
.	
.	
.	
.	
BRZ(NBRES)	Last location.
BR(NBRES)	Corresponding resistance.

File [C13]	"Tube Thermal Properties" (8F10.0) One Card

N.B. File required if and only if JHTW ≠ 0. (See File [M2].)

KW	Thermal conductivity (lbf/sec/R).
ALPHAW	Thermal diffusivity (in²/sec).
ALFAW	Emissivity factor (-).

File [C14]	"Tube Initial Temperature Profile" (8F10.0) One to Three Cards

N.B. File required if and only if NTEM ≠ 0. (See File [M4].)

ZW(1)	First axial location relative to breech (in).
TEMW(1)	Corresponding wall temperature (R).
.	
.	
.	
.	
ZW(NTEM)	Last location.
TEMW(NTEM)	Corresponding temperature.

File [M13]	"Projectile and Rifling Characteristics" (8F10.0) One Card

ZBPR	Initial axial location of base of projectile relative to breech (in).
WTPR	Mass of projectile (1bm).
PRIN	Polar moment of inertia of projectile (1bm-in^2).
RIF	Angle of rifling(^{o}).

File [C18]	"Ith Forward Compactible Filler Element Properties" (3F10.0,2I5) One Card

N.B. File required if and only if NEL ≠ 0. (See File [M4].) File is repeated NEL times.

XEL(I)	Position of left-hand boundary of Ith element (in). The array must be well ordered with respect to I. We require XEL(I) ≥ XEL(I-1). Forward elements are ordered so that the first is to the left.
MEL(1)	Mass of Ith element (1bm). If < 10^{-10} element is interpreted as a space. MEL(I) must be greater than 10^{-10}.

115

FEL(I)   Initial resistance to motion of Ith element (1bf).

NTYPE(I)   If NTYPE(I) = 0, element is treated as perfectly plastic
                        (deformation under loading only).
                        If NTYPE(I) = 1, element is treated as elastic.
                        If NTYPE(I) = 2, element is treated as rigid.
                        If NTYPE(I) = 3, element is treated as incompressible.
                        $0 \leq NTYPE(I) \leq 3$.

NDATA(I)   Number of pairs of entries in stress-strain table of
                        Ith element. $0 \leq NDATA(I) \leq 10$.

File [C19]   "Constitutive Data for Ith Forward Element"   (8F10.0)
                        One to Three Cards

N.B. File required if and only if MEL(I) $> 10^{-10}$ and NTYPE(I) $<$ 2. (See
      File [C18].) File is repeated for each element for which NDATA $>$ 0.
      Files [C19], as a group, follow Files [C18], as a group.

YEL(I,1)[*]   First engineering strain taken positive in compression
                        (dimensionless). Must be zero.

RESEL(I,1)[**]   Corresponding stress taken positive in compression (psi).
  .
  .
  .
  .
RESEL(I,NDATA(I))   Last engineering stress. Should exceed maximum pressure
                        in gun.

---

[*]   The array YEL must be well ordered. All entries must be in the
        interval [0,1].

[**]   The array RESEL must have non-zero entries and must be non-decreasing
        for each element.

116

File [C19.1]	"Ith Rear Compactible Filler Element Properties" (3F10.0,2I5) One Card

N.B. File required if and only if NBL ≠ 0. (See File [M4].) File is repeated NBL times.

XBL(I) Position of right-hand boundary of Ith element (in). The array must be well ordered with respect to I. XBL(I) observes the opposite convention from that of XEL(I), that is XBL(I) $\leq$ XBL(I-1) for all I. Rear elements are tabulated so that the first is to the right.

MBL(I) Mass of Ith element (lbm). If $< 10^{-10}$ element is interpreted as a space. MBL(I) must be greater than 10^{-10}.

FBL(I) Initial resistance to motion of Ith element (lbf).

NTYPB(I) If NTYPB(I) = 0, element is treated as perfectly plastic (deformation under loading only).
If NTYPB(I) = 1, element is treated as elastic.
If NTYPB(I) = 2, element is treated as rigid.
If NTYPB(I) = 3, element is treated as incompressible.
$0 \leq$ NTYPB(I) ≤ 3.

NDATB(I) Number of pairs of entries in stress-strain table of Ith element. $0 \leq$ NDATB(I) ≤ 10.

File [C19.2]	"Constitutive Data for Ith Rear Element" (8F10.0) One to Three Cards

N.B. File required if and only if MEL(I) $> 10^{-10}$ and NTYPE(I) < 2. (See File [C19.1].) File is repeated for each element for which NDATB > 0. Files [C19.2], as a group, follow Files [C19.1], as a group.

YBL(I,1)[*] First engineering strain taken positive in compression (dimensionless). Must be zero.

RESBL(I,1)[**] Corresponding stress taken positive in compression (psi).
.
.
.
.

RESBL(I,NDATB(I)) Last engineering stress. Should exceed maximum pressure in gun.

---

[*] The array YBL must be well ordered. All entries must be in the interval [0,1].

[**] The array RESBL must have non-zero entries and must be non-decreasing for each element.

File [C23]	"Positions for Pressure Table Storage" (8F10.0) One Card

N.B.   File required if and only if NZPT ≠ 0.   (See File [M4].)

ZPT(1)   First position, relative to breech (in).

.
.
.
.

ZPT(NZPT)[*]   Last position.

_____

[*]   Output consists of tables of pressure at each of the NZPT positions
      together with value less that at the NZPTth position.

File [C23.01]	"Projectile Afterbody Pressure History Option" (8I5) One Card

N.B.   File required if and only if NZPT ≠ 0 and MODET = 1.   (See File [M4].)

IZPT(1)   0 if ZPT(1) is fixed in the tube reference frame.
.   1 if ZPT(1) is fixed in the projectile afterbody
.   reference frame.
.
.

IZPT(NZPT)

File [C23.1]	"Kinetics Option Counters" (3I5) One Card

N.B.   File required if and only if KMODE ≠ 0.   (See File [M2].)

NSPEC   Number of species. $1 \leq NSPEC \leq 10$.

NGASR   Number of reactions occurring in the mixture of combustion
                       products. $0 \leq NGASR \leq 10$. If NGASR > 0, File [C23.7] is
                       required.

NSOLR   Number of reactions occurring in the solid-propellant.
                       $0 \leq NSOLR \leq 10$. If NSOLR > 0, File [C23.8] is required.

File [C23.2]   "Properties of Species"   (2A4,1X,A1,6F10.0)   NSPEC Cards

N.B. File required if and only if KMODE ≠ 0. (See File [M2].)

SPCNAM(I)   Name of species, up to 8 alphanumeric characters.

FAZE(I)   Phase of species: G = gas or vapor; L = liquid; S = solid.
                    One alphanumeric character.

SPCV(I)   Specific heat at constant volume (lbf-in/lbm-R).

SPCP(I)   Specific heat at constant pressure (lbf-in/lbm-R).

SPBV(I)   Covolume (in^3/lbm). Only required if FAZE = G.

SPMOL(I)   Molecular weight (lbm/lbmol). Only required if FAZE = G.

SPDEN(I)   Density (lbm/in^3). Only required if FAZE = L or S.

CLOS(I)   Transfer coefficient in correlation for rate of deposition
                    of condensed species on surface of solid propellant
                    (sec/in^2). Only required if FAZE = L or S. If CLOS = 0,
                    the rate of deposition is zero.

N.B. The following File [C23.3] is repeated NPROP times, once for each type
of solid propellant.

File [C23.3]   "Composition of Propellant Near Field Combustion Products"
                    (8F10.0) NPROP to 2*NPROP Cards

N.B. File required if and only if KMODE ≠ 0. (See File [M2].)

ECHO(I)   Chemical energy released in near field combustion
                    (lbf-in/lbm).

YO(I,1)   Mass fraction of near field combustion products
  .   corresponding to species type 1 (-).
  .
  .
  .
  .
YO(I,NSPEC)   Mass fraction of near field combustion products
                    corresponding to species type NSPEC (-).

119

File [C23.4]	"Composition of Igniter Discharge Combustion Products" (8F10.0) One to Two Cards.

N.B. File required if and only if KMODE $\neq$ 0. (See File [M2].)

ECHO(I)	Chemical energy released by combustion of igniter material prior to injection (lbf-in/lbm).
YO(I,1)	Mass fraction of igniter products corresponding to species type 1 (-).
YO(I,NSPEC)	Mass fraction of igniter products corresponding to species type NSPEC (-).

File [C23.5]	"Composition of Initial Ambient Gas" (8F10.0) One to Two Cards

N.B. File required if and only if KMODE $\neq$ 0. (See File [M2].)

ECHO(I)	Internal energy (thermal component) of ambient gas (or mixture if condensed species are initially present) (lbf-in/lbm).
YO (I,1)	Mass fraction of species 1 (-).
YO(I,NSPEC)	Mass fraction of species NSPEC (-).

N.B.   The following File is repeated NPROP times, once for each type of
       solid propellant. Present storage limits only support the case
       NPROP = 1 with KMODE =2.

File [C23.6]   "Initial Composition of Solid Propellant"   (8F10.0)
                    NPROP to 2*NPROP Cards

N.B.   File required if and only if KMODE = 2. (See File [M2].)

ECHO(I)   Inactive.

YO(I,1)   Mass fraction of solid propellant corresponding to
  .   species 1 (-).
  .
  .
  .
YO(I,NSPEC)   Mass fraction of solid propellant corresponding to species
                    NSPEC (-).

File [C23.61]   "Composition of Traveling Charge Near Field Combustion
                    Products"   (8F10.0)   One to Two Cards

N.B.   File required if and only if KMODE ≠ 0 and NTC = 1.   (See File [M2].)

ECHTCO   Chemical energy released in near field combustion of
                    traveling charge (1bf-in/1bm).

YTCO(I)   Mass fraction of species 1 (-).
  .
  .
  .
  .
YTCO(NSPEC)   Mass fraction of species NSPEC (-).

File [C23.62]   "Types of Reactions in Mixture of Combustion Products"
                    (10I5)   One Card

N.B.   File required if and only if KMODE ≠ 0, NGASR ≠ 0 and NTC = 1.   (See
       Files [M2] and [C23.1].)

KRCTYP(1)   If 0, reaction 1 is of the Arrhenius type and is described
  .   by File [C23.7].
  .   If 1, reaction 1 is of the pressure dependent type and is
  .   described by [C23.71].
  .   If NTC = 0, KRCTYP(I) defaults to zero for all I.
  .
  .
  .
KRCTYP(NGASR)   Type of reaction NGASR

File [C23.63]   "Species Thermal Equilibration Switches" (10I5) One Card

N.B.   File required if and only if KMODE ≠ 0, NGASR ≠ 0 and NTC = 1.
        (See Files [M2] and [C23.1].)

KTEQL(1)   If 0, species 1 is assumed to be in constant thermal
  .   equilibrium with mixture of combustion products.
  .   If 1, species 1 is assumed to be thermally insulated from
  .   mixture of combustion products. If NTC = 0, KTEQL(I)
  .   defaults to zero for all I.
  .
  .
  .
  .
KTEQL(NSPEC)   Thermal equilibration switch for species NSPEC.

File [C23.7]   "Description of Arrhenius Reactions in Mixture of
                   Combustion Products"
                   (8I5/8F10.0/F10.0,D10.4,F10.0,D10.4,4F10.0/F10.0)
                   Four Cards For Each Such Reaction

N.B.   File required if and only if KMODE ≠ 0, NGASR ≠ 0 and KRCTYP(I) = 0.
        (See Files [M2], [C23.1] and [C23.62].)

KRCNTB(1,I)*   Pointer to first species acting as a reactant in
  .   reaction I.   0 ≤ KRCNTB ≤ NSPEC.
  .
  .
  .
KRCNTB(4,I)   Pointer to fourth species acting as a reactant in
                   reaction I.

KPRODB(1,I)*   Pointer to first species acting as a product in reaction I.
  .   0 ≤ KPRODB ≤ NSPEC.
  .
  .
  .
KPRODB(4,I)   Pointer to fourth species acting as a product in
                   reaction I.

STOIB(1,I)   Stoichiometric coefficient corresponding to first reactant
  .   species (-). Starts a new card.
  .
  .
  .
STOIB(4,I)   Stoichiometric coefficient corresponding to fourth reactant
                   species (-).

STOIB(5,I)	Stoichiometric coefficient corresponding to first product species (-).
.	
.	
.	
.	
STOIB(8,I)	Stoichiometric coefficient corresponding to fourth product species (-).
ECHB(I)	Chemical energy released by reaction (lbf-in/lbm). Starts a new card.
ARCB(I)	Pre-exponential factor in Arrhenius rate law (units yield lbm/in^3-sec).
ARXB(I)	Temperature exponent in Arrhenius rate law (-).
AREB(I)	Activation energy in Arrhenius rate law (lbf-in/lbmol).
AROB(1,I)	Order of reaction with respect to concentration of first reactant species (-).
.	
.	
.	
.	
AROB(4,I)	Order of reaction with respect to concentration of fourth reactant species (-).
AROB(5,I)	Order of reaction with respect to concentration of gas-phase (-). Starts a new card.

---

* The most general reaction supported involves four reactant and four product species. At least one reactant pointer and one product pointer must be different from zero. A zero entry simply implies a reduction in generality of the reaction.

File [C23.71]	"Description of Pressure-Dependent Reactions in Mixture of Combustion Products" (8I5/ 8F10.0/ 8F10.0) Three Cards For Each Such Reaction

N.B. File required if and only if KMODE $\neq$ 0, NGASR $\neq$ 0 and KRCTYP(I) = 1. (See Files [M2], [C23.1] and [C23.62].)

KRCNTB(1,I)*	Pointer to first species acting as a reactant in reaction I. 0 $\leq$ KRCNTB $\leq$ NSPEC.
. . . .	
KRCNTB(4,I)	Pointer to fourth species acting as a reactant in reaction I.
KPRODB(1,I)*	Pointer to first species acting as a product in reaction I. 0 $\leq$ KPRODB $\leq$ NSPEC.
. . . .	
KPRODB(4,I)	Pointer to fourth species acting as a product in reaction I.
STOIB(1,I)	Stoichiometric coefficient corresponding to first reactant species (-). Starts a new card.
. . . .	
STOIB(4,I)	Stoichiometric coefficient corresponding to fourth reactant species (-).
STOIB(5,I)	Stoichiometric coefficient corresponding to first product species (-).
. . . .	
STOIB(8,I)	Stoichiometric coefficient corresponding to fourth product species (-).
ECHB(I)	Chemical energy released by reaction (1bf-in/1bm). Starts a new card.

DIAB(I)	Particle diameter, assumed constant (in).
B1B(I)	Burn rate additive constant (in/sec).
B2B(I)	Burn rate pre-exponential factor (in/sec-psi^{BNB}).
BNB(I)	Burn rate exponent (-)

---

*   The most general reaction supported involves four reactant and four product species. At least one reactant pointer and one product pointer must be different from zero. A zero entry simply implies a reduction in generality of the reaction.

File [C23.8]	"Description of Reactions in Solid Propellant" (8I5/8F10.0/F10.0,D10.4,F10.0,D10.4,4F10.0) 3*NSOLR Cards

N.B.   File required if and only if KMODE $\neq$ 0 and NSOLR $\neq$ 0. (See Files [M2] and [C23.1].)

KRCNTS(1,I)*	Pointer to first species acting as a reactant in reaction I. 0 $\leq$ KRCNTS $\leq$ NSPEC.
KRCNTS(4,I)	Pointer to fourth species acting as a reactant in reaction I.
KPRODS(1,I)*	Pointer to first species acting as a product in reaction I. 0 $\leq$ KPRODS $\leq$ NSPEC.
KPRODS(4,I)	Pointer to fourth species acting as a product in reaction I.
STOIS(1,I)	Stoichiometric coefficient corresponding to first reactant species (-). Starts a new card.
STOIS(4,I)	Stoichiometric coefficient corresponding to fourth reactant species (-).

STOIS(5,I)	Stoichiometric coefficient corresponding to first product species (-).
.	
.	
.	
.	
STOIS(8,I)	Stoichiometric coefficient corresponding to fourth product species (-).
ECHS(I)	Chemical energy released by reaction (1bf-in/1bm). Starts a new card.
ARCS(I)	Pre-exponential factor in Arrhenius rate law (units yield lbm/in^3-sec).
ARIS(I)	Temperature exponent in Arrhenius rate law (-).
ARES(I)	Activation energy in Arrhenius rate law (1bf-in/1bmol).
AROS(1,I)	Order of reaction with respect to concentration of first reactant species (-).
.	
.	
.	
.	
AROS(4,I)	Order of reaction with respect to concentration of fourth reactant species (-).

---

* The most general reaction supported involves four reactant and four product species. At least one reactant pointer and one product pointer must be different from zero. A zero entry simply implies a reduction in generality of the reaction.

File [C23.9]	"Solid Propellant Thermal Response Parameters" (3I5,5F10.0) One Card

N.B. File required if and only if KMODE = 2. (See File [M2].)

NZC — Number of stations for analysis of thermal response of solid propellant. $0 \leq NZC \leq 21$.

NZCBC — If 0, pyrolysis law is assumed to gover regression of surface of solid propellant.
If 1, evaporative (Clausius Clapeyron) law is assumed to govern regression of surface of solid propellant.

NOFLAM — If 0, heat feedback from the gas-phase is considered according to the Zel'dovitch formulism.
If 1, heat feedback from the gas-phase is neglected.

AS — Pre-exponential factor in solid propellant surface regression law. If NZCBC = 0, units are in/sec. If NZCBC = 1, units are psi.

ES — Activation energy (NZCBC = 0) or heat of vaporization (NZCBC = 1) in solid propellant surface regression law (lbf-in/lbmol).

TSEN — Temperature sensitivity of propellant steady state burn rate (1/R).

TTRANS — Time interval over which external stimulus drops to zero following ignition of the surface of the propellant (sec).

PTRANS — Pressure above which thermal analysis is discontinued and steady state combustion is assumed to occur (psi).

File [C24]	"Parameters to Define Mesh in Invariant Embedding Analysis" (F10.0,3I5) One Card

N.B. File required if and only if KMODE = 2. (See File [M2].)

DELX*   Mesh spacing in group closest to heated surface ($sec^{1/2}$)
             DELX > 0.

N**   Number of intervals per group.

MDELX   Integer multiple by which mesh spacing increases from group
             to group as we move away from heated surface.

NGRP   Number of groups. $1 \leq NGRP \leq 10$.

---

*   Refers to computational coordinate $x/\sqrt{\alpha}$ where x is distance from
     heated surface and α is thermal diffusivity.

** $N*NGRP \leq 200$.

File [C25]	"Tank Gun Option Control Data" (16I5) One Card

N.B. File required if and only if MODET = 1. (See File [M2].)

NAFT   Number of pairs of data to describe projectile afterbody.
             NAFT may be zero. Otherwise $2 \leq NAFT \leq 10$.

JIS(1)   Switch to define level of modeling of surface source term
             attributed to tube wall.

JIS(1)	Model
0	No source term
1	Tabular source term
2	Rate of source determined according to ignition and combustion submodels.

JIS(2)   Switch to define level of modeling of surface source term
             attributed to centerline of tube.

JIS(3)   Switch to define level of modeling of surface source term
             attributed to afterbody of projectile.

NENDL	Number of endwalls defined by packaging of charge. $0 \leq$ NENDL ≤ 21.
NPRM	Number of permeability data sets. $0 \leq$ NPRM ≤ 10.
NRCT	Number of reactivity data sets. $0 \leq$ NRCT ≤ 9.
NSEGS(1)	Number of segments having different properties in tube wall surface source. $0 \leq$ NSEGS(1) ≤ 3. Default value is 1.
NSEGS(2)	Number of segments in centerline surface source.
NSEGS(3)	Number of segments in afterbody surface source.
KCTRL	If 0, control charge not present. If 1, control charge is present. Files [C28] – [C28.7] required.
NZCRE	Number of data to describe external geometry of ballistic control tube.
INHBCR(1)	If 0, control charge not deterred. If 1, control charge is deterred.

File [C25.1]	"Geometry of Projectile Afterbody" (8F10.0) One to Three Cards.

N.B. File required if and only if MODET = 1 and NAFT ≥ 2.
      (See Files [M2] and [C25].)

ZAFT(1)*	First axial position on afterbody (in).
RAFT(1)	Corresponding radius of afterbody (in).
.	
.	
.	
.	
ZAFT(NAFT)	Last axial position.
RAFT(NAFT)	Corresponding radius of afterbody.

---

* The origin of the coordinate ZAFT is independent of that used to describe the gun tube. INOVAT internally reconciles the coordinate frames by assuming that ZAFT(NAFT) coincides with ZBPR. (See File [M13].)

N.B. The following files, [C25.2] through [C26.3] are repeated, as needed, as a group for each of the three types of reactive layers whose presence is indicated by a non-zero value of JIS(I). (See File [C25].)

File [C25.2] "Thickness and Density Counters for Reactive Layer I" (4I5) One Card

---

N.B. File required if and only if MODET = 1 and JIS(I) ≠ 0. (See Files [M2] and [C25].)

NSTAC(I)   Number of data to describe thickness of reactive layer I. $2 \leq$ NSTAC(I) ≤ 10.

NRHOS(I,1)   Number of data to describe density of first segment of reactive layer I as a function of pressure. $1 \leq$ NRHOS(I) ≤ 10.

NRHOS(I,2)   Number of data for second segment of reactive layer I.

NRHOS(I,3)   Number of data for third segment.

File [C25.3] "Thickness of Reactive Layer I" (8F10.0) One to Three Cards

---

N.B. File required if and only if MODET = 1 and JIS(I) ≠ 0. (See Files [M2] and [C25].)

ZAC(1,I)*   First axial position (in).

THC(1,I)   Corresponding thickness of reactive layer (in).
   •
   •
   •
   •

ZAC(NSTAC(I),I)   Last axial position.

THC(NSTAC(I),I)   Corresponding thickness.

---

*   When I = 1 or 2, ZAC is assumed to refer to the coordinate system used to define the tube geometry. When I = 3, ZAC is assumed to correspond to the coordinate system used to define the afterbody of the projectile. The thickness of layer I is taken to be zero outside the table range.

File [C25.31] "Segment Pointers for Reactive Layer I (8I5) One Card

---

N.B. File required if and only if MODET = 1, JIS(I) $\neq$ 0 and NSEGS(I) > 1.
(See Files [M2] and [C25].)

NSG(1,I)   Segment property type for axial positions between ZAC(1,I)
                  and ZAC(2,1).

.
.
.
.

NSG(NSTAC(I)-1,I) Segment property type for axial positions between
                   ZAC(NSTAC(I)-1,I) and ZAC(NSTAC(I),I).

NSG(NSTAC(I),I)   Not used.

N.B. If Reactive Layer I consists of more than one segment, the following
     Files [C25.4] through [C26.3] are repeated as a group for each of the
     segments of the layer. The subscript pertaining to the segment is
     suppressed in the following discussion.

File [C25.4]   "Density of Reactive Layer I" (8F10.0) One to Three Cards

---

N.B. File required if and only if MODET = 1 and JIS(I) $\neq$ 0.
(See Files [M2] and [C25].)

RHOS(1,I)*   Value of density at first pressure (lbm/in^3).

PRHOS(1,I)   First value of pressure (psi).

.
.
.
.

RHOS(NRHOS(I),I)   Last value of density.

PRHOS(NRHOS(I),I) Last value of pressure.

---

* Outside the table range, the first or the last value of RHOS applies. If
  a single value is specified, the density is taken to be constant and
  therefore independent of pressure.
  At present, case compressibility is only modeled if JIS(I) = 2. (See File
  [C25].)

File [C25.5] "Counter to Describe Discharge of Reactive Layer I" (2I5)
One Card

N.B. File required if and only if MODET = 1 and JIS(I) = 1.
(See Files [M2] and [C25].)

IIS(I)   Number of axial positions in discharge table.
                $2 \leq IIS(I) \leq 10$.

JJS(I)   Number of times in discharge table. $2 \leq JJS(I) \leq 10$.

File [C25.6] "Positions to Describe Discharge of Reactive Layer I"
(8F10.0) One to Two Cards

N.B. File required if and only if MODET = 1 and JIS(I) = 1.
(See Files [M2] and [C25].)

ZPHIS(1,I)*   First position (in).
  .
  .
  .
  .
ZPHIS(IIS(I),I) Last position (in).

* The coordinate frame for ZPHIS is assumed to accord with that for ZAC.
(See File [C25.3].)

File [C25.7] "Times to Describe Discharge of Reactive Layer I" (8F10.0)
One to Two Cards

N.B. File required if and only if MODET = 1 and JIS(I) = 1.
(See Files [M2] and [C25].)

TPHIS(1,I)   First time (msec).
  .
  .
  .
  .
TPHIS(JJS(I),I) Last time (msec).

File [C25.8]   "Rate of Discharge of Reactive Layer I"   (8F10.0)
               One to Thirteen Cards

N.B.   File required if and only if MODET = 1 and JIS(I) = 1.
       (See Files [M2] and [C25].)

PHIS(1,1,I)   Rate of discharge at first position and first time
               (1bm/in-sec).

PHIS(2,1,I)   Rate of discharge at second position and first time.
   .
   .
   .
   .
PHIS(IIS(I),1,I)   Rate of discharge at last position and first time.
   .
   .
   .
   .
PHIS(IIS(I),JJS(I),I)   Rate of discharge at last position and last time.

File [C25.9]   "Burn Rate Counters for Reactive Layer I"   (2I5)   One Card

N.B.   File required if and only if MODET = 1 and JIS(I) = 2.
       (See Files [M2] and [C25].)

KBRDS(I)   Number of burn rate data. $1 \leq$ KBRDS $\leq$ 10.

KNHIB(I)   If 0, layer I is not deterred.
               If 1, layer I is deterred.

File [C26]   "Burn Rate Data for Reactive Layer I"   (8F10.0)
               One to Three Cards

N.B.   File required if and only if MODET = 1 and JIS(I) = 2.
       (See Files [M2] and [C25].)

UPPRS(1,I)*   First pressure limit (psi).

B22S(1,I)   Value of pre-exponent for pressures less than UPPRS(1,I)
               $(in/sec-psi^{BNNS})$.

BNNS(1,I)   Value of exponent for pressures less than UPPRS(1,I) (-).

.

.

.

.

UPPRS(KBRDS(I),I)*   Last pressure limit (psi).

B22S(KBRDS(I),I)   Value of pre-exponent for pressures less than
                     UPPRS(KBRDS(I),I) but greater that UPPRS(KBRDS(I)-1,I).

BNNS(KBRDS(I),I)   Corresponding exponent (-).

---

* Outside the table range the first and last values are used.

File [C26.1]   "Ignition Data for Reactive Layer I"   (8F10.0) One Card

---

N.B.   File required if and only if MODET = 1 and JIS(I) = 2.
       (See Files [M2] and [C25].)

B1S(I)   Burn rate additive constant (in/sec).

TMPIGS(I)   Ignition temperature (R).

KPS(I)   Thermal conductivity (lbf/sec-R).

ALPHAS(I)   Thermal diffusivity (in^2/sec).

File [C26.2]   "Thermochemical Data for Reactive Layer I"   (8F10.0) One Card

---

N.B.   File required if and only if MODET = 1 and JIS(I) = 2.
       (See Files [M2] and [C25].)

EIGS(I)   Chemical energy released during combustion (lbf-in/lbm).

GMS(I)   Molecular weight of products of combustion (lbm/lbmol).

GAMAS(I)   Ratio of specific heats (-).

File [C26.21] "Composition of Reactive Layer Near Field Combustion
Products" (8F10.0) One Card

N.B. File required if and only if MODET = 1, KMODE = 1 and JIS(I) = 2.
(See Files [M2] and [C25].)

YSO(I,1)   Mass fraction of species 1 (-).

.

.

.

.

YSO(I,NSPEC)   Mass fraction of species NSPEC (-).

File [C26.3] "Properties of Deterred Layer of Reactive Layer I" (8F10.0)
One Card

N.B. File required if and only if MODET = 1, JIS(I) = 2 and KNHIB(I) = 1.
(See Files [M2], [C25] and [C25.9].)

ECHIS(I)*   Internal energy released in combustion at start of deterred
                layer (lbf-in/lbm).

ECHIS2(I)   Internal energy released in combustion at end of deterred layer
                (lbf-in/lbm).

RGFAS(I)*   Factor by which burn rate is multiplied at start of deterred
                layer (-).

RGFAS2(I)   Factor by which burn rate is multiplied at end of deterred
                layer (-).

HIBS(I)   Depth of deterred layer (in).

---

*   Values within deterred layer deduced by linear spacewise interpolation
    with an allowance for compression of the reactive layer. Final values
    need not be the same as those of the undeterred layer.

File [C26.4]   "Endwall Property Pointers"   (4I5)   NENDL Cards

N.B.   File required if and only if MODET = 1 and NENDL ≠ 0.
(See Files [M2] and [C25].)

NBAGL(I)   Pointer to propellant increment to which Ith endwall is attached. If NBAGL(I) = 0, the endwall is assumed to be attached to the breech of the gun. An increment may include several parallel packaged bundles of propellant.

NBAGE(I)   If 0, endwall is at rear of increment.
If 1, endwall is at front of increment.

NREACT(I)   Pointer to reactivity models associated with endwall. NREACT is interpreted as a four digit number. Each digit points to a different model. A zero value implies no reactivity. The digits have the following meanings

Digit	Source of Reactivity
1	Internal attached component
2	Interior of endwall
3	Exterior of endwall
4	External attached component

NPERM(I)   Pointer to permeability model associated with endwall.

File [C26.5]   "Permeability Model Data"   (8F10.0)   NPRM Cards

N.B.   File required if and only if MODET = 1 and NPRM ≠ 0.
(See Files [M2] and [C25].)

PRM(I)   Initial flow resistance coefficient for Ith model (-).

RUPSTR(I)   Pressure differential at which rupture of endwall commences (psi).

RUPINT(I)   Time interval over which rupture of endwall is completed (msec).

N.B. The following Files, [C26.6] through [C27], are repeated as a group for each of the NRCT reactivity models.

File [C26.6] "File Counters for I-th Reactivity Model" (3I5) One Card

---

N.B. File required if and only if MODET = 1 and NRCT ≠ 0.
(See Files [M2] and [C25].)

KBRDE(I)   Number of data in modeled burn rate description (-). If
                KBRDE(I) = 0, it is assumed that tabular discharge data are
                specified. 0 ≤ KBRDE(I) ≤ 10.

IGCRIT(I)   Ignition criterion for modeled burn rate description.
                Ignition is determined by reference to VALIG(I)
                (File [C26.8]) as follows.

IGCRIT(I)	VALIG(I)
1	Time Delay (μsec)
2	Ambient gas temperature (R)
3	Neighboring propellant temperature (R)

JRCT(I)   Number of data in tabular burn rate description (-).
                JRCT(I) = 0 or 2 ≤ JRCT(I) ≤ 8.

File [C26.7] "Thermochemical Data for I-th Reactivity Model" (8F10.0)
One Card

N.B. File required if and only if MODET = 1 and NRCT ≠ 0.
(See Files [M2] and [C25].)

RHOE(I)   Density (lbm/in^3).

EIGE (I)   Chemical energy released during combustion ($lbf-in/lbm$).

GME(I)   Molecular weight of combustion products ($lbm/lbmol$).

GAMAE(I)   Ratio of specific heats of combustion products (-).

File [C26.71] "Composition of Near Field Combustion Products of I-th
Reactivity Model" (8F10.0) One Card

N.B. File required if and only if MODET = 1, KMODE = 1 and NRCT ≠ 0.
(See Files [M2] and [C25].)

YEE(I,1)   Mass fraction of species 1 (-).
.
.
.
.

YEE(I,NSPEC)   Mass fraction of species NSPEC (-).

File [C26.8] "Ignition Value for I-th Reactivity Model" (8F10.0) One Card

N.B. File required if and only if MODET = 1, NRCT ≠ 0 and KBRDE(I) ≠ 0.
(See Files [M2], [C25] and [C26.6].)

VALIG(I)   Value of time delay (msec), gas temperature (R) or propellant
                temperature (R) in accordance with IGCRIT(I) as defined above.
                (See File [C26.6].)

File [C26.9] "Burn Rate Data for I-th Reactivity Model" (8F10.0)
             One to Three Cards

N.B. File required if and only if MODET = 1, NRCT ≠ 0 and KBRDE(I) ≠ 0.
(See Files [M2], [C25] and [C26.6].)

UPPRE(1,I)*   First pressure limit (psi).

B22E(1,I)   Value of pre-exponent for pressures less than UPPRE(1,I)
                (in/sec-psi^{BNNE}).

BNNE(1,I)   Value of exponent for pressures less than UPPRE(1,I) (-).
.
.
.
.

UPPRE(KBRDE(I),I)* Last pressure limit (psi).

B22E(KBRDE(I),I)   Value of pre-exponent for pressures less than
                    UPPRE(KBRDE(I),I) but greater than UPPRE(KBRDE(I)-1,I).

BNNE(KBRDE(I),I)   Corresponding exponent (-).

---
* Outside the table range the first and last values are used.

138

File [C27]   "Tabular Description of I-th Reactivity Model"   (8F10.0)
             One or Two Cards

N.B.   File required if and only if MODET = 1, NRCT ≠ 0, KBRDE(I) = 0 and
       $2 \leq JRCT(I) \leq 8$. (See Files [M2], [C25] and [C26.6].)

TRCT(1,I)   First value of time (msec).

FLORCT(1,I)   Corresponding rate of combustion (lbm/in^2-sec).
  .
  .
  .
  .
TRCT(JRCT(I),I)   Last value of time.

FLORCT(JRCT(I),I)   Corresponding rate of combustion.

File [C28]   "Internal Properties of Control Charge Combustion Chamber"
             (8F10.0)   One Card

N.B.   File required if and only if MODET = 1 and KCTRL ≠ 0.
       (See Files [M2] and [C25].)

CDCR   Discharge coefficient for venting to gun chamber (-).

RCRI   Internal radius of bore (in).

VCRO   Initial chamber volume corresponding to zero afterbody
            offset (in^3).

ZCRO   Initial afterbody offset (in).

File [C28.1] "External Properties of Control Charge Combustion Chamber"
(3F10.0) NZCRE Cards

N.B. File required if and only if MODET = 1 and KCTRL ≠ 0.
(See Files [M2] and [C25].)

ZCRE(1)   First axial position relative to breechface of gun (in).

RCRE(1)   Corresponding external radius of chamber (in).

AVENT(1)   Total sidewall vent area exposed when base of afterbody is at
               ZCRE(1) (in^2).

ZCRE(2)   Second axial position. (New Card)
  •
  •
  •
  •
ZCRE(NZCRE)   Last axial position. (New Card)

RCRE(NZCRE)

AVENT(NZCRE)

File [C28.2] "Control Charge Type" (5A4,2F10.0) One Card

N.B. File required if and only if MODET = 1 and KCTRL ≠ 0.
(See Files [M2] and [C25].)

GENMCR   Name of propellant. Up to 20 alphanumeric characters.

WGTCR   Mass of control charge (lbm).

RHOPCR   Density of propellant (lbm/in^3).

File [C28.3] "Control Charge Form Function"   (I5,4F10.0)   One Card

N.B.   File required if and only if MODET = 1 and KCTRL ≠ 0.
(See Files [M2] and [C25].)

NFRMCR   Form function indicator. See discussion of File [M8].
              Allowable values of NFRMCR are 1, 2, 5, 6 and 7.

ODCR   Grain dimension (in). See File [M8].

DPRFCR   Grain dimension (in). See File [M8].

GLENCR   Grain length (in).

NPRFCR   Number of perforations (-).

File [C28.4]   "Control Charge Burn Rate Counter"   (I5)   One Card

N.B.   File required if and only if MODET = 1 and KCTRL ≠ 0.
(See Files [M2] and [C25].)

NBRDCR   Number of sets of values used to describe burn rate.
              $1 \leq$ NBRDCR ≤ 10.

File [C28.5]   "Control Charge Burn Rate Description"   (8F10.0)
                   One to Four Cards

N.B.   File required if and only if MODET = 1 and KCTRL ≠ 0.
(See Files [M2] and [C25].)

UPPCR(1)   Maximum value of pressure for corresponding values of burn rate
              pre-exponential and exponential factors (psi)

B22CR(1)   Burning rate pre-exponential factor (in/sec-psi^n).

BNNCR(1)   Burning rate exponent (-).
  .
  .
  .

UPPCR(NBRDCR) Maximum value for last set of burn rate data.

B22(NBRDCR)   Corresponding pre-exponent.

BNN(NBRDCR)   Corresponding exponent.

B1CR   Burning rate additive constant (in/sec).

DELCR   Ignition delay (msec).

141

File [C28.6] "Control Charge Thermochemistry" (8F10.0) One Card

---

N.B. File required if and only if MODET = 1 and KCTRL ≠ 0.
(See Files [M2] and [C25].)

ECHCR   Internal energy released in combustion (1bf-in/1bm).

WMCR   Molecular weight of combustion products (1bm/1bmol).

AMACR   Ratio of specific heats (-).

File [C28.7] "Properties of Deterred Layer" (8F10.0) One Card

---

N.B. File required if and only if MODET = 1 and KCTRL ≠ 0 and INHBCR = 1.
(See Files [M2] and [C25].)

ECRIB*   Internal energy released in combustion at start of
           deterred layer (1bf-in/1bm).

ECRIB2   Internal energy released in combustion at end of
           deterred layer (1bf-in/1bm).

RGFCR   Factor by which burn rate is multiplied at start of
           deterred layer (-).

RGFCR2   Factor by which burn rate is multiplied at end of
           deterred layer (-).

HIBXCR   Depth of inhibited layer (in).

---

*   Values within deterred layer deduced by linear spacewise
    interpolation. Final values need not be the same as those of the
    undeterred propellant.

File [TC1]	"Traveling Charge Control Data" (7I5)	One Card TC-Mandatory

IDEAL
: Propellant burn rate indicator.
0 – Measured burn rate data. See Files [TC5]-[TC8].
1 – Not supported.
2 – Ideal burning with prespecified value of pressure on either side of gas/traveling charge interface or of projectile acceleration. Note the discussion of SIGMAX, MACH, APMAX in File [TC2].

NPRC
: 0 – Traveling charge treated as rigid.
1 – Traveling charge treated as a continuum with analytical description of rheology. File [TC9] required.
2 – Traveling charge treated as continuum with tabular description of rheology. Files [TC10] and [TC11] required.

NPROP
: Number of traveling charge increments (maximum of 20).

NWFR
: Propellant Wall Friction Parameter.
0 – Friction between propellant and tube not considered.
1 – Friction due to gas film. File [TC12] required.
>0 – Number of entries in velocity dependent coefficient of friction table (maximum of 10). File [TC13] required.

NBRES1
: 0 – Obturator resistance not given as table.
>0 – Number of entries in table of resistive pressure versus travel (maximum of 10). File [TC14] required.

NBRES2
: 0 – Resistance due to shocked air not considered.
1 – Resistance due to shocked air considered. File [TC15] required.

NBRES3
: 0 – Obturator resistance not proportional to setback pressure.
>0 – Number of entries in table of velocity-dependent coefficient of friction of obturator (maximum of 10). Files [TC16] and [TC17] required.

File [TC2]	"Mesh Parameters" (I5,F10.0)	One Card TC-Mandatory

MAXDIM
: Maximum number of mesh points to be used in continuum representation of traveling charge (≤ 100).

DXMIN
: Minimum mesh size for continuum representation (in).

File [TC3]   "General Properties"   (6F10.0)   One Card   TC-Mandatory

DB   Diameter of tube (in).

XIB   Initial length of gas column (in).

PRM   Mass of projectile (lbm).

SIGMAX   Maximum value of pressure at gas/propellant interface (psi).
                If SIGMAX = 0, no restriction is considered. SIGMAX pertains
                to the reacted or the unreacted side of the flame according
                as NPORS(KK) = 0 or 1 respectively. (See File [TC5].)

MACH   Maximum value of Mach number of combustion products relative
                to regressing surface. If MACH = 0, no restriction is
                considered.

APMAX   Maximum value of acceleration of projectile (gravities). If
                APMAX = 0, no restriction is considered.

N.B.   Files [TC4] through [TC13] pertain to a specific type of
        propellant. The sequence [TC4] through [TC13], subject to
        relevant contingencies, is repeated for each type of traveling
        charge propellant in the problem. The index KK used in the
        following file descriptions runs through the values
        1,2, . . ., NPROP, where NPROP is defined in File [TC1].

File [TC4]   "Propellant Thermochemical Properties"   (8F10.0)   One Card
                                                                    TC-Mandatory

XGAM(KK)   Ratio of specific heats of gas (--).

XBV(KK)   Covolume (in^3/lbm).

XMOL(KK)   Molecular weight (lbm/lbmol).

XECHEM(KK)   Chemical energy of propellant (lbf-in/lbm).

XRHOP(KK)   Density of solid propellant at zero pressure (lbm/in^3).

XCM(KK)   Mass of propellant (lbm).

XCRIT(KK)   Time delay following first exposure of increment base before
                combustion begins (msec).

XDEL(KK)   Time interval over which increment combustion rate increases
                to steady-state value (msec).

File [TC5] "Burn Rate Switches" (2I5) One Card TC-Mandatory

MNBR1(KK) 0 — Exponential form for measured burn rate description of propellant KK.
 — Tabular form for measured burn rate description of propellant KK.

NPORS(KK) 0 — Measured burn rate data are given as function of pressure on reacted side of flame. Ideal burn rate value SIGMAX (see File [TC3]) pertains to reacted side.
 1 — Measured burn rate data are given as function of pressure on unreacted side of flame. Ideal burn rate value SIGMAX pertains to unreacted side.

File [TC6] "Tabular Burn Rate Data" (2I5,F10.0) One Card TC-Contingent

---

N.B. File is required if and only if IDEAL = 0 and MNBR1(KK) = 1. (See Files [TC1] and [TC5]).

NBRP(KK) Number of pairs of data in KK-th tabular description of burn rate (maximum of 20.)

INTD Number of table entries to use in divided difference interpolation. The same value is assumed for all propellants.

B1(KK) Burn rate additive constant for KK-th increment (in/sec).

File [TC7] "Tabular Burn Rate Data (cont'd)" (2F10.0) NBRP(KK) Cards
 TC-Contingent

N.B. File is required if and only if IDEAL = 0 and MNBR1(KK) = 1. (See Files [TC1] and [TC5].)

PE(1,KK) First value of pressure in tabular description of burn rate of propellant KK (psi).

RP(1,KK) First value of burn rate of propellant KK corresponding to PE(1,KK) (in/sec).

.
.
.
.

PE(NBRP(KK),KK)

RP(NBRP(KK),KK)

File [TC8]   "Exponential Burn Rate Data"   (3F10.0)   One Card   TC-Contingent

---

N.B.   File required if and only if IDEAL = 0 and MNBR1(KK) = 0.
        (See Files [TC1] and [TC5].)

B1(KK)   Burn rate additive constant for KK-th propellant (in/sec).

B2(KK)   Burn rate pre-exponential coefficient for KK-th propellant
              (in/sec-psi^{BN}).

BN(KK)   Burn rate exponent for KK-th propellant (--).

File [TC9]   "Propellant Analytical Rheology Data"   (2F10.0)   One Card
                                                                   TC-Contingent

---

N.B.   File required if and only if NPRC = 1.   (See File [TC1].)

XAUP(KK)   Compressive wave speed at zero pressure in analytical
              description of propellant rheology (in/sec).

XADWN(KK)   Expansion wave speed in analytical description of propellant
              rheology (in/sec). If XADWN(KK) is entered so that it is
              less than the nominal compressive wave speed, the loading
              value is used. By entering XADWN(KK) = 0, a reversible law
              is defined.

File [TC10]   "Propellant Tabular Rheology Data"   (I5)   One Card
                                                             TC-Contingent

---

N.B.   File required if and only if NPRC = 2.   (See File [TC1].)

MNSS(KK)   Number of pairs of entries in tabular description of
              propellant rheology (maximum of 20).

File [TC11]   "Propellant Tabular Rheology Data (cont'd)"   (3F10.0)
                                        MNSS(KK) Cards   TC-Contingent
---

N.B.   File required if and only if NPRC = 2.   (See File [TC1].)

PSTA(1,KK)   First value of percent strain in tabular description of
               propellant rheology (-).

STRL(1,KK)   Corresponding value of pressure on nominal loading
               (compression curve (psi)).

STRU(1,KK)   Corresponding value of pressure on nominal unloading
    .   (expansion curve (psi)).
    .
    .

    .
PSTA(MNSS(KK),KK)

STRL(MNSS(KK),KK)

STRU(MNSS(KK),KK)

File [TC12]   "Ablative Film Data"   (2F10.0)   One Card   TC-Contingent
---

N.B.   File required if and only if NWFR < 0.   (See File [TC1].)

VISLYR(KK)   Viscosity of gas film used to lubricate propellant
               (1bm/in-sec).

DELYR(KK)   Thickness of film (in).

File [TC13]   "Propellant Friction Data"   (8F10.0)   One to Three Cards
                                                      TC-Contingent
---

N.B.   File required if and only if NWFR > 0.   (See File [TC1].)
       All propellants are assumed to have the same number of data NWFR.

AMUV(1,KK)   First value of velocity of propellant (in/sec).

AMU(1,KK)   Corresponding coefficient of friction on tube (-).
    .
    .
    .

    .
AMUV(NWFR,KK) Last value of velocity (in/sec).

AMU(NWFR,KK)   Corresponding coefficient of friction (-).

147

File [TC14] "Tabular Bore Resistance Data" (8F10.0) One to Three Cards
TC-Contingent

N.B. File required if and only if NBRES1 ≠ 0. (See File [TC1].)

BRX(1)   First value of projectile travel (in).

BR(1)   Corresponding value of resistive pressure due to obturator
                (psi).

.
.
.
.

BRX(NBRES1)   Last value of projectile travel (in).

BR(NBRES1)   Corresponding value of resistive pressure (psi).

File [TC15] "Barrel Shock Resistance Data" (4F10.0) One Card
TC-Contingent

N.B. File required if and only if NBRES2 ≠ 0. (See File [TC1].)

AIRGAM   Ratio of specific heats of air (-).

AIRPO   Pressure of air in barrel (psi).

AIRTO   Temperature of air in barrel (R).

AIRMW   Molecular weight of air in barrel (lbm/lbmol).

File [TC16] "Obturator Setback Resistance Data" (3F10.0) One Card
TC-Contingent

N.B. File required if and only if NBRES3 ≠ 0. (See File [TC1].)

PRMB   Mass of projectile ahead of midpoint of obturating band
                (lbm).

BLB   Length of bearing section of obturating band (in).

ANU   Poisson's ratio of obturating band (-).

File [TC17] "Obturator Friction Data" (8F10.0) One to Three Cards
                                                    TC-Contingent

N.B. File required if and only if NBRES3 ≠ 0. (See File [TC1].)

BMUV(1)   First value of velocity of projectile (in/sec).

BMU(1)   Corresponding value of coefficient of friction between
             obturator and tube (-).

  .
  .
  .
  .

BMUV(NBRES3) Last value of velocity of projectile (in/sec).

BMU(NBRES3) Corresponding coefficient of friction (-).

INTENTIONALLY LEFT BLANK.

150

No of Copies	Organization	No of Copies	Organization
(Unclass., unlimited) 12	Administrator	1	Commander
(Unclass., limited) 2	Defense Technical Info Center		US Army Missile Command
(Classified) 2	ATTN: DTIC-DDA		ATTN: AMSMI-RD-CS-R (DOC)
	Cameron Station		Redstone Arsenal, AL 35898-5010
	Alexandria, VA 22304-6145		

<table>
<tr><td>1</td><td>HQDA (SARD-TR)
WASH DC 20310-0001</td><td>1</td><td>Commander
US Army Tank-Automotive Command
ATTN: AMSTA-TSL (Technical Library)
Warren, MI 48397-5000</td></tr>
<tr><td>1</td><td>Commander
US Army Materiel Command
ATTN: AMCDRA-ST
5001 Eisenhower Avenue
Alexandria, VA 22333-0001</td><td>1</td><td>Director
US Army TRADOC Analysis Command
ATTN: ATAA-SL
White Sands Missile Range, NM 88002-5</td></tr>
<tr><td>1</td><td>Commander
US Army Laboratory Command
ATTN: AMSLC-DL
Adelphi MD 20783-1145</td><td>(Class. only) 1</td><td>Commandant
US Army Infantry School
ATTN: ATSH-CD (Security Mgr.)
Fort Benning, GA 31905-5660</td></tr>
<tr><td>2</td><td>Commander
Armament RD&E Center
US Army AMCCOM
ATTN: SMCAR-MSI
Picatinny Arsenal, NJ 07806-5000</td><td>(Unclass. only) 1</td><td>Commandant
US Army Infantry School
ATTN: ATSH-CD-CSO-OR
Fort Benning, GA 31905-5660</td></tr>
<tr><td>2</td><td>Commander
Armament RD&E Center
US Army AMCCOM
ATTN: SMCAR-TDC
Picatinny Arsenal, NJ 07806-5000</td><td>(Class. only) 1</td><td>The Rand Corporation
P.O. Box 2138
Santa Monica, CA 90401-2138</td></tr>
<tr><td>1</td><td>Director
Benet Weapons Laboratory
Armament RD&E Center
US Army AMCCOM
ATTN: SMCAR-CCB-TL
Watervliet, NY 12189-4050</td><td>1</td><td>Air Force Armament Laboratory
ATTN: AFATL/DLODL
Eglin AFB, FL 32542-5000</td></tr>
<tr><td>1</td><td>Commander
US Army Armament, Munitions
and Chemical Command
ATTN: SMCAR-ESP-L
Rock Island, IL 61299-5000</td><td colspan="2">Aberdeen Proving Ground
Dir, USAMSAA
    ATTN: AMXSY-D
        AMXSY-MP, H. Cohen
Cdr, USATECOM
    ATTN: AMSTE-TO-F
Cdr, CRDEC, AMCCOM
    ATTN: SMCCR-RSP-A
        SMCCR-MU
        SMCCR-MSI
Dir, VLAMO
    ATTN: AMSLC-VL-D</td></tr>
<tr><td>1</td><td>Commander
US Army Aviation Systems Command
ATTN: AMSAV-DACL
4300 Goodfellow Blvd.
St. Louis, MO 63120-1798</td><td></td><td></td></tr>
<tr><td>1</td><td>Director
US Army Aviation Research
and Technology Activity
Ames Research Center
Moffett Field, CA 94035-1099</td><td></td><td></td></tr>
</table>

No. of Copies	Organization	No. of Copies	Organization

1   Commander
USA Concepts Analysis Agency
ATTN: D. Hardison
8120 Woodmont Avenue
Bethesda, MD 20014-2797

1   C.I.A.
01R/DB/Standard
GE47 HQ
Washington, DC 20505

1   US Army Ballistic Missile Defense
Systems Command
Advanced Technology Center
P.O. Box 1500
Huntsville, AL 25807-3801

1   Chairman
DOD Explosives Safety Board
Room 856-C
Hoffman Bldg 1
2461 Eisenhower Avenue
Alexandria, VA 22331-9999

1   Commander
US Army Materiel Command
ATTN: AMCPM-GCM-WF
5001 Eisenhower Avenue
Alexandria, VA 22333-5001

1   Commander
US Army Materiel Command
ATTN: AMCDE-DW
5001 Eisenhower Avenue
Alexandria, VA 22333-5001

5   PEO - Armaments
Project Manager
Autonomous Precision-Guided
Munitions (APGM)
Armament RD&E Center
US Army AMCCOM
ATTN: AMCPM-CW
AMCPM-CWW
AMCPM-CWS, M. Fisette
AMCPM-CWA, H. Haussman
AMCPM-CWA-S, R. DeKleine
Picatinny Arsenal, NJ 07806-5000

2   Commander
Production Base
Modernization Agency
ATTN: AMSMC-PBM, A. Siklosi
AMSMC-PBM-E, L. Laibson
Picatinny Arsenal, NJ 07806-5000

3   PEO-Armaments
Project Manager
Tank Main Armament Systems
ATTN: AMCPM-TMA, K. Russell
AMCPM-TMA-105
AMCPM-TMA-120
Picatinny Arsenal, NJ 07806-5000

1   Commander
Armament RD&E Center
US Army AMCCOM
ATTN: SMCAR-AEE
Picatinny Arsenal, NJ 07806-5000

8   Commander
Armament RD&E Center
US Army AMCCOM
ATTN: SMCAR-AEE-B,
A. Beardell
D. Downs
S. Einstein
S. Westley
S. Bernstein
C. Roller
J. Rutkowski
B. Brodman
Picatinny Arsenal, NJ 07806-5000

3   Commander
Armament RD&E Center
US Army AMCCOM
ATTN: SMCAR-FSB-I, D. Spring
SMCAR-AEE
SMCAR-AES, S. Kaplowitz
Picatinny Arsenal, NJ 07806-5000

4   Commander
Armament RD&E Center
US Army AMCCOM
ATTN: SMCAR-FSS
SMCAR-HFM, E. Barrieres
R. Davitt
SMCAR-CCH-V, C. Mandala
Picatinny Arsenal, NJ 07806-5000

1   Commander
Armament RD&E Center
US Army AMCCOM
ATTN: SMCAR-FSA-T, M. Salsbury
Picatinny Arsenal, NJ 07806-5000

1   Commander
CECOM R&D Technical Library
ATTN: ASQNC-ELC-I-T. Myer Center
Fort Monmouth, NJ 07703-5001

No. of Copies	Organization	No. of Copies	Organization
1	Commandant US Army Armor School ATTN: ATZK-CD-MS, M. Falkovitch Armor Agency Fort Knox, KY 40121-5215	1	AF Astronautics Laboratory AFAL/TSTL (Technical Library) Edwards AFB, CA 92523-5000
2	Commander US Naval Surface Warfare Center ATTN: J. P. Consaga C. Gotzmer Indian Head, MD 20640-5000	1	AFSC/SDOA Andrews AFB, MD 20334
		1	AFATL/DLYV Eglin AFB, FL 32542-5000
4	Commander Naval Surface Warfare Center ATTN: Code 240, S. Jacobs Code 730 Code R-13, K. Kim R. Bernecker Silver Spring, MD 20903-5000	1	AFATL/DLXP Eglin AFB, FL 32542-5000
		1	AFATL/DLJE Eglin AFB, FL 32542-5000
		1	NASA/Lyndon B. Johnson Space Center ATTN: NHS-22 Library Section Houston, TX 77054
2	Commanding Officer Naval Underwater Systems Center ATTN: Code 5B331, R. S. Lazar Technical Library Newport, RI 02840	3	AAI Corporation ATTN: J. Herbert J. Frankle D. Cleveland P.O. Box 126 Hunt Valley, MD 21030-0126
5	Commander Naval Surface Warfare Center ATTN: Code G33, J. L. East W. Burrel J. Johndrow Code G23, D. McClure Code DX-21 Tech Lib Dahlgren, VA 22448-5000	1	Aerojet Ordnance Company ATTN: D. Thatcher 2521 Michelle Drive Tustin, CA 92680-7014
		1	Aerojet Solid Porpulsion Company ATTN: P. Micheli Sacramento, CA 95813
3	Commander Naval Weapons Center ATTN: Code 388, C. F. Price T. Parr Info Sci Div China Lake, CA 93555-6001	1	Atlantic Research Corporation ATTN: M. King 5390 Cherokee Avenue Alexandria, VA 22312-2302
1	Program Manager AFOSR Directorate of Aerospace Sciences ATTN: L. H. Caveny Bolling AFB, Washington DC, 20332-0001	3	AL/LSCF ATTN: J. Levine L. Quinn T. Edwards Edwards, CA 92523-5000
		1	AVCO Everett Research Laboratory ATTN: D. Stickler 2385 Revere Beach Parkway Everett, MA 02149-5936
5	Commander Naval Ordnance Station ATTN: L. Torreyson T. C. Smith D. Brooks W. Vienna Technical Library Indian Head, MD 20640-5000	2	Calspan Corporation ATTN: C. Murphy P.O. Box 400 Buffalo, NY 14225-0400

154

No. of Copies	Organization	No. of Copies	Organization
1	General Electric Company Armament Systems Department ATTN: M. J. Bulman 128 Lakeside Avenue Burlington, VT 95491-4985	1	Princeton Combustion Research Laboratory, Inc. ATTN: M. Summerfield 475 US Highway One Monmouth Junction, NJ 08852-9650
1	IITRI ATTN: M. J. Klein 10 W. 35th Street Chicago, IL 60616-3799	2	Rockwell International Rocketdyne Division ATTN: BA08, J. E. Flanagan J. Gray 6633 Canoga Park, CA 91303-2703

1	Hercules, Inc.
	Allegheny Ballistics Laboratory
	ATTN: William B. Walkup
	P.O. Box 210
	Rocket Center, WV 26726
		3	Thiokol Corporation
			Huntsville Division
			ATTN: D. Flanigan
			          J. Deur
			          Technical Library
			Huntsville, AL 35807

1	Hercules, Inc. Radford Army Ammunition Plant ATTN: J. Pierce Radford, VA 24141-0299	2	Thiokol Corporation Elkton Division ATTN: R. Biddle Technical Library P.O. Box 241 Elkton, MD 21921-0241
2	Lawrence Livermore National Laboratory ATTN: L-355, A. Buckingham M. Finger P.O. Box 808 Livermore, CA 94550-0622	1	Veritay Technology, Inc. ATTN: E. Fisher 4845 Millersport Highway P.O. Box 305 East Amherst, NY 14501-0305
1	Lawrence Livermore National Laboratory ATTN: L-324, M. Constantino P.O. Box 808 Livermore, CA 94550-0622	1	Universal Propulsion Company ATTN: H. J. McSpadden Black Canyon Stage 1 Box 1140 Phoenix, AZ 85029
1	Olin Corporation Badger Army Ammunition Plant ATTN: R. J. Thiede Baraboo, WI 52913	1	Battelle Memorial Institute ATTN: Technical Library 505 King Avenue Columbus, OH 43201-2693
1	Olin Corporation Smokeless Powder Operations ATTN: D. C. Mann P.O. Box 222 St. Marks, FL 32355-0222	1	Brigham Young University Dept. of Chemical Engineering ATTN: M. Beckstead Provo, UT 84601
1	Paul Gough Associates, Inc. ATTN: P.S. Gough P.O. Box 1614 1048 South Street Portsmouth, NH 03801-1614	1	California Institute of Technology 204 Karman Laboratory Main Stop 301-46 ATTN: F.E.C. Culick 1201 E. California Street Pasadena, CA 91109
1	Physics International Company ATTN: Library, H. Wayne Wampler 2700 Merced Street San Leandro, CA 98457-5602	1	California Institute of Technology Jet Propulsion Laboratory ATTN: L. D. Strand 4800 Oak Grove Drive Pasadena, CA 91109-8099

No. of Copies	Organization
1	University of Illinois Dept. of Mech/Indust Engineering ATTN: H. Krier 144 MEB; 1206 N. Green Street Urbana, IL 61801-2978
1	University of Massachusetts Dept. of Mechanical Engineering ATTN: K. Jakus Amherst, MA 01002-0014
1	University of Minnesota Dept. of Mechanical Engineering ATTN: E. Fletcher Minneapolis, MN 55414-5368
1	Case Western Reserve University Division of Aerospace Sciences ATTN: J. Tien Cleveland, OH 44135
3	Georgia Institute of Technology School of of Aerospace Engineering ATTN: B. T. Zinn E. Price W. C. Strahle Atlanta, GA 30332
1	Institute of Gas Technology ATTN: D. Gidaspow 3424 S. State Street Chicago, IL 60616-3896
1	Johns Hopkins University Applied Physics Laboratory Chemical Propulsion Information Agency ATTN: T. Christian Johns Hopkins Road Laurel, MD 20707-0690
1	Massachusetts Institute of Technology Dept. of Mechanical Engineering ATTN: T. Toong 77 Massachusetts Avenue Cambridge, MA 02139-4307
1	Pennsylvania State University Applied Research Laboratory ATTN: G. M. Faeth University Park, PA 16802-7501
1	Pennsylvania State University Dept. of Mechanic Engineering ATTN: K. Kuo University Park, PA 16802-7501

No. of Copies	Organization
1	Purdue University School of Mechanical Engineering ATTN: J. R. Osborn TSPC Chaffee Hall West Lafayette, IN 47907-1199
1	SRI International Propulsion Sciences Division ATTN: Technical Library 333 Ravenswood Avenue Menlo Park, CA 94025-3493
1	Rensselaer Polytechnic Institute Department of Mathematics Troy, NY 12181
2	Director Los Alamos National Laboratory ATTN: TS, D. Butler M. Division, B. Craig P.O. Box 1663 Los Alamos, NM 87545
1	General Applied Sciences Laboratory ATTN: J. Erdos 77 Raynor Avenue Ronkonkama, NY 11779-6649
1	Battelle Pacific Northwest Laboratory ATTN: Mr. Mark Garnich P.O. Box 999 Richland, WA 99352
1	Stevens Institute of Technology Davidson Laboratory ATTN: R. McAlevy, III Castle Point Station Hoboken, NJ 07030-5907
1	Rutgers University Dept. of Mechanical and Aerospace Engineering ATTN: S. Temkin University Heights Campus New Brunswick, NJ 08903
1	University of Southern California Mechanical Engineering Department ATTN: OHE200, M. Gerstein Los Angeles, CA 90089-5199
2	University of Utah Department of Chemical Engineering ATTN: A. Baer G. Flandro Salt Lake City, UT 84112-1194
1	Washington State University Department of Mechanical Engineering ATTN: C. T. Crowe Pullman, WA 99163-5201

No. of
Copies   Organization

1   Honeywell, Inc.
         ATTN: R. E. Tompkins
                MN38-3300
         10400 Yellow Circle Drive
         Minnetonka, MN 55343

1   Science Applications, Inc.
         ATTN: R. B. Edelman
         23146 Cumorah Crest Drive
         Woodland Hills, CA 91364-3710

         Aberdeen Proving Ground

         Cdr. CSTA
           ATTN: STECS-LI, R. Hendricksen

INTENTIONALLY LEFT BLANK.

USER EVALUATION SHEET/CHANGE OF ADDRESS

This Laboratory undertakes a continuing effort to improve the quality of the reports it publishes. Your comments/answers to the items/questions below will aid us in our efforts.

1. BRL Report Number ___BRL-CR-627___ Date of Report ___FEB 90___

2. Date Report Received _____

3. Does this report satisfy a need? (Comment on purpose, related project, or other area of interest for which the report will be used.) _____

_____

_____

4. Specifically, how is the report being used? (Information source, design data, procedure, source of ideas, etc.) _____

_____

_____

5. Has the information in this report led to any quantitative savings as far as man-hours or dollars saved, operating costs avoided, or efficiencies achieved, etc? If so, please elaborate. _____

_____

_____

6. General Comments. What do you think should be changed to improve future reports? (Indicate changes to organization, technical content, format, etc.) _____

_____

_____

_____

	Name
CURRENT ADDRESS	Organization
	Address
	City, State, Zip Code

7. If indicating a Change of Address or Address Correction, please provide the New or Correct Address in Block 6 above and the Old or Incorrect address below.

	Name
OLD ADDRESS	Organization
	Address
	City, State, Zip Code

(Remove this sheet, fold as indicated, staple or tape closed, and mail.)

---FOLD HERE---

:PARTMENT OF THE ARMY
rector
5. Army Ballistic Research Laboratory
TN: SLCBR-DD-T
erdeen Proving Ground, MD 21005-5066
  OFFICIAL BUSINESS

BUSINESS REPLY MAIL
FIRST CLASS PERMIT No 0001, APG, MD

POSTAGE WILL BE PAID BY ADDRESSEE

Director
U.S. Army Ballistic Research Laboratory
ATTN: SLCBR-DD-T
Aberdeen Proving Ground, MD 21005-9989

---FOLD HERE---